

---

# Protein Stability

---

A STUDY OF THE STABILITY OF HEN EGG-WHITE LYSOZYME EXPOSED TO  
CHEMICAL AND THERMAL DENATURATION AT PH 4, PH 7, AND PH 10

## AUTHORS

ANDERS SØBYE  
ASGER KOLDING  
MARIE-LOUISE KNOP LUND  
MIA DALGAARD JENSEN



**AALBORG UNIVERSITY**  
STUDENT REPORT

SCHOOL OF ENGINEERING AND SCIENCE

AALBORG UNIVERSITY 2015

GROUP 4.212





**AALBORG UNIVERSITY**  
STUDENT REPORT

Fourth Semester, School of  
Engineering and Science  
Nanotechnology  
Skjernvej 4A  
9220 Aalborg Ø  
<http://www.nano.aau.dk>

**Title:**

Protein Stability

**Project:**

P4

**Project Period:**

February 2015 - May 2015

**Projectgroup:**

4.212

**Participants:**

Anders Søbye  
Asger Kolding  
Marie-Louise K. Lund  
Mia Dalgaard Jensen

**Supervisors:**

Peter Fojan  
Leonid Gurevich

**Printed Copies: 7**

**Total Page Number: 95**

**Appendix: 1**

**Finished: May 29<sup>th</sup>, 2015**

**Abstract:**

The motivation for this project is to investigate the stability of Hen Egg-White Lysozyme (HEWL) during different environmental conditions. The effects of temperature and the denaturant GuHCl (0 - 7 M) at pH 4, pH 7, and pH 10 have been investigated. The results are obtained by steady-state fluorescence and circular dichroism spectroscopy, in order to determine the tertiary and secondary structures of HEWL, respectively, as HEWL is denatured. In this project, HEWL was successfully thermally denatured at pH 10 at 69 °C. However at pH 7 no denaturation is observed, and at pH 4 the results are discussed, as one small peak in the derivative of the emission spectrum is observed at 73 °C. Furthermore, HEWL was successfully chemically denatured at pH 4, pH 7, and pH 10 at GuHCl concentrations 5 - 7 M, indicating transition points of 6.1238, 6.2286, and 6.0656 M, respectively. A reduced stability of HEWL at pH 10 is observed, compared to the stability at pH 4 and pH 7. However, the tendency is not elucidated during chemical denaturation as during thermal denaturation. An obtained molten globule state is discussed.

*The content of this report is freely available, but publication (with source reference) may only take place in agreement with the authors.*



---

# Preface

---

This project is written by group 4.212 consisting of fourth semester Nanotechnology students of Aalborg University from February 3<sup>rd</sup> to May 29<sup>th</sup>. Lector Peter Fojan and Lector Leonid Gurevich are the primary supervisors. The topic of this project is characterization and modeling of nanostructures. This project will concern protein folding during environmental changes.

This project will introduce the topic of protein folding. Furthermore, this project includes a State of the Art chapter, which concerns with fatal protein misfoldings. The project includes theoretical chapters describing proteins, amino acids, protein stability, circular dichroism spectroscopy, and steady-state fluorescence spectroscopy. A description of the experiment and results will follow, which leads to a discussion and conclusion of the experiments according to relevant theory.

Throughout this project, each chapter and section will have numbered titles. Furthermore, all figures, significant equations, and tables will be numbered. The reference system applied is the numerical system and every reference is then represented by a [number], which refers directly to a specific source in the bibliography. Figures with no reference number are composed by the group itself.

---

Anders Søbye

---

Asger Kolding

---

Marie-Louise Knop Lund

---

Mia Dalgaard Jensen



---

## List of Abbreviations

---

<b>CD:</b>	Circular dichroism
<b>GuHCl:</b>	Guanidine hydrochloride
<b>HEWL:</b>	Hen Egg-White Lysozyme
<b>MG:</b>	Molten globule
<b>UV:</b>	Ultraviolet



---

# Table of Contents

---

<b>1</b>	<b>Introduction</b>	<b>11</b>
<b>2</b>	<b>State of the Art</b>	<b>13</b>
<b>3</b>	<b>Proteins</b>	<b>17</b>
3.1	Amino Acids . . . . .	17
3.2	Protein Structures . . . . .	19
3.2.1	Secondary Structures . . . . .	21
3.2.2	Tertiary Structures . . . . .	23
3.3	Hen Egg-White Lysozyme . . . . .	25
<b>4</b>	<b>Protein Stability</b>	<b>27</b>
4.1	Thermodynamic Considerations . . . . .	28
4.2	Environmental Impact . . . . .	29
4.2.1	Temperature . . . . .	29
4.2.2	pH . . . . .	30
4.2.3	Denaturants . . . . .	32
4.2.4	Guanidine Hydrochloride . . . . .	32
4.2.5	Ultraviolet Light . . . . .	34
<b>5</b>	<b>Circular Dichroism Spectroscopy</b>	<b>37</b>
5.1	Polarization of Light . . . . .	37
5.2	Principles of Circular Dichroism Spectroscopy . . . . .	37
5.3	Applications of Circular Dichroism Spectroscopy . . . . .	40
<b>6</b>	<b>Steady-State Fluorescence Spectroscopy</b>	<b>43</b>
6.1	Principles of Steady-State Fluorescence Spectroscopy . . . . .	43
6.2	Applications of Steady-State Fluorescence Spectroscopy . . . . .	45
<b>7</b>	<b>Materials and Methods</b>	<b>47</b>
7.1	Stock Buffer Solutions . . . . .	47
7.2	Stock Denaturant Solutions . . . . .	48
7.3	Thermal Denaturation: Fluorescence Spectroscopy . . . . .	48
7.4	Thermal Denaturation: Circular Dichroism Spectroscopy . . . . .	49
7.5	Chemical Denaturation: Fluorescence Spectroscopy . . . . .	50
7.6	Chemical Denaturation: Circular Dichroism Spectroscopy . . . . .	51
<b>8</b>	<b>Results</b>	<b>53</b>
8.1	Preparation of Stock Buffer Solutions . . . . .	53
8.2	Thermal Denaturation . . . . .	54
8.2.1	Sodium Acetate Buffer: pH 4 . . . . .	54
8.2.2	Sodium Citrate Buffer: pH 7 . . . . .	57

8.2.3	Sodium Carbonate Buffer: pH 10 . . . . .	60
8.3	Chemical Denaturation . . . . .	63
8.3.1	Sodium Acetate Buffer: pH 4 . . . . .	63
8.3.2	Sodium Citrate Buffer: pH 7 . . . . .	66
8.3.3	Sodium Carbonate Buffer: pH 10 . . . . .	69
8.4	Helical Content . . . . .	72
<b>9</b>	<b>Discussion</b>	<b>73</b>
9.1	Considerations in Relation to Buffer Solutions . . . . .	73
9.2	Thermal Denaturation . . . . .	74
9.3	Chemical Denaturation . . . . .	77
9.4	Further Studies . . . . .	81
<b>10</b>	<b>Conclusion</b>	<b>85</b>
	<b>Bibliography</b>	<b>87</b>
	<b>Appendix A</b>	<b>95</b>

---

# 1. Introduction

---

Proteins are among the most fundamental and versatile organic macromolecules in organisms, and they are crucial for normal cell and corpus functionality. Some proteins function as catalysts in chemical reactions, while others can transport or store molecules, provide mechanical structural support or immune protection, or control growth etc. The specific and crucial protein functionality depends directly on the three-dimensional protein structure, and thus the amino acid sequence. It is obvious that protein dysfunctionality is devastating for organisms and potentially deadly. During the last decade well-known and aetiologically distinct diseases have been connected to protein misfolding of specific proteins into aggregates. These disorders, including Alzheimer's disease and diabetes, are among the most debilitating, socially disruptive, and costly diseases in the modern world, and they are becoming more prevalent as the society age and become more dependent on new agricultural and dietary practices. [1]

In many cases, it is easy to reproduce the structural transitions of normal functional proteins into denatured, misfolded, or aggregated proteins in vitro by exposure to denaturing conditions. However, the mechanisms in which normal functional proteins misfold into aggregates in vivo are not yet well understood, and it is unclear how distinct proteins can change structurally into a highly organized common aggregate structure such as amyloid fibrils that is extremely thermodynamically stable. [2]

In order to deal with and potentially treat or prevent these human diseases, it is important to understand the mechanisms and principles underlying protein folding, denaturation, and misfolding. Thus, this project will concern the denaturation of a model protein, Hen Egg-White Lysozyme both thermal and chemical by the denaturant guanidine hydrochloride.



---

## 2. State of the Art

---

The ability of proteins to fold correctly into their native and functional form is one of the most fundamental phenomena in nature, and crucial for normal functionality of cells and organisms. Due to the complexity of the protein folding process, it would be astonishing if misfoldings never occurred. To compensate for misfoldings, the cell have evolved several intracellular regulatory systems to sense, respond to, and target misfolded proteins. Of particular importance are molecular chaperones, which are found in a large number and variety in all cell types and cellular compartments. Some ribosomal chaperones enable efficient protein folding and assembling, some can solubilize specific forms of protein aggregates, ultimately inducing refolding in some cases, and others can interact with highly aggregation-prone protein regions in the misfolded or partially folded protein such as exposed hydrophobic surfaces protecting them from aggregation. A great number of chaperones are found in The Endoplasmic Reticulum, and they serve as a strict quality control of all synthesized proteins. The importance of this control system is evident from studies suggesting that up to half of all synthesized polypeptide chains fail to satisfy the quality control mechanism. [1, 3]

Furthermore, during protein folding into the native and functional form, the assembling occurs rapidly, allowing the proteins to escape and reduce aberrant side-reactions that potentially can lead to the formation of aggregates. Since the native proteins are a thermodynamic meta-stable structure, the proteins must be kinetically trapped in their native form in order to stay functional. [2]

Despite the complex intracellular regulatory systems, protein misfolding and aggregation occurs intra- and extracellularly, particularly as organisms age, or by the fact that small local environmental changes can induce unfolding events. These event can result in denatured proteins prone to aggregation, resulting in devastating protein aggregation pathologies including Alzheimer's, Parkinson's, Type II Diabetes, Cystic Fibrosis, Huntington's, and Creutzfeldt-Jakob's disease. [2, 3]

One characteristic of many protein aggregation diseases is the deposition of misfolded proteins in the form of amyloid fibrils, which are fibrous structures resistant to protease digestion and with special optic and dye-binding properties. Depending on the disease involved, the deposits can form in brain tissue, vital organs or skeletal tissue, and, in some cases of systemic diseases, kilograms of aggregate can be isolated from such deposits [1]. It was generally believed that only a few proteins, mainly those involved in known pathologies, were able to form amyloid fibrils, and that those proteins possessed specific sequence motifs, encoding the amyloid structure. However, recent study suggests that the ability to form amyloid fibrils is a genetic feature of all polypeptide chains when presented with some stimulating environment, and, fibrils formed from both large proteins and from those of only a handful of residues are very similar in overall appearance and properties. [1, 2]

Although the ability to form amyloid fibrils appears genetic, the faculty and propensity to aggregate in this fashion can vary dramatically between different polymer sequences. Some amino acids are much more soluble than others resulting in different concentration

requirements for aggregation to occur, and the aggregation process is nucleation dependent, where it is evident that even a single amino acid in the protein sequence can affect the rate of nucleation. [1]

The general appearance of amyloid fibrils is a cross- $\beta$  structure where continuous  $\beta$ -sheets are formed with  $\beta$ -strands running perpendicular to the axis of the fibril. This structure is remarkable in its high thermodynamic stability and high insolubility, and by the fact that the proteins comprising the fibril structure have no sequence or structural similarities. [1, 2, 3]

The core structure of the fibrils are primarily stabilized by hydrogen bonds involving the protein backbones, which explains why the general appearance of the amyloid fibrils from different proteins are similar. The side chains are incorporated in the fibril structure in whatever manner is the most favourable. They only affect the details of the amyloid fibril, and not the general appearance. [1]

Amyloid fibrils are included as one of the types of aggregates proteins can form. The fibrils have a unique kinetic stability due to the highly organized hydrogen bond structure, and the highest thermodynamic stability of all protein aggregates. [2]

Conditions that favour fibril aggregation from native proteins are those that involve partially unfolded proteins. In the case of globular proteins, low pH, high temperatures, addition of denaturants, and amino acid substitution all destabilizes the native protein exposing aggregate-prone regions, inducing fibril formation. However, the identity of specific amyloid precursor structures are not yet determined for any protein, but it is indicated by electron and atomic force microscopy that small amorphous aggregate structures initiates the formation of fibril-like structures with more distinctive morphologies that eventually assembles into mature amyloid fibrils by some sort of structural reorganization. This nucleation of fibrils is very distinct from the nucleation of native globular proteins, indicating that evolution have selected the nucleation that favours folding over aggregation. [2]

Intra- and extracellular aggregation is often accompanied with cytotoxicity caused by mechanisms such as lipid membrane permeabilization, oxidative stress and mitochondrial dysfunction. Amyloid fibrils can interact with lipid membranes inducing membrane permeabilization through pores or by disrupting membrane integrity through surface electrostatic interactions that ultimately disintegrate the bilayer structure of the membrane. Oxidative stress is suggested to be the major cytotoxic mechanism in the pathology of most protein misfolding diseases. Many proteins comprising the amyloid fibrils are capable of generating reactive oxygen species. Also, Endoplasmic reticulum stress has been observed in hippocampal neurons caused by amyloid  $\beta$ -peptides. Lastly, during the process of amyloidogenesis the mitochondrial signalling pathway is affected leading to mitochondrial dysfunction as cytochrome C and apoptosis induce factor are released from the mitochondria, which in turn induces DNA damage and cell apoptosis. [4]

The most common protein aggregation disease is Alzheimer's disease, and like most other amyloidosis diseases, the patients have a prolonged preclinical period before clinical manifestation, indicating that time rather than old age is required in amyloidosis diseases. One striking example is Alzheimer's patients with Down's syndrome, where aggregates comprised of Amyloid  $\beta$ -peptides are developed in the brain as early as the age of ten due to life-long overexpression of the amyloid precursor protein, which is encoded in chromosome

21. [5]

In the case of Alzheimer's disease, deposition of Amyloid- $\beta$  aggregates is found both extra- and intracellularly. It has been proven, that in the brain of patients with only mild clinical impairment, the concentration of aggregate in the cerebral cortex correspond to the degree of synaptic loss [5]. The amyloid fibrils and their precursor assemblies might act as amphiphiles bonding non specifically to, and perturbing multiple cell-surface receptors and channels. In the case of Alzheimer's they can bind to receptors and channels in the synaptic plasma membrane, thus interfering with numerous signal-transduction cascades by enhancement of the generation of free radicals or alter the calcium homeostasis. [5]

The second most common neurodegenerative disease is Parkinson's disease. Here, the protein  $\alpha$ -synuclein misfold and accumulate in spherical filaments in selected neuronal cells, in particular the dopaminergic and noradrenergic brainstem neurons, whose premature death defines the disease biochemically.

Another case of protein misfolding diseases in the central nervous system is Huntington's disease where unstable DNA mutations in different genes ultimately results in misfolding and accumulation of proteins in the nuclei and cytoplasm of certain neuron cells, leading to gradual dysfunction and death of the host neurons. [5]

Type II Diabetes has been recognized as a protein aggregation disease since the hormone Amylin can aggregate and accumulate extracellularly in the pancreas, and it is suggested that this deposition can lead to cell-death in insulin-producing  $\beta$ -cells. However, it is unknown if this accumulation causes the Diabetes, or if it is a result of the disease. [5]

Lastly, one of the most remarkable cases of protein misfolding diseases is Creutzfeldt-Jakob's disease. Here the cellular prion protein can mutate its conformation, resulting in a meta-stable conformer, which can bind to and convert another wild-type prion into the same pathological isoform. This reaction can occur spontaneously at a very low frequency, but can also occur more rapidly if the proteins bear certain mutations. Most remarkable, the disease can occur in infectious form, where small amounts of pathologically conformed but non-mutant prion proteins cause Creutzfeldt-Jakob's disease in healthy subjects after exposure [5].

During the last two decades, intensive research have been carried out in the need of therapeutics that can somehow reduce cases of amyloidosis, or at least limit further development in patients. It is well known which proteins cause these aggregation diseases. However, it is not well defined how those can aggregate into pathogenic species, and it is not clear how to prevent the formation of the amyloid fibrils, remove them effectively, or block their interactions [3].

Where most research have been concerning the understanding of the development of the diseases, some drug candidates targeting amyloidogenic peptides have been proposed and are under development. Those include therapeutics that reduce the expression level of the amyloidogenic peptides, increases the removal rate of misfolded amyloidogenic peptides, increase the stability of functional native amyloidogenic peptides, and inhibit the self-assembling into misfolding such as amyloid fibrils. Some reported inhibitors that are currently being clinically tested include polyphenols and non-polyphenols. Polyphenols are aromatic compounds naturally occurring in a wide range of foods and herbal medicines such as wine, coffee, and tea. They contain one or more phenolic hydroxyl groups, which their anti-amyloidogenic activity is suggested to rely on as they may interact with aromatic residues in amyloidogenic peptides inducing  $\pi$ -stacking, which could prevent

$\pi$ - $\pi$  interactions that lead to self-assembling into fibrils. Non-polyphenols include small molecules such as glycosides and alkaloids, and contains one or several aromatic rings, and thus also relies on the  $\pi$ -stacking principle. Most studies are performed on the amyloid- $\beta$  peptide, and it was believed that those inhibitors found on aggregates would have a generally inhibitory effect on all amyloidogenic peptides. However, recent studies suggest that this might not be the case as where some inhibitors (i.e. polyphenols extracted from coffee) had an excellent inhibitory effect on amyloid- $\beta$  aggregates, they showed acceleration effects on fibrillization of Lysozyme. [4]

Furthermore, short peptides have shown inhibitory effects on amyloid formation as they can be designed to bind to aggregation-prone regions in amyloidogenic peptides and thus preventing aggregation. Lastly, antibodies have been designed to recognize specific secondary and tertiary structures, or structural motifs, in native amyloidogenic peptides, and by antibody-antigen interaction inhibit aggregation. Despite failures to demonstrate effective therapeutic efficacy, anti-bodies are a promising approach in accelerating removal of amyloidogenic peptides, especially as they can be designed to interact with receptors specific for every known amyloidosis disorder. [4]

---

## 3. Proteins

---

Proteins are organic polymers, comprised by a repeating framework of amino acids, and possess diverse abilities depending on their physiochemical properties. Beside the polypeptide chain, proteins often contain co-factors including small molecules, ions, or sugars etc. The co-factors can be linked to the polypeptide chain by chemical bonds, or bound into cavities by other interactions where they often confer to and participate in protein functionality. [6]

The proteins reside in different *in vivo* environments, which leave an obvious mark on their three-dimensional structure, and, along with their stabilizing interactions and architecture, divide the proteins into three categories; Fibrous, membrane, and globular proteins. Fibrous proteins are often very large and elongated with mostly structural main functionality. They often possess a higher order of secondary structures and are usually highly hydrogen-bonded, very flexible, and insoluble. Membrane proteins reside in the water-deficient cell membrane, and they possess functionalities such as molecular transport and metabolism regulation or membrane signalling. Furthermore, they have a very regular structure, and are highly hydrogen-bonded. Lastly, globular proteins are water-soluble proteins with less regular structures. The functions of globular proteins are often catalytic, making them enzymes. As the name indicates, they have tight bonded spherical tertiary structures. [7]

This project will mainly concern the structure and stability of globular proteins, in particular smaller ones, in accordance with the enzyme Hen Egg-White Lysozyme (HEWL). The applied HEWL structure in this project is deduced by nuclear magnetic resonance spectroscopy. Thus some secondary structures are left out in comparison to those deduced by x-ray crystallography. These residue regions are denoted green in every figure showing the tertiary structure of HEWL.

### 3.1 Amino Acids

Amino acids are colourless organic monomer units, which serve as building blocks for proteins. By principle, there exist an infinite number of possible amino acids, which can be synthesized. However, all proteins found in different species of organisms, including bacterial, archaeal, and eukaryotic, are composed of the same set of 20 specific amino acids, see Appendix A, with only a few exceptions. Amino acids are often designated by either a three-letter abbreviation or a one-letter symbol. The three-letter abbreviation is deduced from the three first letters in the amino acid name with exceptions of Asparagine, Glutamine, Isoleucine, and Tryptophan. [7]

The general appearance of amino acids is a composition of a carboxylic acid- and an amine functional group along with a distinctive side chain, which all are linked by a central  $\alpha$ -carbon. Four different chemical groups are bound to the  $\alpha$ -carbon, and thus it is defined as a chiral center. Consequently, the amino acids can exist in one of its two configurations; the Laevus (L) isomer or the Dexter (D) isomer, which are enantiomers. In proteins, amino acids only exist as L isomers, which refer to a composition where the amino group

is projected left when projected in a Fischer projection. One exception is the hydrophobic amino acid Glycine whose  $\alpha$ -carbon is achiral owing to its hydrogen side chain, and thus it exists in both L and D configurations. [7]

Furthermore, L isomers often have an absolute Sinister (S) configuration meaning the direction of highest to lowest priority substituents is counter clockwise around the  $\alpha$ -carbon, and indicates that the chiral center is at S configuration. One exception is the polar Cysteine, which have an absolute Rectus (R) configured  $\alpha$ -carbon, and thus have clockwise priority of substituents. [7]

The 20 natural amino acids can be categorized into four groups depending on their general chemical characteristics, which ultimately refer to the characteristics of the side chains. There exist apolar, polar, alkaline, and acidic amino acids. Since free amino acids have both alkaline and acidic functional groups they exist primarily as dipolar ions, zwitterions, at pH 7. [7]

Among the hydrophobic apolar amino acids, Proline is particularly interesting as its side chain is bonded to its amine group and thus it is essentially an imino acid rather than an amino acid. Furthermore, Tryptophan and Phenylalanine, along with the polar uncharged Tyrosine, have aromatic side chains and are therefore fluorophores. The benzene ring is a perfect conjugated system comprised by six  $sp^2$ -hybridized carbon atoms, which provide a planar ring structure and results in high thermodynamic stability and thus less reactivity [8]. The bonds between the carbon atoms are chemical covalent bonds, and to form such bonds carbon orbitals must overlap in order to form shared molecular orbitals in which most atoms come to obey the octet rule, and shares one electron pair. The hybridization is a pure quantum effect. As most organic molecules, including oxygen and nitrogen, carbon valence electrons reside in 2p-orbitals. The p-orbital is an 8-shaped orbital with a transverse horizontal nodal plane perpendicular to the orientation plane of the orbital. At the nodal plane there is zero possibility of interaction with the electron and thus the wave function is equal to zero. The wave function has a positive phase sign on one side of the nodal plane, and a negative one on the other side. When two orbitals overlap, the two electron wave functions in the overlap-regions are superimposed and thus by Schrödinger's linearity resulting in a new valid wave function for the resulting molecular orbital that is more energetically favourable. The orbital overlap can be either positive, resulting in a bonding molecular orbital, or negative, resulting in an anti-bonding molecular orbital in which the shared electron density is reduced and intermolecular repulsion is increased. [6, 9]

The resultant orbital overlap in the benzene ring is a  $\pi$ -system of covalent  $\pi$ -bonds between carbon atoms owing to the involved valence electrons originated from p-orbitals. Furthermore, the benzene ring is at resonance structure, which is evident from the bond length between the carbon atoms as they are shorter than those of pure double bonds, but longer than those of pure single bonds. It is said that the  $\pi$ -electrons are equally delocalized over all six carbon atoms and thus the bonding  $\pi$ molecular orbital involves all six atoms. Due to the linearity of the benzene ring, the orbital overlap results in pairs of  $\pi$ -molecular orbitals since there is two similar p-orbitals ( $p_x$  and  $p_y$ ) on each atom, thus resulting in two equivalent  $\pi$ molecular orbitals and two equivalent anti  $\pi$  ( $\pi^*$ ) molecular orbitals. Furthermore, all single bonds are  $\sigma$ -bonds, and the combination of a  $\sigma$ -bonds and a  $\pi$ -bond is what is normally referred to as a double bond. [9]

Conjugated systems have characteristic spectral absorptions in the ultraviolet (UV) region.

In a pure conjugated system, the energy difference between bonding and anti-bonding molecular orbitals are small and thus the compound have intense absorption at longer wavelengths. [8]

Lastly, the  $\pi^*$  orbital is always present. However, it is electron deficient when electrons of the ring is at ground state and located in the bonding orbital. If the electrons are to be excited to a higher energy level (i.e.  $\pi^*$  orbital) by absorbing energy, the  $\pi$ -bond is temporarily destroyed allowing rotation and change in conformation around the  $\sigma$ -bond. The  $\pi$ -bond is reformed when the electron is restored to ground state. [8]

## 3.2 Protein Structures

To form a protein, amino acids are linked into a polypeptide chain by peptide bonds between the carboxylic acid group of one amino acid and the amino group of another amino acid from N-terminus to C-terminus. This unique sequence of amino acids is the primary structure of the protein, which is a result from the biochemical matrix synthesis in accordance with the gene coding (i.e. polymerization by translation), and determines the three-dimensional structure and thereby functionality of the protein. [6]

The formation of a peptide bond between two amino acids results in the elimination of a water molecule. During most conditions, the equilibrium of this reaction is displaced toward the hydrolysis rather than synthesis, and thus the biosynthesis of the peptide bond requires some input of free energy. The peptide bond is quite kinetically stable since the rate of hydrolysis is extremely slow. [7]

The peptide bond is a chemical covalent bond that resides in the planar rigid peptide unit, which is comprised of six atoms places in the same plane, see Figure 3.1. The planar structure is provided by the  $sp^2$ -hybridization of carbon and nitrogen electrons in the peptide bond. To form the bond, the carbon and nitrogen orbitals must overlap in order to form shared molecular orbitals in which they come to obey the octet rule. [6, 9]

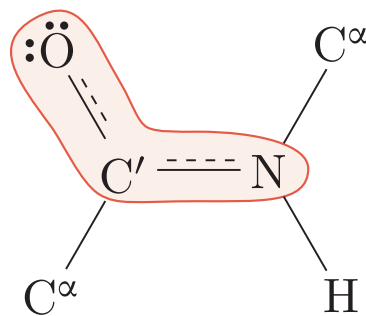


**Figure 3.1.** Schematic representation of the planar rigid peptide unit comprised of six atoms of the protein backbone. The electrons of nitrogen, carbon, and oxygen are delocalized, inducing resonance stabilization of the three atoms. The resultant peptide bond is a covalent  $\pi$ -bond delocalized over the  $N-C'=O$ .

The  $sp^2$ -hybridization is a superposition of one s-orbital and two p-orbitals per participating atom resulting in three  $sp^2$ -orbitals, each containing one single unpaired electron, and involves the atoms in three covalent bonds ( $N-C=O$ ). Note that in the case of N-C  $sp^2$ -hybridization, one non-hybridized non-bonding p-orbital remains, which also contains one single unpaired electron. Ultimately, the creation of a covalent bond involves

a delocalized electron hybrid orbital surrounding the participating atoms, which obey the Pauli exclusion principle, and when pairing two electrons with opposite spin moment from two different atoms a tight covalent bond is formed. [6, 9]

The covalent bond in the peptide unit is a  $\pi$ -bond owing to its involved electrons originated from p-orbitals [10]. Due to its linearity, the peptide bond also forms  $\pi$ -molecular orbitals in pairs. [9]

Furthermore, the peptide unit is in a resonance structure since the lone pair electrons of oxygen and nonbonding nitrogen and carbon (i.e. uninvolved in  $sp^2$ -hybridization) electrons also bond and delocalize, and therefore the double bonds  $O=C'$  and  $N=C'$  are drawn partially. The  $\pi$ -bond is equally distributed and delocalized over the three atoms rather than just nitrogen and carbon, see Figure 3.1. In contrast, the bonds  $N-C^\alpha$  and  $C^\alpha-C'$  are pure single bonds,  $\sigma$ -bonds. [6, 9]

The conformation the polypeptide chain is described in terms of angular rotations (dihedral angles) around the covalent bonds, and give rise to different orientations of the peptide unit and folding possibilities of the whole peptide chain. [6]

The rotation angles of the side-chains are denoted  $\chi$  angles, which is the rotation around the covalent bond between the  $sp^3$ -hybridized atoms  $C^\alpha$  and  $C^\beta$  where four bonds are directed from each center atom forming a tetrahedron, see Figure 3.2. The rotation angle around the  $sp^2$ -hybridized peptide bond  $C'-N$  is termed  $\omega$ , see Figure 3.2. The potential energy barriers in this bond are high, owing to the non-bonding p-electrons originated from the nitrogen atom that is perpendicular to the plane of the  $sp^2$ -hybridization resulting in a rigid structure and blockage of large angle rotations around the peptide bond. Furthermore, this angle gives rise to cis/trans conformation as its potential minimums are at  $0^\circ$  (cis) and  $180^\circ$  (trans). Lastly, the rotation angles around the bond between  $sp^3$ -hybridized and  $sp^2$ -hybridized atoms are denoted  $\phi$  and  $\psi$ , and include the  $N-C^\alpha$  and the  $C^\alpha-C'$  bond, respectively, see Figure 3.2. Around such bonds there is nearly free rotation, giving the polypeptide chain its flexibility.

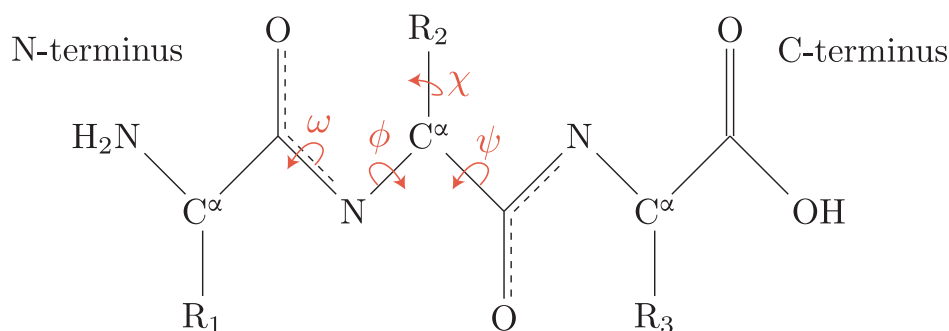


**Figure 3.2.** Schematic representation of a protein backbone from the N-terminus to the C-terminus. The dihedrals are denoted red. The  $\omega$  rotation angle is the rotation around the peptide bond,  $\phi$  is the rotation around the  $N-C^\alpha$  bond,  $\psi$  is the rotation around the  $C'-C^\alpha$  bond, and  $\chi$  is the rotation angle of the side chains.

However, not all combinations of dihedral angles in the polypeptide chain are possible due to steric collision between atoms. The allowed angle pairs of  $\phi$  and  $\psi$  are plotted in a two-dimensional Ramachandran diagram. Such angle pairs determine whether the residue is part of an  $\alpha$ -helix,  $\beta$ -structure, loop, or turn. If the angles are determined through x-ray diffraction, they can be plotted in an Ramachandran diagram, visualizing if the

proposed protein structure is sterically allowed or disfavoured. Only a third of the angle combinations are allowed. Note that Glycine and Proline are exceptions to the general Ramachandran diagram, as Glycine is not chiral and Proline prefer cis configuration, and thus when plotted in a Ramachandran diagram they will differentiate from the allowed regions. [6, 7]

See Figure 3.3 for a Ramachandran diagram of HEWL.

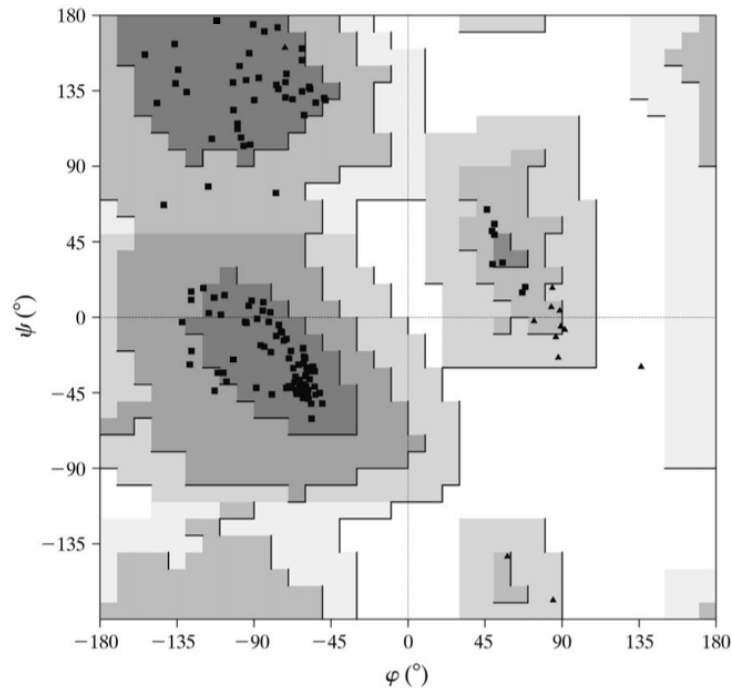


**Figure 3.3.** Ramachandran diagram of HEWL. A total of 136 angle pairs are plotted (■). Glycine residues are denoted ▲. Dark grey areas are the normally allowed regions and include fully allowed conformations that is mostly preferred. The lighter grey regions are the partially allowed regions with partially allowed conformations. The large upper region is conformations comprising  $\beta$ -structures. The large lower region is conformations comprising the right-handed  $\alpha$ -helix, and lastly the smaller middle region is conformations comprising the left-handed  $\alpha$ -helix. [11]

### 3.2.1 Secondary Structures

Folded proteins have regular secondary structures, which includes the  $\alpha$ -helix and the  $\beta$ -structure. The folding process into these structures is essentially thermodynamic, and the number of stable possible folded protein conformations are restricted by the dihedral angles  $\psi$  and  $\phi$ . Furthermore,  $\alpha$ -turns and  $\omega$ -loops have been identified. Although they are not characterized by a regular periodic conformation, as the  $\alpha$ -helix and the  $\beta$ -structures, they are well defined and contribute, along with the  $\alpha$ -helix and the  $\beta$ -structures, to the final protein structure. [7]

The  $\alpha$ -helix is a rod-like secondary structure, in which the side chains of the amino acids constitute the outer part of the structure, and the backbone of the polypeptide chain constitute the inner core, see Figure 3.4.

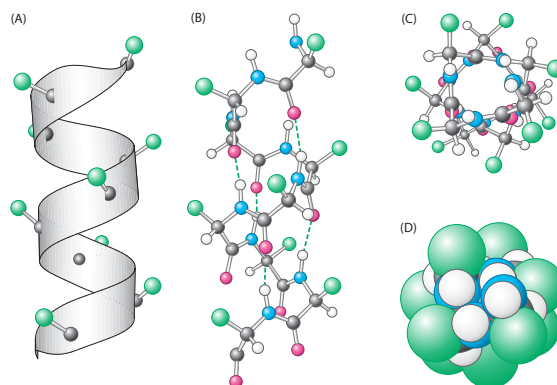


**Figure 3.4.** The structure of the  $\alpha$ -helix showing A) the rod-like representation with  $C^\alpha$  (black) and side chains (green), B) Ball-and-stick representation of the helix structure with hydrogen bonds between  $C=O$  and  $N-H$  groups, C) a top view of the helix with side chains pointing outward, and D) a top view of an atomic representation showing the closed packed interior of the helix. [7]

The  $\alpha$ -helix is stabilized by hydrogen-bonds between  $N-H$  groups, which are great hydrogen-bond donors, and  $C=O$  groups, which are great hydrogen-bond acceptors. When a hydrogen-bond is formed between a donor and an acceptor within a protein, it replaces two hydrogen-bonds between the polypeptide chain and the surrounding water, and forms an additional hydrogen-bond between the two freed water molecules. Any donor and acceptor in a protein free of bonding within the protein itself are hydrogen bonded to surrounding water molecules in aqueous environments. In the  $\alpha$ -helix, each participating  $C=O$  group forms a hydrogen bond with the  $N-H$  group that is four residues ahead in the amino acid sequence, see Figure 3.5. Consequently, the number of residues per turn in an  $\alpha$ -helix is 3.6. The screw sense of the helix can be either right-handed or left-handed, and both are sterically allowed conformations. However, the right-handed  $\alpha$ -helix is far the most common in proteins, owing to its more energetically favourable conformation caused by less steric hindrance between side-chains and the backbone. Furthermore, not all amino acids can be accommodated to the helix structure; Valine, Threonine, and Isoleucine tend to destabilize the  $\alpha$ -helix due to steric hindrance, and Serine, Aspartate, and Asparagine tend to disrupt the structure since their side chains contain hydrogen-bond acceptors or donors, and lastly, Proline breaks an  $\alpha$ -helix since its ring structure prevents the amino acid in complying with the needed  $\phi$  angle to fit into a helix structure. [7]

In contrast, Alanine prefer the  $\alpha$ -helix, and partially the  $\beta$ -structure, over irregular conformations such as turns and loops, explained by its restricted conformations in the Ramachandran diagram. Lastly, negatively charged residues prefer the N-terminus of the helix. [6]

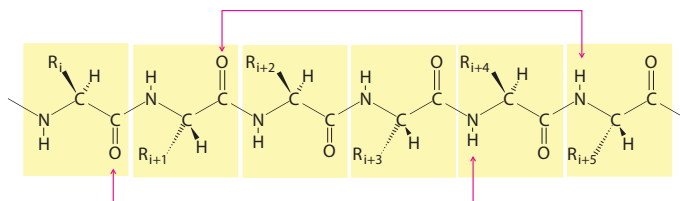


**Figure 3.5.** Protein residues of the  $\alpha$ -helix which form hydrogen bonds between the  $C=O$  and the  $N-H$  group four residues ahead in the amino acid sequence. [7]

The  $\beta$ -sheet is a periodic structural motif, or super-secondary structure, composed of two or more  $\beta$ -strands, which is a true secondary structure. The  $\beta$ -sheets are, like the  $\alpha$ -helix, stabilized by hydrogen bonds between adjacent  $\beta$ -strands. In the case of the antiparallel  $\beta$ -sheet, the  $\beta$  strands run in the opposite direction to each other, and are linked by hydrogen bonds between the C=O group and the N-H group of two neighbouring amino acids on two adjacent  $\beta$ -strands, see Figure 3.6. The  $\beta$ -sheet can also be parallel, however, the antiparallel is the most common and most stable of the two. Furthermore, the  $\beta$ -sheet can be purely antiparallel, parallel, or mixed. The form of the  $\beta$ -sheet is somewhat between almost flat to some twisted shape that is a more energetically advantageous conformation, and the  $\beta$ -strands are schematically represented as arrows in the protein running from the N-terminus to the C-terminus indicating the produced type of motif. [6, 7]

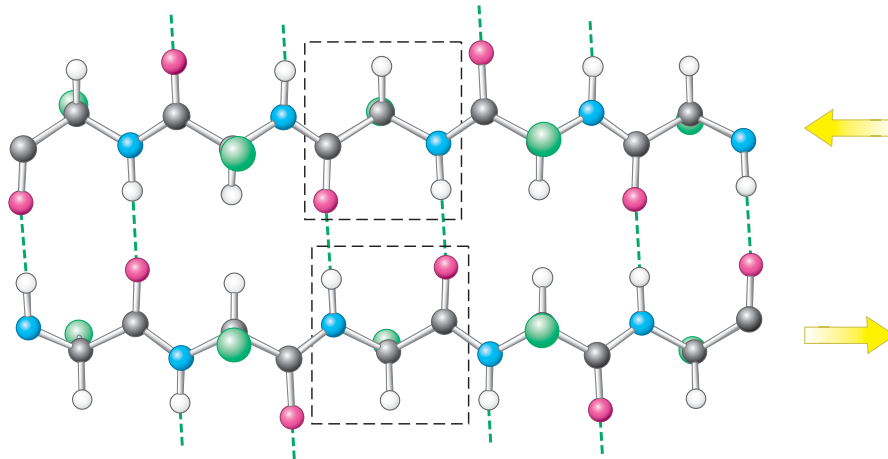


**Figure 3.6.** Adjacent  $\beta$ -strands, which constitute an antiparallel  $\beta$ -sheet structure. The structure is stabilized by hydrogen bonds between the N-H and C=O groups on neighbouring  $\beta$ -strands. [7]

Hydrophobic residues most often prefer the  $\beta$ -structure, since this structure is less tightly packed compared to the  $\alpha$ -helix and thus gives more room to large  $\gamma$ -atoms (carbon atom bonded to the  $\beta$ -atom in the side chain) of the hydrophobic residues. In contrast, polar amino acids prefer irregular surface regions where they easily can participate in hydrogen bonds with both water and the polypeptide chain itself. Exceptions are Tryptophan and Tyrosine. They have small dipoles and a large hydrophobic part, and cysteine whose S-H group have extremely weak hydrogen bonds. Together, the behaviour of all three residues is similar to that of hydrophobic residues. Lastly, Glycine dislike both the  $\beta$ -structure and the  $\alpha$ -helix, and prefer irregular regions since it can adopt a variety of conformations, giving it broad regions in its Ramachandran diagram. [6]

### 3.2.2 Tertiary Structures

When the secondary structures along with the loops and turns are arranged in three-dimensional space into a tight packed globular formation, the tertiary structure of the proteins appears, see Figure 3.7 for the tertiary structure of HEWL.

A general tendency between proteins in aqueous solutions are that they are driven by hydrophobic interactions in order to pack the nonpolar hydrophobic residues inside the protein structure to exclude them from water. This leaves the more hydrophilic (i.e. polar charged) residues on the outer side of the protein in contact with water where they can

participate in hydrogen bonds. This formation is more thermodynamically stable and confer the globular protein its solubility in water, as overall hydrophilic substances are soluble in hydrophilic environments and vice versa. Indeed there exist exceptions where hydrophilic residues reside in the protein interior; however, they are all connected with coordinate bonding of metal ions or with functionalities of active sites of enzymes. [6, 7] Furthermore, the hydrophobic protein interior must comprise only hydrophobic side chains from secondary structures while polar side chains must remain on the outer side, inducing an ordering of hydrophobic and hydrophilic residues in secondary structures as to obey the thermodynamic stable conformation of the protein. Turns and loops also tend to reside on the surface of the protein, and thus often participate in interactions with other proteins and molecules, and yield the protein a higher order of stability. [6]

The architecture and folding pattern of the tertiary protein structure can represent different domains and structural motifs. Domains are spatial structures of the globules and are composed of regular secondary structures. As an example, HEWL is composed of two domains linked by a long  $\alpha$ -helix; one domain consisting of the  $\beta$ -sheet and the other consisting of two  $\alpha$ -helices. As for most enzymes, the active site of HEWL is located between the domains, see Figure 3.7.

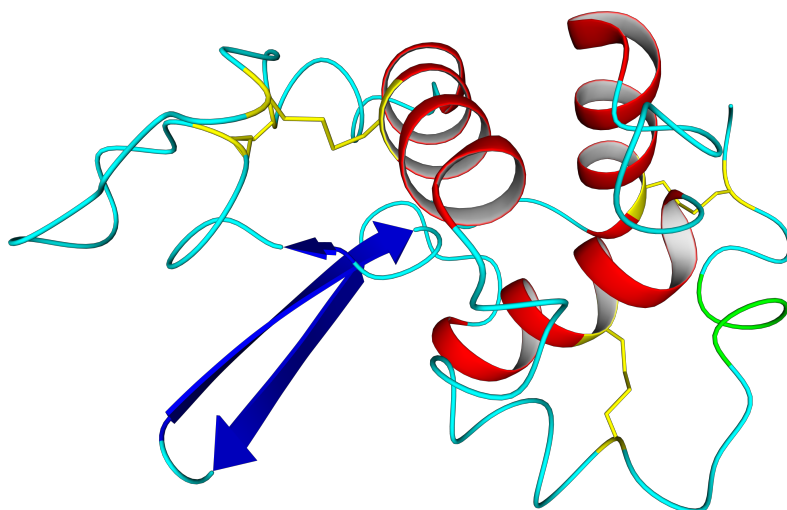


**Figure 3.7.** Tertiary structure of HEWL, which is composed of one  $\alpha$ -domain and one  $\beta$ -domain linked by one long  $\alpha$ -helix. In between HEWL's two domains reside its active site. HEWL's four disulphide bonds are denoted yellow.

A structural motif composition gives rise to a classification of small globular proteins or domains. The protein can be either a pure  $\beta$ -, a pure  $\alpha$ -, or a mixed protein. HEWL is a mixed protein since it contains both  $\beta$ -structures and  $\alpha$ -helices, and is thus defined as a  $\alpha + \beta$  protein since the  $\beta$ -sheet is anti-parallel. As for the motifs within these domains, HEWL contain one helix-loop-helix motif and a meander pattern of the  $\beta$ -sheet consisting of  $\beta$ -hairpins, see Figure 3.8. [6]

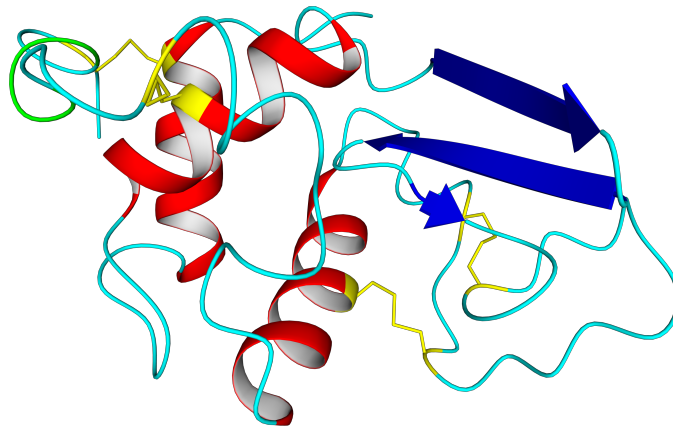


**Figure 3.8.** Tertiary structure of the  $\alpha + \beta$  protein HEWL, which is composed of one helix-loop-helix motif (red - not including the longest  $\alpha$ -helix) and a meander pattern of the  $\beta$ -sheet consisting of  $\beta$ -hairpins (blue). HEWL's four disulphide bonds are denoted yellow.

In some proteins, the tertiary structure is stabilized by cross-linkage by disulphide bonds formed by oxidation of a pair of Cysteine thiol groups, see Figures 3.7 and 3.8. The disulphide bond is a covalent bond, however, it is not as strong as the covalent peptide bond as an example. Disulphide bonds can only be formed when two cysteines are brought close enough by other interactions, since, intracellularly, there is a high concentration of Glutathione in bond breaking form (GSH), which shift the reaction toward breaking. Thus only proteins residing extracellularly are stabilized by disulphide bonds, which are formed when the synthesized proteins are secreted. The bonds become frozen and risk no breaking or rearrangement since GSH is only present intracellularly. [6]

Furthermore, Van der Waals interactions between the side chains contribute to the protein stability since maximizing of the Van der Waals interactions requires a very intimate contact between atoms. Electrostatic interactions between charged side chains also contribute to the protein stability. Although covalent bonds, hydrogen bonds, hydrophobic interactions, disulphide bonds, Van der Waals interactions, and electrostatic interactions all contribute to the folded protein stability, the covalent bond is far the strongest interaction, and thus most chemical and thermal denaturants tends to disrupt the non-covalent bonds in the polypeptide chain. [7]

Furthermore, the peptide bond is uncharged, which allows the polypeptide chain to fold into a tightly packed globular structure. [6]

Lastly, some proteins may have a quaternary structural organization meaning the functional protein consist of more than one polypeptide chain. [7]

### 3.3 Hen Egg-White Lysozyme

Lysozyme is a small globular enzyme, with a somewhat elliptical structure, which first was discovered in 1921 by Alexander Fleming while he was searching for antibiotics. By accident, he showed that his own nasal mucus inhibited the growth of a *Micrococcus* species. [12]

Lysozyme has since that been identified in mammalian saliva, blood, milk, and tears where it acts as part of the immune response, and furthermore, in plants and eggs. Hen egg-white has a particularly high level of Lysozyme [12]. HEWL is one of the most studied globular proteins and the first protein whose primary and tertiary structure was determined by x-ray crystallography in the 1960s. [13]

HEWL consists of 129 amino acids, see Figure 3.9, which are closely packed comprising an apolar protein interior and polar surface to accommodate high stability. The structure is, as mentioned, a mixed tertiary structure ( $\alpha + \beta$ ) where the  $\beta$ -sheets are primarily anti parallel, and the family of HEWL is the C-type (chicken or conventional type) lysozyme. [13, 14]

Lysozymes isolated from different species differentiates in the primary amino acid sequence, however, they possess the same substrate specificity and their catalytic activity commonly relies on hydrolysis of  $\beta$ -glycosidic bonds between the C-1 and N-acetylmuramic acid and the C-4 on N-acetylglucosamine of bacterial peptidoglycan resulting in disturbance of structural integrity of the bacteria, thus resulting in bacteria lysing. Furthermore, Lysozymes enzymatic activity is lost if at least two of its four disulphide bonds are not intact. Its enzymatic activity is pointed toward gram-positive bacterium, as their cell envelopes consist of a thick outer cell wall comprised by peptidoglycan. Lysozymes activity against gram-negative bacterium is restricted as they have difficulties in penetrating the outer membrane of the gram-negative bacterium. [13]

Lys - Val - Phe - Gly - Arg - Cys - Glu - Cys - Ala - Ala - Ala - Met - Lys - Arg - His - Gly - Leu - Asp - Asn - Tyr - Arg - Gly - Tyr - Ser - Leu - Gly - Asn - Trp - Val - Cys - Ala - Ala - Lys - Phe - Glu - Ser - Asn - Phe - Asn - Thr - Gln - Ala - Thr - Asn - Arg - Asn - Thr - Asp - Gly - Ser - Thr - Asp - Tyr - Gly - Ile - Leu - Gln - Ile - Asn - Ser - Arg - Trp - Trp - Cys - Asn - Asp - Gly - Arg - Thr - Pro - Gly - Ser - Arg - Asn - Leu - Cys - Asn - Ile - Pro - Cys - Ser - Ala - Leu - Leu - Ser - Ser - Asp - Ile - Thr - Ala - Ser - Val - Asn - Cys - Ala - Lys - Lys - Ile - Val - Ser - Asp - Gly - Asn - Gly - Met - Asn - Ala - Trp - Val - Ala - Trp - Arg - Asn - Arg - Cys - Lys - Gly - Thr - Asp - Val - Gln - Ala - Trp - Ile - Arg - Gly - Cys - Arg - Leu

**Figure 3.9.** The primary amino acid sequence of HEWL, containing hydrophobic (green), polar (blue), alkaline (purple), and acidic (red) amino acids. Cysteine and Glycine are both hydrophobic and polar since Cysteine by itself is polar, but the pair of Cysteine forming a disulphide bond are apolar, and Glycine can exist in both hydrophobic and hydrophilic environments due to its small side chain. [6]

---

## 4. Protein Stability

---

When talking about protein stability, one often seeks to understand why and when the native form in a protein is favoured over the denatured form. To understand the mechanisms, thermodynamics plays a crucial role, and it will be examined in detail in the following chapter. First, however, the different forms of the protein will be outlined.

The native form of a protein refers to an optimal folded form, where the protein is functional and operative. The denatured form is thus the opposite; when the protein is unfolded and non-operational. These two forms are in equilibrium, when they are both equally thermodynamically favourable, as will be described later. This point is termed the transition point. The transition between a native protein and a denatured one is a first-order transition, meaning it is an all-or-none transition without intermediates, which can be described as



Initially it was assumed that the denatured protein is always a random coil. This was true for denatured proteins in concentrated solutions of denaturants such as urea or GuHCl. However, numerous structural studies report some intermediates between the random coil and the native protein, but only in some proteins, where others completely denature into the random coil. One especially interesting denatured protein form is one termed the *molten globule* (MG). [6, 15, 16]

The MG is often introduced in proteins as they are subjected to any moderate denaturing environment, and it will decay into an random coil in concentrated denaturant solutions. The MG is characterized by a swelling in the entire protein, but with the secondary structures resembling the native form. The tertiary structure of the MG deviates heavily from both the native and the denatured protein. The nature of the MG is not relevant for all proteins, as some smaller proteins may convert directly into random coils by either temperatures or denaturing agents. [6]

The MG form often occurs in smaller proteins after acidic or thermal denaturation (melting of the protein), while agents such as urea convert the protein directly into a random coil. The transition from a native protein to a MG is a first-order transition, meaning there are no intermediate between the states. The MG, however, can be seen as an intermediate between the native and denatured protein. [6]

The MG form have been reported in HEWL in different environments. Hameed *et al.* reported an induced MG form in HEWL at a pH value of 12.3 [17]. Furthermore, Ohkuri *et al.* recorded the MG form in HEWL after from thermal and chemical denaturation and refolding, where GuHCl was used as the denaturing agent [18].

In contrast to these studies, however, Chang *et al.* does not observe the MG state in HEWL at all, when using either GuHCl and thermal denaturation [19]. They are in agreement with studies done by Pardon *et al.*, and Sugai *et al.* [20, 21]. The equilibrium between the native, MG, and denatured form can be described as



## 4.1 Thermodynamic Considerations

In order to understand the stability of proteins, one must first study thermodynamics, since the stability of proteins can be defined using the Gibbs Free Energy  $G$ . The change in Gibbs Free Energy,  $\Delta G$ , is an important factor, when evaluating whether a chemical reaction will proceed spontaneously or not. Often, the change in Gibbs Free Energy is defined as

$$\Delta G = \Delta H - T \cdot \Delta S, \quad (4.3)$$

where  $T$  is the temperature at which the reaction occurs [22, 23]. This definition introduces a number of terms, which must be examined further.  $\Delta H$  denotes the change in enthalpy, or internal energy, during the chemical reaction. Under constant pressure, the change in enthalpy is measured as the release or absorbance of heat during the reaction. A slightly more important factor in Equation (4.3) is the change in entropy,  $\Delta S$ , which describes the change in disorder in the system. According to the second law of thermodynamics, the entropy of the entire universe will always rise towards a higher state of disorder. [22, 23] From Equation (4.3), with the aforementioned definitions in mind, one can deduce that a negative value of  $\Delta G$  results in a rise in entropy,  $T$  times larger than any rise in enthalpy, and thus the reaction is favourable to proceed, or in other words; the products of the reaction is favoured.

In an effort to relate this to the stability of proteins, the change in Gibbs Free Energy can also be described as the difference in free energy between the products and the reactants of a reaction,

$$\Delta G = G_D - G_N = \Delta G_{D-N}. \quad (4.4)$$

The indices, D and N, relates to a case relevant to this project; the denatured and native state of a protein. Equation (4.4) could refer to the transition between any two forms, however.

The unfolded protein is the product and the folded protein is the reactant, and thus, a negative value of  $\Delta G$  means that an unfolded protein is favoured. For this to be the case, the free energy of the folded protein must be higher than the free energy of the unfolded protein. If the inverse is true, meaning the unfolded protein has a higher free energy than the folded,  $\Delta G$  will have a positive value, and the folded protein will be favoured. [22, 23] In Figure 4.1, a reaction proceeding from a higher free energy form toward a lower free energy form can be seen. It is however evident, that an activation energy  $\Delta G^\ddagger$  is needed for the reaction to proceed.

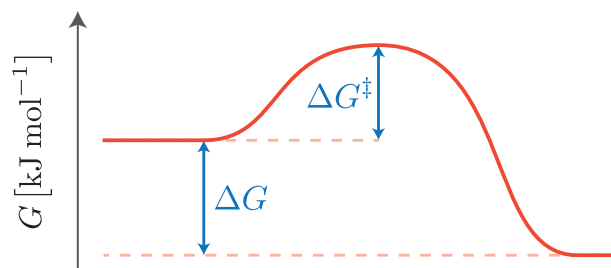


**Figure 4.1.** Energy diagram showing the Gibbs Free Energy during a chemical reaction. The constant  $\Delta G^\ddagger$  describes the activation energy of the reaction.

This activation energy leads into another important part of protein stability; kinetics. The kinetics of a reaction, in short, describes the reaction speed, and it depends strongly on  $\Delta G^\ddagger$ . Proteins fold into the native form rapidly, because of a low activation energy, where they become kinetically trapped, due to a large activation energy for the reaction into the unfolded form [2]. A reaction with a negative  $\Delta G$ , that has a high activation energy, will thus react over long periods of time, and thus both terms must be taken into account when describing the stability of a protein. [24]

As stated, the value of  $\Delta G$  determines the spontaneity of a reaction. If the value is negative, the products are favoured, and if the value is positive, the reactants are favoured. If the value, however, is zero, neither of the products and reactants are favoured, and the reaction enters an equilibrium at a transition point.

Proteins are in an equilibrium state between native and denatured, when they are numerous in a solution. The stability of a protein is heavily influenced by the environment in which the protein resides. Thus specific environments, and their impact on protein stability must be examined.

## 4.2 Environmental Impact

The previous thermodynamic considerations can be used to describe how stable a protein is in different environments. Relevant to this project are environments with different temperatures, dielectric constants, different amounts of UV radiation, and pH values.

### 4.2.1 Temperature

The change in Gibbs Free Energy can be plotted as a function of the temperature at which the reaction occurs. This plot can be seen in Figure 4.2.

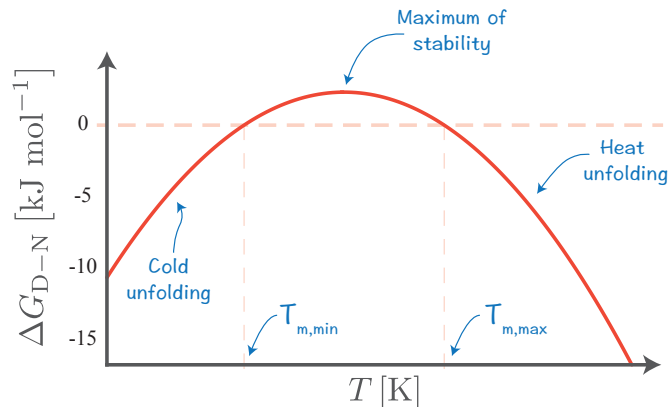


**Figure 4.2.** The relationship between the change in Gibbs Free Energy and the temperature of a solution in which a protein is residing. As the temperature deviates from a value of maximum stability of the protein it can either unfold due to cold or heat. The temperatures at the two transition points are labelled  $T_{m,max}$  and  $T_{m,min}$ . Adapted from [25].

Figure 4.2 visualizes that there is a certain temperature, at which the protein is at its most stable form. But then, as the temperature increases or decreases, the value of  $\Delta G$  changes to favour the unfolded protein, and it therefore becomes more unstable.

When  $T = T_m$  then  $\Delta G = 0$ , and there is an equilibrium. The Gibbs Free Energy can be

expressed as:

$$\Delta G = -R \cdot T \cdot \ln(K), \quad (4.5)$$

where  $R$  is the gas constant, and  $K$  is the equilibrium constant. Equation (4.5) can be developed to ultimately describe the signal of either CD or fluorescence:

$$y = \frac{A + B \cdot T + (C + D \cdot T) e^{-\Delta G/(R \cdot T)}}{1 + e^{-\Delta G/(R \cdot T)}}. \quad (4.6)$$

The constants,  $A$ ,  $B$ ,  $C$ , and  $D$  comes from the fact that before and after denaturation, it is assumed that the experimental data will behave linearly, which is a good approximation and makes physical sense. The denaturation is assumed to be a first order reaction, and so until denaturation, no major event will take place.  $A$  and  $C$  are the intersections with the second axis, before and after denaturation respectively, and  $B$  and  $D$  are the slopes of the linear dependences before and after denaturation respectively. It is also assumed, that during denaturation, the data will fit an exponential curve. The Gibbs Free Energy in Equation (4.6) is given by

$$\Delta G = \Delta H \left(1 - \frac{T}{T_m}\right) - \Delta C_p \left[ (T_m - T) + T \ln \left(\frac{T}{T_m}\right) \right], \quad (4.7)$$

where  $C_p$  is the specific heat capacity of the protein. Equation (4.6) can be used to fit a curve to experimental data showing a protein being denatured by thermal denaturation, and this gives information about the change in heat capacity and enthalpy. These parameters are useful for describing the denaturation event. [20, 26]

When the function described in Equation (4.6) has been fitted to the experimental data, it is possible to calculate the fractions of folded and unfolded protein during the denaturation event. Using the fitted linear relations before,  $y_N$ , and after  $y_D$  denaturation, the fraction of denatured protein can be determined using:

$$f_D = \frac{y_N - y}{y_N - y_D} = \frac{A + B \cdot T - y}{(A + B \cdot T) - (C + D \cdot T)}, \quad (4.8)$$

where  $y$  is the fluorescence or CD signal. [27]

Calorimetric studies performed on HEWL by Arai *et al.* showed a transition temperature,  $T_m$ , on thermograms at 73 °C in pH 2.8, 77 °C in pH 4.8, and at 73 °C in pH 7.2 [28]. Blumlein *et al.* showed a  $T_m$  for HEWL at approximately 73 °C in pH 5 [29].

### 4.2.2 pH

The pH value of the solvent in which the proteins are dissolved, have been shown to drastically alter their stability. An example is showed by Arai *et al.*, as written earlier, where the thermal stability of HEWL varied with changing pH value. The effect, the pH value has on the stability of the protein is a testament to the importance of the ionizable groups of the protein. The pH value of the solvent induces a change in the overall charge of the protein, as the titration groups or sites of the protein are ionized, which ultimately affects the electrostatic interactions comprising protein stability. Each titration site is either a polar, alkaline, or acidic residue side chain, which in the case of HEWL amounts to 32 titratable sites when assuming only two possible protonation states for each titration site. HEWL contains 11 Arginines, 7 Aspartic acids, 2 Glutamic acids, 1 Histidine, 6 Lysines, 3 Tyrosines, and an N- and C-terminus. See Figure 4.3 for pH dependence of

protonation of the 32 sites. The titration curve of an unfolded protein is approximately equal to the sum of the titration curves of the titratable sites. [30]

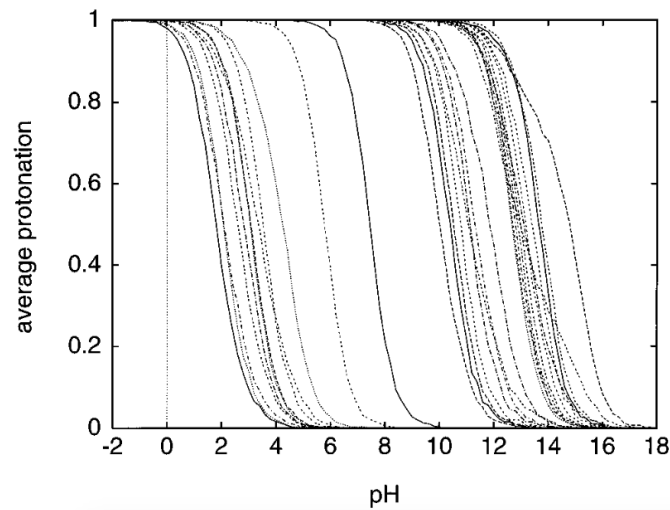


**Figure 4.3.** The pH dependence of protonation of 32 titratable sites in HEWL. The curves are theoretical and calculated by Monte Carlo titration program by Schaefer *et al.* estimating an dielectric constant equal to 20 for the protein interior. [30]

The charge of the protein is, however, not distributed evenly around the protein, as the Linderstrom-Lang model approximates [31]. This model proposes that the pH corresponding to the isoelectric point (pI) is where the protein is most stable, which, for HEWL, is at pH 11 [17]. The net charge of the protein is zero at this pH, but it is seen, that the pI not always corresponds to the pH of maximum stability. The most stable pH value for HEWL is around pH 5 [32, 33, 34].

The stability of proteins as a function of the pH value of the solvent is still subject to investigation and research. Evidence mounts towards the fact, that it is not only the charged residues on the surface of the protein which must be taken into account. The charge of the side chains remains as the protein denatures, and as such they will affect the conformation, and thereby the Gibbs Free Energy of the denatured state. This will have an impact on the stability of the protein, and it is a point, which has been missed in many earlier reports. [35]

HEWL is one of the most heat-stable enzymes, and can remain native during boiling for 1 - 2 minutes at pH 4. HEWL is stable in most acidic solutions, but is limited in stability in alkaline environments. Furthermore, HEWL is denaturated by high temperatures at pH higher than 7 due to reduced stability, which is thought to be a result of reduction of at least one disulphide bond. It has been observed that between 85 °C and 95 °C, HEWL is most stable at pH 5.5. HEWL is usually not affected by temperatures up to 55 °C, and a decomposition of all most every amino acid is observed at higher temperatures (250 °C). [12]

Furthermore, most stability predictions of HEWL concerning pH of the solvent only range from pH 1 - 7, as it is difficult to determine any stability relation between native and unfolded HEWL above pH 7 since HEWL tends to aggregate in alkaline conditions. [30]

### 4.2.3 Denaturants

Some molecules lead to the denaturing of proteins if dissolved in the same solution. These molecules are termed chaotropic agents, and examples of such agents are urea and guanidine hydrochloride (GuHCl). The mechanics of these chaotropic agents are still investigated, but one model postulates, that they disturb the hydrogen bonding network of the solvent, which weakens the hydrophobic effect of the protein, thus destabilizing it [36, 37, 38]. Another model states that the chaotropic agent is able to migrate inside the native protein and form hydrogen bonds to atoms in the backbone [39]. Often, it is a good estimation, to assume that there is a linear relation between the change in Gibbs Free Energy and the concentration of an added denaturant  $[D]$  [25], see Figure 4.4.

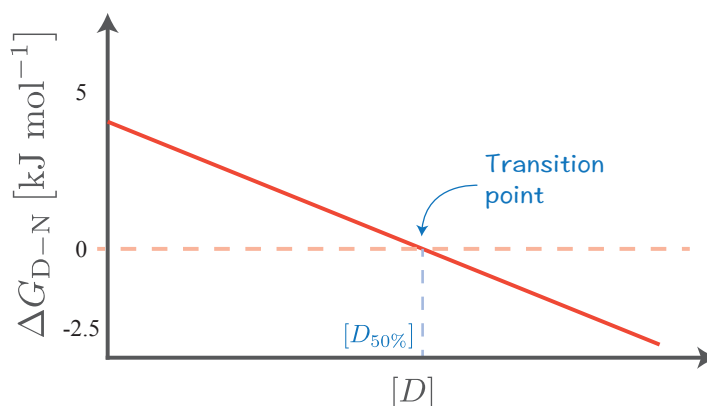


**Figure 4.4.** The relation between the change in Gibbs Free Energy and concentration of the denaturant added. Adapted from [25].

$[D_{50\%}]$  refers to a transition point, where the concentration of denaturant induces an equilibrium between the native and denatured proteins. This dependence is often written as

$$\Delta G_{D-N}([D]) = \Delta G_{\text{solvent}} - m \cdot [D], \quad (4.9)$$

where  $m$  is the slope of the relation, and  $\Delta G_{\text{solvent}}$  is the change in Gibbs Free Energy when no denaturant is added. When the specific concentration  $[D_{50\%}]$  of denaturant is added,  $\Delta G_{D-N}([D_{50\%}]) = 0$ , which gives:

$$\Delta G_{\text{solvent}} = m \cdot [D_{50\%}]. \quad (4.10)$$

A study done by Ahmad *et al.* establishes the  $m$  value of the denaturation of HEWL with GuHCl to be  $1.88 \text{ kcal} \cdot \text{mol}^{-1} \cdot \text{M}^{-1}$  at pH 7 [40].

In HEWL, a study done by Emadi *et al.*, showed a decrease in protein structure when GuHCl was added in a concentration of 0.5 M. Between 4.0 and 5.0 M the protein was partially denatured, and had no longer any helical structure [41].

### 4.2.4 Guanidine Hydrochloride

This project will utilize GuHCl as a denaturant, since it is one of the strongest denaturants used in physiochemical studies [42], and it is suggested that GuHCl is 1.5 - 2 times more effective than urea [43]. Furthermore, GuHCl is preferred since it is suspected that urea solutions may contain and spontaneously produce cyanate, which can carbamylate amino

groups of proteins [44].

The effect of different salt species on protein stability has been investigated by Frans Hofmeister resulting in the Hofmeister series, see Figure 4.5 for a partial series. The Hofmeister series classifies the effectiveness of different cations and anions on protein stability, primarily relying on salting in (right) and salting out (left) effects [45]. These ion specific effects is suggested to rely on the field strength of the ion (i.e. ion size, charge density, and polarizability) [46].

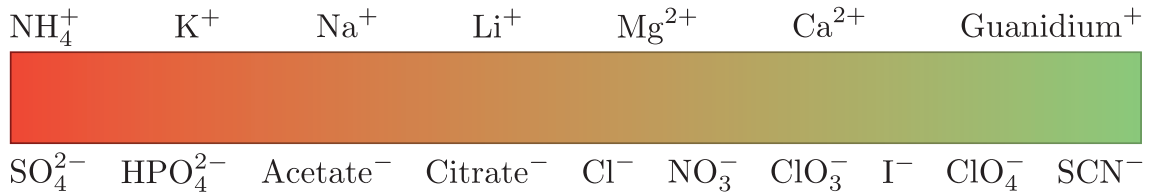


**Figure 4.5.** The Hofmeister series, describing the effect of cations and anions on protein stability. Moving from left to the right, the cations and anions shift from salting out toward salting in effects.

When salting out ions are added to an aqueous protein solution, they will precipitate the native protein, increase surface tension of water, and thus decrease the solubility of apolar molecules in the solution. This all favours aggregation and precipitation over dissolution, since the hydrophobic core of the proteins will have a decreased susceptibility to move out into the aqueous solution, the solubility of the protein is decreased, and the protein-protein interactions will be strengthened. [45, 46]

In contrast, when adding salting in ions to an aqueous protein solution, the surface tension is less affected, increasing the solubility of the apolar molecules. These conditions destabilize the native protein due to the increased propensity of buried hydrophobic residues to move out into the aqueous solution. [45, 46]

Furthermore, addition of ions (ionic entities with high dipole moments) will increase the dielectric constant of the solution as the polarity of the solvent is increased.

From the Hofmeister series, it is observed that the guanidium ion is classified as a salting in ion, and hence destabilizes the native protein in aqueous solutions [45]. In order to destabilize a native protein by the guanidium ion, one can dissolve GuHCl in an aqueous solution, resulting in the guanidium cation and an chloride anion. See Figure 4.6 for the chemical representation of GuHCl.

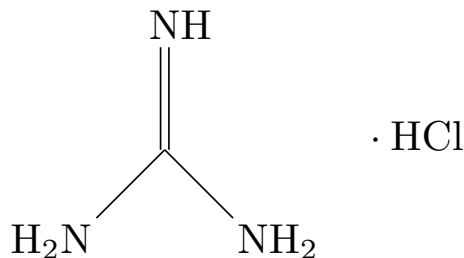


**Figure 4.6.** Chemical representation of GuHCl ( $\text{CH}_6\text{ClN}_3$ ).

According to Mayr *et al.*, low concentrations of GuHCl (0 - 0.3 M) acts in an unusual manner as a structure stabilizing agent, whereas the overall view showed that in concentrations from 0 - 6 M GuHCl acts as a classical denaturant, destabilizing proteins [47].

In order for GuHCl to denature proteins, it is suggested that it disrupts the hydrophobic effect and the hydrogen bonds between water and the protein. Manson *et al.* suggest that GuHCl dissolves into its polar ions in a solution, and that the guanidium cation will tend to form approximately 4.5 hydrogen bonds with surrounding water on average, and by principle can contain up to 6 hydrogen bonds, thus disrupting the hydrogen bond network of the solution. Furthermore, it is suggested that the denaturing effect of GuHCl, along with the relatively strong hydrogen bonding to water and chloride counter ions, relies on the tendency of the guanidium cation to self-associate in a stacking fashion. The faces of the guanidium cation tend to interact with hydrophobic surfaces where the equator tends to interact with water molecules. The hydrophobic property of the guanidium ion forces the ions to stack by hydrophobic interactions. The stacking can include hydrophobic aromatic amino acid side chains. The resulting environment increases the solubility of hydrophobic groups, and thus shifts the native-denatured equilibrium toward the denatured form. This effect is, however, weak and requires high concentrations of GuHCl. Manson *et al.* have tested 3 M solutions. Furthermore, the hydrophobic interactions are likely to be accompanied by favourable hydrogen-bonding interactions with the weakly hydrated backbone amide groups that are exposed during protein unfolding. Moreover, chloride as a counter ion for the guanidium cation, results in a greater level of stacking, and hence GuHCl is a powerful denaturant. [48]

#### 4.2.5 Ultraviolet Light

This project primarily utilizes measurement methods relying heavily on UV light, and therefore the study of how UV light affects proteins is of great importance. According to Davidson *et al.*, HEWL can be inactivated by UV radiation, which follows first-order kinetics [12].

Xie *et al.* showed that if HEWL was exposed to 200  $\mu\text{W}/\text{cm}^2$  UV light around 280 nm, the proteins would form aggregates visible with atomic force microscopy after 10 minutes of exposure. After 6 hours of exposure, the aggregates would be visible to the naked eye in the form of a milky white colouration of the solution. Besides aggregation, structural changes takes place as well. Xie *et al.* define the structure as partially unfolded, because the protein partially retain a native secondary structure and radically loose tertiary structure. Xie *et al.* argues that the native disulphide bonds are reduced by inner excitations of Tryptophan, diminishing the stability of the tertiary structure. Another interesting aspect of the study done by Xie *et al.* is the effect of pH values on the aggregation of HEWL. In solutions with pH values of 3 - 5 the diameter of the aggregate is about 0 nm at both half an hour and at one hour. But when the pH value of the solution is 9, the size of the aggregate is 375 nm at half an hour and 875 nm at one hour. [49]

Another study done by Wu *et al.* showed that prolonged exposure to UV light was followed by conformational changes within the protein, mainly the breakage of disulphide bonds, which are critical to the integrity of the protein structure [50]. They found that the main site for the interaction with UV light in HEWL is the six Tryptophans, as is to be expected. In Figure 4.7, the wavelength and intensity of the maximum emission intensity of HEWL can be seen as time of exposure to UV light increases.

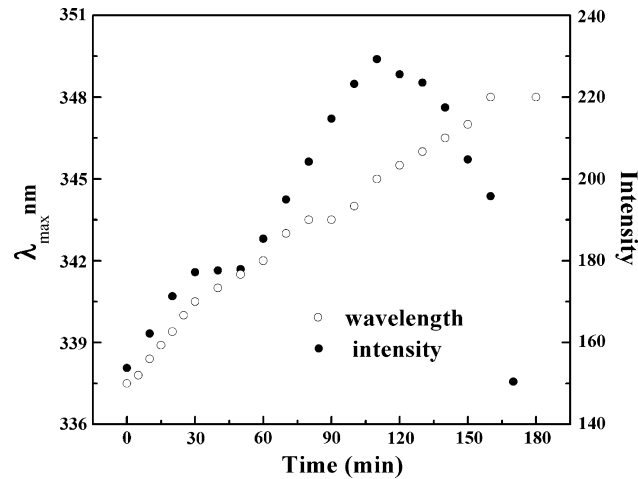


**Figure 4.7.** A study by Wu *et al.* shows how the wavelength and intensity of the maximum emission intensity spectrum of HEWL changes as the protein is exposed to UV light over time [50].

The graph made by Wu *et al.* shows that the intensity of the maximum emission intensity increases until 30 minutes has passed, and then begins to increase again after 60 minutes of exposure. The intensity then dramatically increases until it reaches its maximum at approximately 110 minutes, and then it decreases until the end of the experiment. The wavelength steadily increases throughout the entire experiment. The decrease in intensity at the end is argued to be because of photobleaching of Tryptophan. Photobleaching is a process, where a fluorophore undergoes chemical or conformational changes due to it entering an excited state. Photobleaching can, however, be minimized by using a small intensity in measurements using UV light, or by a gentle stirring of the sample during measurements. [50, 51]



---

## 5. Circular Dichroism Spectroscopy

---

Circular dichroism (CD) spectroscopy is a measurement method, which is often used when looking at macromolecules. The method allows one to study the conformation and structure of especially proteins.

Before the principles behind CD spectroscopy is explained, the polarization of light must first be discussed.

### 5.1 Polarization of Light

The polarization of a light wave describes the direction with which the electric field of a electromagnetic wave oscillates. In linearly polarized light, the oscillations are confined to a single plane, and any other polarization can be described as a sum of two linearly polarized states perpendicular to each other. It can also be described as the superposition of two circularly polarized light waves (CPL) with equal amplitudes. In a CPL, the components of the electric field are out of phase by  $\pi/2$ , and so the total electric field changes direction with time. The CPL can be either right-handed ( $\mathcal{R}$ -state) or left-handed ( $\mathcal{L}$ -state). [52] Linearly polarized light can be converted to CPL by using a quarter-wave plate, as seen on Figure 5.1.

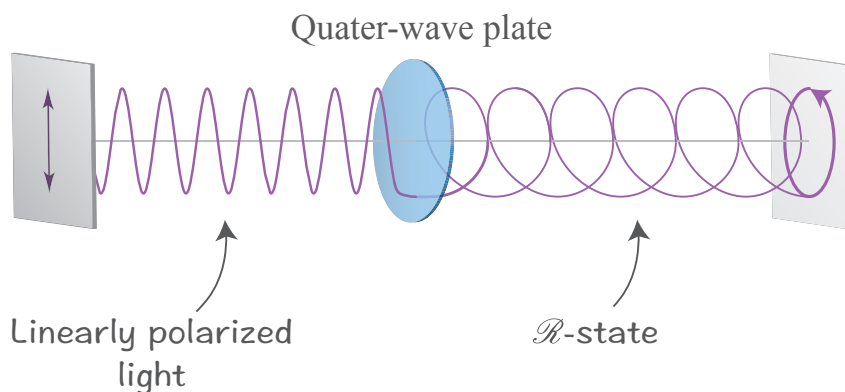


**Figure 5.1.** An illustration of how the quarter wave plate converts linearly polarized light into either  $\mathcal{R}$ - or  $\mathcal{L}$ -CPL. On the figure, the light is converted to  $\mathcal{R}$ -CPL.

The quarter-wave plate works by introducing a relative phase shift of  $\pi/2$  between the components in the light wave. This converts a linearly polarized wave to a CPL, if the quarter-wave plate is tilted by  $45^\circ$  in relation to the plane of polarization of the incident light wave. [52]

### 5.2 Principles of Circular Dichroism Spectroscopy

The generally used apparatus is a CD spectrophotometer, and the principles behind the machinery can be seen in Figure 5.2.

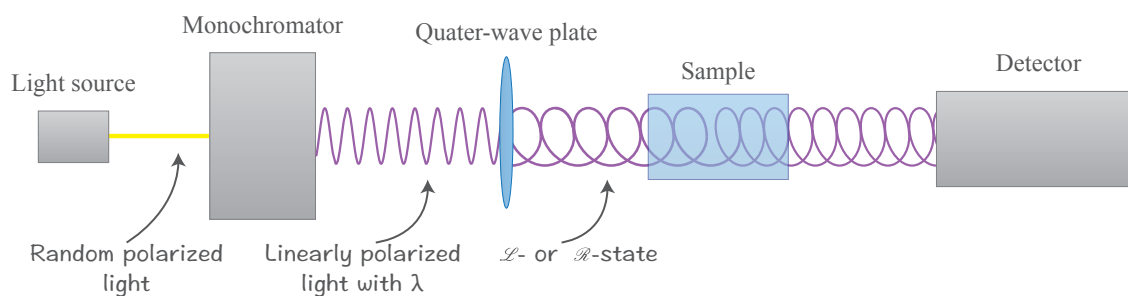


**Figure 5.2.** The lineup of the CD spectrophotometer. A lamp emits randomly polarized light through a monochromator, which linearly polarizes the light. The light travels through the quarter wave-plate, which circularly polarizes the light, and lastly through the sample onto the detector.

The CD spectrophotometer works by a lightsource sending random polarized light through a monochromator, which converts the light to monochromatic, linearly polarized light with a specific wavelength, which typically lies in the UV region. The linearly polarized light then travels through a quarter-wave plate, which is tilted  $45^\circ$  in relation to the plane of polarization of the incident light wave. The quarter-wave plate converts the light into CPL, alternately  $\mathcal{R}$ - and  $\mathcal{L}$ -state, which then travels through the sample before reaching a detector. [25, 53]

If the sample is optically active (chiral), it will absorb different amounts of either  $\mathcal{R}$ - or  $\mathcal{L}$ -CPL, and the difference in absorption is termed the CD. The fact, that the sample absorbs differing amounts of the two states of light, results in the polarity of the light will become elliptical.

The CD can be described with Equation (5.1) [25]:

$$\Delta A = A_L - A_R. \quad (5.1)$$

This difference is also given by the Beer-Lambert law:

$$\Delta A = (\varepsilon_L - \varepsilon_R) \cdot c \cdot d = \Delta\varepsilon \cdot c \cdot d.$$

Here,  $c$  is the molar concentration of the sample,  $d$  is the optical path length of the sample, and  $\Delta\varepsilon$  is the molar extinction coefficient, or molar absorptivity [25, 53]. The difference in the molar extinction coefficients,  $\Delta\varepsilon$ , is often termed the molar circular dichroism or molar ellipticity, and it is often shown in plots and figures. Sometimes, CD spectra is shown as the angle of the elliptically polarized light,  $\theta$ , measured in mdeg. For proteins, the standardized unit, however, is the mean residue molar ellipticity,  $[\theta]$ , of the light, which is measured in  $\text{deg cm}^2 \text{ dmol}^{-1}$ . The mean residue molar ellipticity is calculated using Equation (5.2).

$$[\theta] = \frac{\theta \cdot 100 \cdot M}{c \cdot d \cdot n}, \quad (5.2)$$

where  $n$  is the number of amino acids in the protein,  $\theta$  is the ellipticity of the elliptically polarized light reaching the detector, and  $M$  is the molecular mass of the protein [53]. Conversion between mean residue molar ellipticity and the molar extinction coefficient is easy, since the two quantities is related as  $[\theta] = \Delta\varepsilon \cdot 3298$ . A third unit, which is sometimes depicted in graphs is the mean residual ellipticity,  $\Delta\varepsilon_R$ . It is simply defined as  $\Delta\varepsilon/n$ . [25, 53]

As stated, CD measurements provides information regarding the secondary structure of

the protein, and it is possible to calculate the percentage of a secondary structure of the total protein. What structure is being calculated depends on what wavelength is being used in the calculations, and the calculations themselves. It is generally accepted, that the ellipticity at 222 nm is proportional to the helical content of the protein even though some question this assumption [54]. As such, it is the wavelength which will be used, when calculating the percentage of  $\alpha$ -helices in the protein. [17, 53, 55]

Chen *et al.* [56] presents a method for calculating the helical content of a protein, where

$$\% \alpha\text{-helix} = \left( \frac{[\theta]_{222} - 340}{30300} \right) \cdot 100\%. \quad (5.3)$$

An optically active protein sample will absorb either the  $\mathcal{R}$ - or  $\mathcal{L}$ -CPL as described by Beer-Lambert's law, because the protein consists of chiral molecules, which exhibit circular birefringence. In other words, the chiral molecules present an anisotropic solution, through which  $\mathcal{R}$ - or  $\mathcal{L}$ -CPL will propagate with different speeds. This is a result of the fact that the peptide bond in the amino acids, making up the protein, is without a plane of symmetry [53]. Chromophores such as the amide group of the protein backbone and the aromatic amino acids are the ones mainly responsible for the CD spectra. It is the far-UV (190 - 250 nm), which interacts with the peptide bond, corresponding to the  $n \rightarrow \pi^*$  transition, and the near-UV (260 - 330 nm), which interacts with the aromatic amino acids, corresponding to the  $\pi \rightarrow \pi^*$  transition [10]. Thus, the far-UV spectrum reveals information about the secondary structures of the protein. In Figure 5.3, an example of the CD spectrum showing the secondary structures of a protein can be seen. [6, 53, 55]

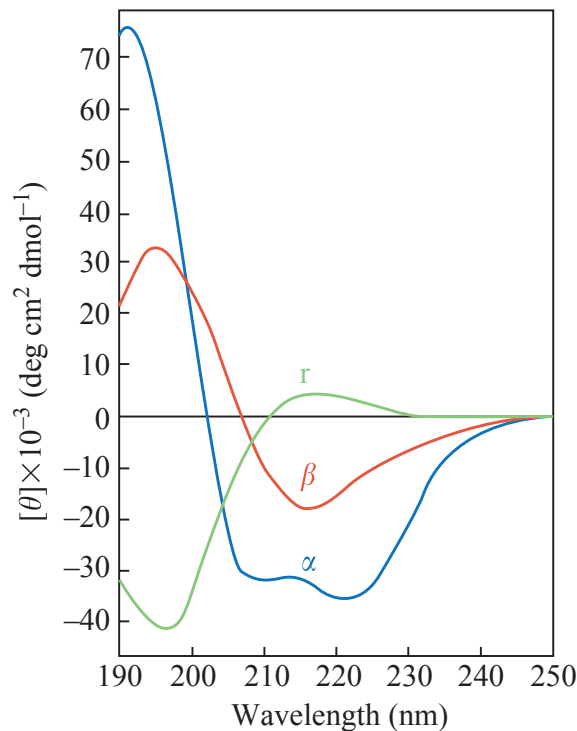


**Figure 5.3.** Far-UV CD spectra for different types of protein structures.  $\alpha$ -helix is denoted blue,  $\beta$ -structures red, and random coil is denoted green. [6]

## 5.3 Applications of Circular Dichroism Spectroscopy

CD spectroscopy is a widely used and useful way to gain information about the stability, conformation, and the folding and unfolding of proteins. It is possible to observe a protein unfold due to certain environmental factors where the unfolded state is thermodynamically and kinetically favoured.

Some studies prefer to display the entire CD spectrum, though this includes more often than not only the far-UV spectrum, since it gives information about the secondary structure of the protein. Examples of full far-UV CD spectra can be seen in Figures 5.4 and 5.5.

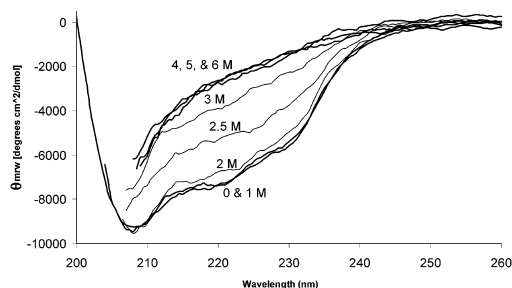


**Figure 5.4.** Mean residue ellipticity in the far-UV region of HEWL, which changes at different concentrations of denaturant [57].

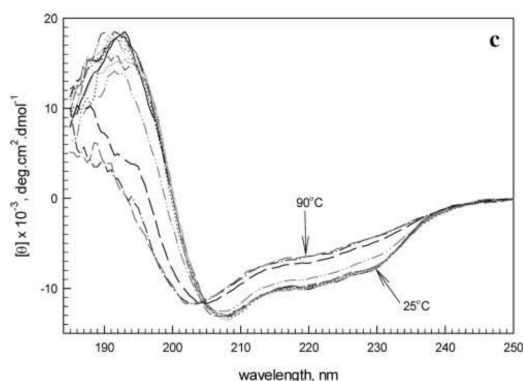


**Figure 5.5.** Mean residue ellipticity in the far-UV region of HEWL, which changes at different temperatures [58].

Figure 5.4 shows how the mean residue ellipticity in the far-UV region of HEWL changes at different concentrations of denaturant. The form of the curve is specific for every protein since it is a linear combination of CD signals from random coils,  $\beta$ -structures, and  $\alpha$ -helices, illustrating the specific composition of those structures in the protein. As the concentration of denaturant increases, the ellipticity approaches zero, which means that the difference in absorption of the two states of CPL decreases as the protein loses structure and thereby chirality. Vernaglia *et al.* states that HEWL is fully denatured at concentrations of 4 and 5 M GuHCl, but still has some structure, and is therefore only partially unfolded [57].

In Figure 5.5, a similar effect is seen, only increasing temperature is used as a denaturing method. As the temperature increases, the protein begins to denature, which is indicated by the loss of chirality, as the mean residue ellipticity approaches zero [58].

Often, denaturation of proteins is visualized using the ellipticity at 222 nm. The helical content is often measured instead of the  $\beta$ -structures because the CD spectrum of  $\beta$ -structures is more susceptible to noise, distortion, and influence of the aromatic side chains of the protein. As Figures 5.6 and 5.7 shows, the ellipticity around 222 nm makes it possible to deduce when a protein unfolds.

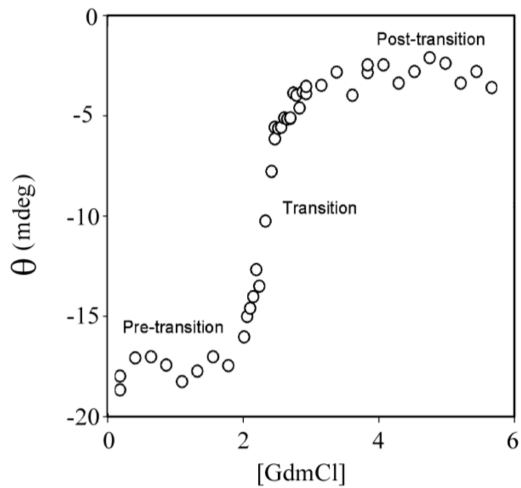


**Figure 5.6.** Far-UV ellipticity at 220 nm of human frataxin at different concentrations of GdmCl (GuHCl) at pH 7. At the transition point, there exist equilibrium between denatured and native proteins. At the pre-transition and post-transition point most of the proteins are native and denatured, respectively. [55]

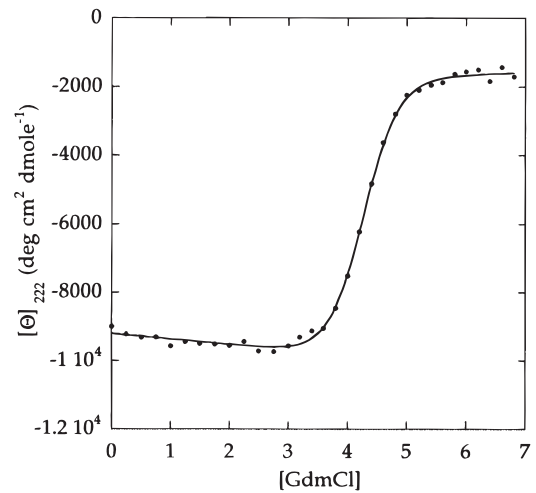


**Figure 5.7.** Far-UV mean residue ellipticity at 222 nm of HEWL at different concentrations of GdmCl (GuHCl) at pH 4. [59]

From Figures 5.6 and 5.7, it can be seen how, the ellipticity is more or less stable until a certain concentration of denaturant, after which the protein denatures, and stays in that conformation irregardless of the further increase in denaturant concentration. The point of transition, where the slope is the steepest, is where there would be a peak in the derivative of the curve. The concentration of denaturant corresponding to the maximum of the peak in the derivative is labelled  $[D_{50\%}]$ .



---

## 6. Steady-State Fluorescence Spectroscopy

---

In the examination of HEWL, steady-state fluorescence spectroscopy is needed in addition to CD spectroscopy.

### 6.1 Principles of Steady-State Fluorescence Spectroscopy

Where CD spectroscopy relies solely on the absorption of light by chromophores in the protein, fluorescence spectroscopy relies on the process of absorption and a following emission of light from certain residues within the protein. The steady-state technique relies on a continuous illumination (i.e. when the incident light intensity is constant) [51]. The set up of fluorescence spectroscopy used in this project can be seen in Figure 6.1.

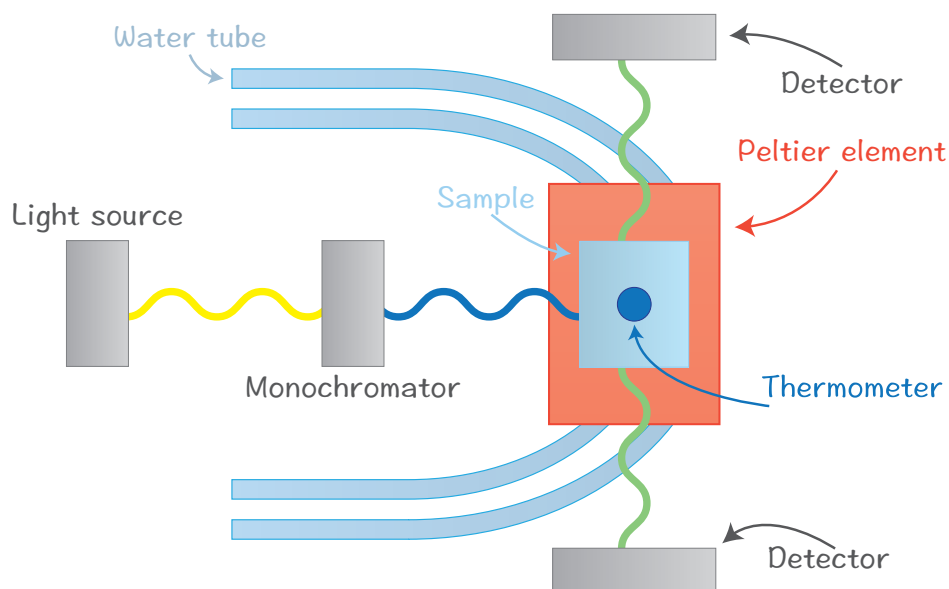


**Figure 6.1.** An illustration showing the fluorescence spectroscopy setup used in this project. The light, emitted by the light source, travels through a monochromator and reaches the sample. The fluorescence of the sample is then collected by two detectors. The peltier element works as a heating element, and the water tubes will provide a temperature baseline for the peltier element, as the air in the chamber will increase in temperature.

The light, which is emitted by the light source, travels through a monochromator. It reaches the sample, and the fluorescence of the sample is detected by the two detectors. For measurements including a change in temperature, the peltier element works as a heating element, while the water tubes provide a baseline in temperature for the peltier element. The temperature of the air in the chamber will increase, since the chamber is black and thus will absorb UV light, and a constant water flow through the tubes will therefore provide a constant temperature baseline.

When performing fluorescence spectroscopy on a protein, it is the fluorescence of the three fluorescent amino acids, which are being measured. The specific amino acids are the ones

containing aromatic side chains (Tryptophan, Phenylalanine, and Tyrosine). Of these three amino acids, Tryptophan is the far most prevailing fluorophore primarily due to its high quantum yield [60], thus this project will only concern Tryptophan. The quantum yield of a fluorophore is defined as the ratio between absorbed and emitted photons. The quantum yield of Tryptophan is typically 0.13 [61], but varies with the surrounding environment. In HEWL, Imoto *et al.* showed that out of the six Tryptophans, Trp62 and Trp108 are mainly responsible for the emission spectrum [62]. The wavelength used to excite Tryptophan is often 295 nm. This is due to the fact, that the absorption spectrum of Tyrosine and Tryptophan overlap, but at 295 nm none of the Tyrosines are being excited along with most of the Tryptophans. [62, 63, 64]

The process of absorption and emission can be visualized using a Jablonski Diagram [61] as seen in Figure 6.2.

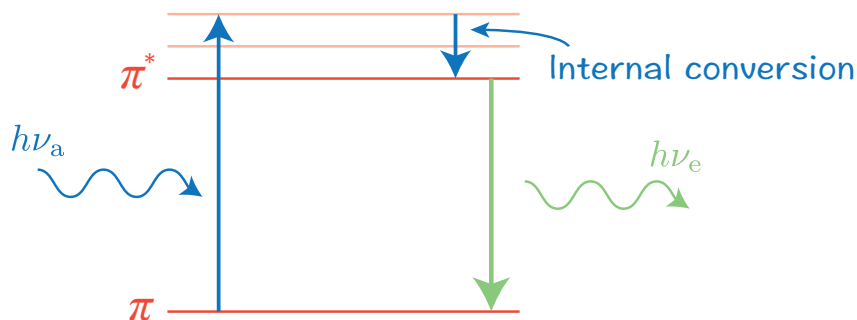


**Figure 6.2.** An illustration showing the process of fluorescence. Light with the energy  $h\nu_a$  is absorbed by an electron in a ground state ( $\pi$ ), which is then excited to a higher vibrational energy in a higher energy level ( $\pi^*$ ). The electron then relaxes to the bottom of the energy level by an internal energy conversion, which does not emit radiation. Lastly, the electron retreats into the ground state by emission of a photon with energy  $h\nu_e$ . Adapted from [61].

The Jablonski diagram shows how a photon with frequency  $\nu_a$  and energy  $h\nu_a$  is absorbed by an electron in a ground state ( $\pi$ ) which is then excited to a higher energy level ( $\pi^*$ ). In the case of the indol ring in Tryptophan, an electron experiences a  $\pi \rightarrow \pi^*$  transition. The electron then relaxes by an internal conversion of energy to a lower vibrational energy level, and lastly the electron relaxes to the ground state by emission of a photon with energy  $h\nu_e$ . The emitted photon typically has a smaller energy and thereby longer wavelength compared to the absorbed photon. This red shift is termed the Stokes Shift. [61]

The process described above is susceptible to several interactions with the environment of the fluorophore. One example of interactions between the fluorophore and its immediate environment is quenching.

Quenching is a phenomenon which occurs when quenchers decrease the intensity of the emitted light from the fluorophore [61]. Water is known to act as a quencher of Tryptophan. Tryptophan can however also be quenched by other residues in the protein when in its native state. Denton *et al.* found the quantum yield of Tryptophan to be only approximately 30 % of the value for a free Tryptophan [63]. In fact, almost every polar residue is able to act as quencher, and disulfide bonds is the strongest quencher of Tryptophan [65, 66]. Chen *et al.* has showed that the peptide bond in residues also has a quenching effect on Tryptophan [67]. If a protein denatures, it would be water acting as the main quencher of Tryptophan and not the rest of the protein. Since water should act

as a weaker quencher, it has been postulated by Khalifeh *et al.*, that as HEWL unfolds, the emission intensity of Tryptophan increases [68]. This discussion can be complicated further by the fact that the pH is shown to affect the emission intensity of Tryptophan by Ansari *et al.* [69]. This could be due to a change in the charge of some of the polar amino acids, which then affects the quenching of Tryptophan. A study done by Yamamoto *et al.* shows that the emission intensity of free Tryptophan decreases as the temperature of the solvent increases. They conclude that this is due to thermal quenching, which is the effect of an increase in the quenching effects of the solvent as it is heated. [70]

Another interaction between the fluorophore and its environment manifests itself as a red shift in the emitted light. It has been shown, that a red shift in emission occurs when proteins containing Tryptophan unfolds and thereby exposing the residues to the solvent [61]. This can be seen in Figure 6.3.

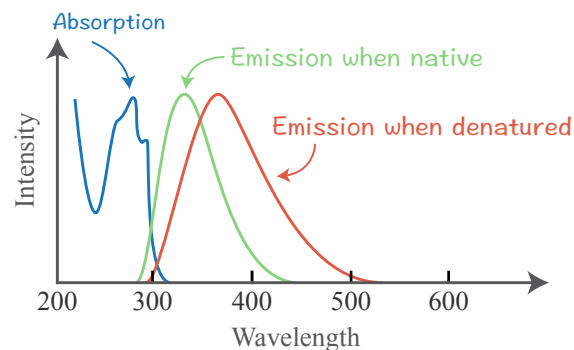


**Figure 6.3.** The absorption (blue) and emission spectra of a protein containing Tryptophan when native (green) and denatured (red). The red shift, when the protein containing Tryptophan denatures is clear. Adapted from [61].

The red shift in emission can be attributed to hydrogen bonding with the solvent by the imide group in Tryptophan. The hydrogen bonding of the imide group changes the electron structure of the aromatic side chain, resulting in the red shift. The red shift can also be viewed as a result of the phenomenon termed solvent relaxation. Solvent relaxation occurs in polar solvents with dipole moments which affects the dipole moment of the excited Tryptophan. The dipoles in the solvent can reorient around the dipole of the excited residue, lowering the energy of the excited state. A more polar solvent results in a larger decrease in energy of the excited state, and so the dielectric constant of the solvent becomes an important factor in solvent relaxation. The relaxation occurs on a much smaller time scale (10 - 100 ps) than the fluorescent emission (1 - 10 ns). [61]

When the protein is in its native form, Tryptophan will absorb light with wavelengths from approximately 250 - 295 nm, and it will emit a broad peak with a maximum somewhere around 340 nm. The emission spectrum is, extremely sensitive to the local environment and solvent [61].

## 6.2 Applications of Steady-State Fluorescence Spectroscopy

Steady-state fluorescence spectroscopy is an important tool when investigating proteins, and both the stability and folding and unfolding kinetics can be explored. The effects of solvent relaxation and hydrogen bonding of Tryptophan with water are showed by Laurents

*et al.*, as can be seen in Figure 6.5 [59]. In a study done by Khalifeh *et al.*, it is clear how the fluorescence spectrum is red shifted and increases in intensity as the protein unfolds, see Figure 6.4 [68].

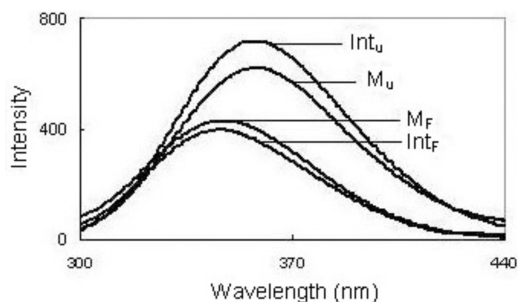


**Figure 6.4.** Fluorescence spectra of HEWL at both a folded (F) state and at an unfolded (U) state. The experiment was done with an intact (Int) sample of HEWL, and with a modified (M) sample of HEWL, and the proteins were denatured using GuHCl. It is clear, how the spectrum increases in intensity, and is red shifted as the protein denatures. [68]

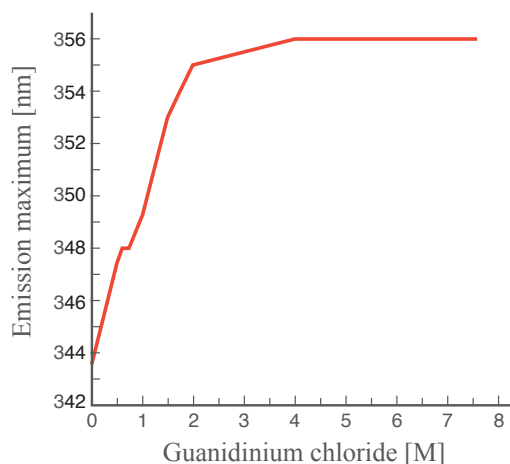


**Figure 6.5.** A graph showing the maximum wavelength of the emission spectrum of HEWL as a function of the concentration of added GuHCl. The maximum wavelength is clearly red shifted, as the protein presumably denatures. [59]

From Figure 6.5, it is evident that as the protein denatures due to a large concentration of a denaturing agent, the more red shifted the emission of Tryptophan becomes due to the solvent relaxation.

---

# 7. Materials and Methods

---

This chapter presents the preparation of buffer- and denaturant solutions used for steady-state fluorescence and CD spectroscopy as to determine the thermal and chemical denaturation by GuHCl of HEWL at different pH values. Furthermore it presents the method applied in usage of steady-state fluorescence and CD spectroscopy. Both in fluorescence and CD spectroscopy, baselines containing only buffer were applied.

## 7.1 Stock Buffer Solutions

### Materials

- 1000 mL Bluecap containers for stock buffer solutions
- 1000 mL volumetric flask
- 250 mL Bluecap container for stock acid and alkaline solutions
- 100 mL volumetric flask
- Plastic pasteur pipettes
- Calibrated MeterLab<sup>TM</sup> PHM210 Standard pH meter
- JP Selecta Autoclave

### Chemicals

- 1.0 mM Sodium acetate anhydrous stock buffer solution (Sigma Aldrich)
- 1.0 mM Sodium citrate dihydrate ( $\geq 99.5\%$ ) stock buffer solution (Sigma Aldrich)
- 1.0 mM Sodium carbonate anhydrous ( $\geq 98.0\%$ ) stock buffer solution (Fluka Chemika)
- 3.0 M Sodium hydroxide ( $\geq 98.0\%$ ) stock solution (Sigma Aldrich)
- $\geq 40.0\% < 50.0\%$  Acetic acid solution (Supplier Unknown)
- 1.0 M Citric acid monohydrate ( $\geq 99.5\%$ ) stock solution (Fluka Chemika)
- Milli-Q water

Three buffers have been selected on the basis of their pH range, their water solubility, and their pH stability during temperature changes. It was decided to produce buffers at concentrations of 1.0 mM in order to minimize salt effects during CD spectroscopy measurements, and in order to present the protein with low ionic strength conditions.

In the case of pH 4, sodium acetate anhydrous ( $C_2H_3O_2Na$ ) was dissolved in Milli-Q water in order to obtain the 1.0 mM pH 4 stock buffer solution. The pH was confirmed with a calibrated pH meter, and adjusted with its conjugated acid-base pair; acetic acid ( $C_2H_4O_2$ ) and sodium hydroxide (NaOH), respectively. In the case of pH 7, sodium citrate dihydrate ( $C_6H_5Na_3O_7 \cdot 2H_2O$ ) was dissolved in Milli-Q water in order to obtain the 1.0 mM pH 7 stock buffer solution. The pH was confirmed with a calibrated pH meter, and adjusted with its conjugated acid-base pair; citric acid monohydrate ( $C_6H_8O_7$ ) and sodium hydroxide, respectively. Lastly, in the case of pH 10, sodium carbonate anhydrous ( $CNa_2O_3$ ) was dissolved in Milli-Q water in order to obtain the 1.0 mM pH 10 stock buffer solution. The pH was confirmed with a calibrated pH meter, and adjusted with its conjugated acid-base pair; carbonic acid ( $H_2CO_3$ ) and sodium hydroxide, respectively. However, since carbonic acid is a gas, this buffer can only be adjusted toward a more alkaline solution.

Furthermore, sodium hydroxide and citric acid monohydrate was prepared in solutions of

3.0 M and 1.0 M, respectively. An acetic acid solution was borrowed from stock solutions belonging to the pH meter lab. It is estimated to have a concentration between 40.0 and 50.0 % acetic acid that is dissolved in Milli-Q water.

The buffers were autoclaved at 121 °C, one bar above atmospheric pressure for 30 minutes. The pH of the buffer solutions was reassured two weeks after preparation.

Every buffer has an optimal pH range in which they are able to moderate changes in proton concentrations. The pH range is a factor of the the pKa of the acid of the buffer. In Table 7.1 the pKa values and pH range of the buffers are displayed.

Buffer	pKa (20 - 25 °C)	pH range (20 - 25 °C)
Sodium acetate anhydrous	4.76	3.6 - 5.6
Sodium citrate dihydrate	3.183, 4.76, 6.40	3.0 - 6.2
Sodium carbonate anhydrous	6.37, 10.25	9.2 - 10.8

**Table 7.1.** The pKa values for each ionization site of the buffers, and their respectively optimal pH range. Data are obtained from chemical suppliers.

## 7.2 Stock Denaturant Solutions

### Materials

- 500 mL Bluecap container for GuHCl solution
- 100 mL volumetric flask
- JP Selecta Autoclave

### Chemicals

- 8 M stock Guanidine hydrochloride solution (Applichem, Biochemika)
- pH 4, pH 7, and pH 10 stock buffer solutions

In order to prepare stock denaturant solutions, GuHCl ( $\text{CH}_5\text{N}_3 \cdot \text{HCl}$ ) was dissolved in 200 mL stock buffer solutions, in order to obtain the 8 M stock denaturant solution at pH 4, one at pH 7, and one at pH 10. Note that the resultant volume is close to 400 mL. GuHCl was dissolved in buffer in order not to dilute the resultant buffer during measurements thus maintaining a constant buffer concentration of 1.0 mM in the system. Stock denaturant solutions were autoclaved at 121 °C, one bar above atmospheric pressure for 30 minutes.

## 7.3 Thermal Denaturation: Fluorescence Spectroscopy

### Materials

- 1 - 5 mL Eppendorf pipette
- 3.00 mL quartz cuvette (10.0 mm)
- 30 mL plastic containers for HEWL solutions
- Photon Technology International (PTI) steady-state Fluorescence Spectrophotometer including software Felix32 Analysis Module
- JP Selecta Autoclave

### Chemicals

- pH 4, pH 7, and pH 10 stock buffer solutions
- 0.1 g/L stock Hen Egg-White Lysozyme ( $\geq 90.0\%$ ) solution
- 2 % Hellmanex (Hellma Analytics)
- 70 % Ethanol (VWR Chemicals)
- Fresh Milli-Q water

Firstly, HEWL was dissolved in buffer, in order to obtain the 0.1 g/L stock HEWL solution. HEWL solutions were prepared fresh before each buffer experiment as to avoid unwanted pH denaturation of the protein during experiment period, since HEWL is less stable in

acidic and alkaline conditions. Furthermore, HEWL solutions were stored at 4 °C in order to slow pH denaturation, and the solutions were prepared in plastic containers since proteins tend to adsorb onto glass surfaces faster than onto plastics. Before application, the plastic containers were cleansed in 2 % Hellmanex, 70 % ethanol, and fresh Milli-Q water, respectively, and blow dried in nitrogen gas. Pipette tips were autoclaved at 121 °C, one bar above atmospheric pressure for 30 minutes. Afterwards they were stored at 60 °C in order to dry the pipette tips.

2.5 mL of 0.1 g/L stock HEWL solution was placed on a magnetic stirrer at 750 RPM while one emission scan (300 - 455 nm) at 295 nm excitation was executed in order to determine the emission spectrum of Tryptophan in native HEWL.

In order to determine the thermal denaturation of HEWL, 2.5 mL of 0.1 g/L stock HEWL solution was placed on a magnetic stirrer at 750 RPM while one temperature scan was executed, scanning 25 - 87 °C, 3 °C per minute, at 350 nm, with 3 nm slit width.

A 10.0 mm quartz cuvette was applied in order to use the build-in magnetic stirrer in the setup. The procedure was repeated for each pH three times. Between each measurement, the cuvettes were cleansed in 2 % Hellmanex, 70 % ethanol, and fresh Milli-Q water, in that order. Furthermore, the cuvettes were blow dried in nitrogen gas, and stock HEWL solutions were stirred before application.

## 7.4 Thermal Denaturation: Circular Dichroism Spectroscopy

### Materials

- 1 - 5 mL Eppendorf pipette
- 100 - 1000 µL Eppendorf pipette
- 10 - 100 µL Eppendorf pipette
- 0.5 - 10 µL Eppendorf pipette
- 450 µL quartz cuvette (1.00 mm)
- 30 mL plastic containers for HEWL solutions
- 1.5 mL Eppendorf tubes
- 500 mL beaker for ice bath
- Glass thermometer
- Stuart Scientific Test tube Heater SHT
- Jasco J-515 Spectropolarimeter including software CD Jasco J-715 Hardware Manager
- JP Selecta Autoclave

### Chemicals

- pH 4, pH 7, and pH 10 stock buffer solutions
- 0.1 g/L stock Hen Egg-White Lysozyme ( $\geq$  90.0 %) solution
- 2 % Hellmanex (Hellma Analytics)
- 70 % Ethanol (VWR Chemicals)
- Fresh Milli-Q water

Firstly, HEWL was dissolved in buffer, in order to obtain the 0.1 g/L stock HEWL solution. HEWL solutions were prepared fresh before each buffer experiment as to avoid unwanted pH denaturation of the protein during the experiment period, since HEWL is less stable in acidic and alkaline conditions. Furthermore, HEWL solutions were stored at 4 °C in order to slow pH denaturation, and the solutions were prepared in plastic containers since proteins tend to adsorb onto glass surfaces faster than onto plastics. Before application, the plastic containers were cleansed in 2 % Hellmanex, 70 % ethanol, and fresh Milli-Q

water, in that order, and blow dried in nitrogen gas. Pipette tips were autoclaved at 121 °C, one bar above atmospheric pressure for 30 minutes. Afterwards they were stored at 60 °C in order to dry the pipette tips.

This section contains three minor temperature experiments. Firstly, the native HEWL structure was determined by CD spectroscopy at 20 °C. One 450 µL 0.1 g/L HEWL sample was tested in far-UV (190 - 250 nm) at 10 accumulations.

Later, 0.1 g/L HEWL solutions in 1.5 mL Eppendorf tubes were placed into a test tube heater at 80 °C for 5 minutes in order to unfold the protein. Afterwards, the solutions were placed on ice for 1.5 minutes in order to lock the protein state. The unfolded HEWL structure was determined by CD spectroscopy. One 450 µL 0.1 g/L HEWL sample was tested in far-UV (190 - 250 nm) at 10 accumulations. Furthermore, one 2.5 mL sample unfolded HEWL was tested by fluorescence spectroscopy. One emission scan (300 nm - 455 nm) at 295 nm excitation was executed at 350 nm.

Lastly, 0.1 g/L HEWL solutions in 1.5 mL Eppendorf tubes were placed into a test tube heater at 80 °C for 5 minutes in order to unfold the protein. Afterwards they were placed for natural cooling for 30 minutes toward 20 - 25 °C in order to refold HEWL. Afterwards, the refolded HEWL solutions were placed on ice for 1.5 minutes in order to lock the protein structure. The refolded protein structure was determined by CD spectroscopy. One 450 µL 0.1 g/L HEWL sample was tested in far-UV (190 - 250 nm) at 10 accumulations. Furthermore, one 2.5 mL sample unfolded HEWL was tested by fluorescence spectroscopy. One emission scan (300 - 455 nm) at 295 nm excitation was executed at 350 nm.

All CD spectroscopy measurements were executed at rate 50 nm per minute with 1 nm intervals.

The procedure was repeated for each pH three times. Between each measurement, the cuvettes were cleansed in 2 % Hellmanex, 70 % ethanol, and fresh Milli-Q water, in that order. Furthermore, the cuvettes were blow dried in nitrogen gas.

## 7.5 Chemical Denaturation: Fluorescence Spectroscopy

### Materials

- 1 - 5 mL Eppendorf pipette
- 100 - 1000 µL Eppendorf pipette
- 10 - 100 µL Eppendorf pipette
- 0.5 - 10 µL Eppendorf pipette
- 3.00 mL quartz cuvette (10.0 mm)
- 30 mL plastic container for stock HEWL solutions
- Photon Technology International (PTI) steady-state Fluorescence Spectrophotometer including software Felix32 Analysis Module
- JP Selecta Autoclave

### Chemicals

- pH 4, pH 7, and pH 10 stock buffer solutions
- 0.8 g/L stock Hen Egg-White Lysozyme ( $\geq 90.0\%$ ) solution
- 8 M stock Guanidine hydrochloride solution (Applichem, Biochemika)
- 2 % Hellmanex (Hellma Analytics)
- 70 % Ethanol (VWR Chemicals)
- Fresh Milli-Q water

Firstly, HEWL was dissolved in buffer, in order to obtain the 0.8 g/L stock HEWL solution. HEWL solutions were prepared fresh before each buffer experiment as to avoid unwanted pH denaturation of the protein during the experiment period since HEWL is less stable

in acidic and alkaline conditions. Furthermore, HEWL solutions were stored at 4 °C in order to slow pH denaturation, and the solutions were prepared in plastic containers since proteins tend to adsorb onto glass surfaces faster than onto plastics. Before application, the plastic containers were cleansed in 2 % Hellmanex, 70 % ethanol, and fresh Milli-Q water, in that order, and blow dried in nitrogen gas. Pipette tips were autoclaved at 121 °C, one bar above atmospheric pressure for 30 minutes. Afterwards they were stored at 60 °C in order to dry the pipette tips.

In order to determine the chemical denaturation of HEWL by GuHCl, 8 concentrations of GuHCl were tested; 0 M, 1 M, 2 M, 3 M, 4 M, 5 M, 6 M, and 7 M. 2.5 mL solution was placed on a magnetic stirrer at 750 RPM for 15 minutes. Each cuvette was prepared by diluting 0.8 g/L stock HEWL solution, stock buffer solutions, and 8 M stock GuHCl solution in order to maintain a concentration of 0.1 g/L HEWL in each cuvette, and GuHCl concentrations between 0 and 7 M.

Afterwards, one emission scan (300 - 455 nm) at 295 nm excitation was executed as to determine the emission spectrum of Tryptophan at concentrations of GuHCl between 0 and 7 M.

A 10.0 mm quartz cuvette was applied in order to use the build-in magnetic stirrer in the setup. The procedure was repeated for each pH three times. Between each measurement, the cuvettes were cleansed in 2 % Hellmanex, 70 % ethanol, and fresh Milli-Q water, respectively. Furthermore, the cuvettes were blow dried in nitrogen gas.

## 7.6 Chemical Denaturation: Circular Dichroism Spectroscopy

### Materials

- 1 - 5 mL Eppendorf pipette
- 100 - 1000 µL Eppendorf pipette
- 10 - 100 µL Eppendorf pipette
- 0.5 - 10 µL Eppendorf pipette
- 50 µL quartz cuvette (0.10 mm)
- 30 mL plastic container for stock HEWL solutions
- 15 mL Greiner tubes for HEWL solutions
- K-MS2 Minishaker from VWR<sup>TM</sup> International
- Jasco J-515 Spectropolarimeter including software CD Jasco J-715 Hardware Manager
- JP Selecta Autoclave

### Chemicals

- pH 4, pH 7, and pH 10 stock buffer solutions
- 8.0 g/L stock Hen Egg-White Lysozyme ( $\geq$  90.0 %) solution
- 8 M stock Guanidine hydrochloride solution (Applichem, Biochemika)
- 2 % Hellmanex (Hellma Analytics)
- 70 % Ethanol (VWR Chemicals)
- Fresh Milli-Q water

Firstly, HEWL was dissolved in buffer, in order to obtain the 8.0 g/L stock HEWL solution. HEWL solutions were prepared fresh before each buffer experiment as to avoid unwanted pH denaturation of the protein during the experiment period since HEWL is less stable in acidic and alkaline conditions. Furthermore, HEWL solutions were stored at 4 °C in order to slow pH denaturation, and the solutions were prepared in plastic containers since proteins tend to adsorb onto glass surfaces faster than onto plastics. Before application,

the plastic containers were cleansed in 2 % Hellmanex, 70 % ethanol, and fresh Milli-Q water, in that order, and blow dried in nitrogen gas. Pipette tips were autoclaved at 121 °C, one bar above atmospheric pressure for 30 minutes. Afterwards they were stored at 60 °C in order to dry the pipette tips.

In order to determine the chemical denaturation of HEWL by GuHCl, 8 concentrations of GuHCl were tested; 0 M, 1 M, 2 M, 3 M, 4 M, 5 M, 6 M, and 7 M.

2.0 mL solution was placed on a minishaker at 750 RPM for 15 minutes. Each solution was prepared by diluting 8.0 g/L stock HEWL, buffer, and 8 M GuHCl in order to maintain a concentration of 1.0 g/L HEWL in each cuvette, and GuHCl concentrations between 0 and 7 M. 50 µL solution was tested by CD spectroscopy in far-UV (190 - 250 nm) at 10 accumulations.

All CD spectroscopy measurements were executed at rate 50 nm per minute with 1 nm intervals. 1.0 g/L HEWL was chosen due to the 0.10 mm quartz cuvette.

A 0.10 mm quartz cuvette was applied in order to minimize the optical path length, thus minimizing scattering salt effects. The procedure was repeated for each pH three times. Between each measurement, the cuvettes were cleansed in 2 % Hellmanex, 70 % ethanol, and fresh Milli-Q water, in that order. Furthermore, the cuvettes were blow dried in nitrogen gas.

---

## 8. Results

---

This chapter will present the results of the experiments described in Chapter 7. Firstly, it will present the results regarding the preparation of the stock buffer solutions, later, the steady-state fluorescence and CD spectroscopy results during thermal and chemical denaturation of HEWL, and, lastly, the calculated  $\alpha$ -helix content in HEWL during denaturation. Results presented from fluorescence spectroscopy are only constituted by one of the detectors as the other gave rise to some problems during some experiments. During all fluorescence spectroscopy measurements, a 3 nm slit width was employed. Furthermore, all results are treated and presented using MatLab, and every normalization of spectra is done by dividing the entire graph with its maximum emission intensity.

### 8.1 Preparation of Stock Buffer Solutions

The three buffers applied during experiments were prepared as described in Section 7.1. After preparation, their initial pH values were adjusted toward the desired values at 20 °C. The preparation and adjustment resulted in one 1.0 mM sodium acetate stock buffer solution with pH 4.13, one 1.0 mM sodium citrate stock buffer solution with pH 7.18, and one 1.0 mM sodium carbonate stock buffer solution with pH 10.81.

Two weeks after preparation, the pH of the solutions were verified by measurements at 20 °C. Furthermore, the pH of the buffer solutions containing GuHCl in concentrations from 1 to 7 M were measured two times at 20 °C. The average pH of these measurements is displayed in Table 8.1 along with the initial pH values. All three buffer solutions had no discolouration or precipitation after autoclaving and storage at 4 °C throughout the experiment period.

Buffer	pH values								
	Initial	0 M	1 M	2 M	3 M	4 M	5 M	6 M	7 M
Sodium acetate	4.13	4.12	3.85	3.765	3.73	3.715	3.69	3.665	3.675
Sodium citrate	7.18	7.115	6.09	5.89	5.745	5.667	5.595	5.57	5.53
Sodium carbonate	10.81	10.63	9.305	8.95	8.795	8.665	8.54	8.465	8.355

**Table 8.1.** A table displaying the initial pH values of the three 1.0 mM buffer solutions applied in the experiments; Sodium acetate, sodium citrate, and sodium carbonate. Furthermore, two weeks after preparation, the pH values of the buffer solutions were ensured by measurements, and the pH of the buffer solutions containing concentrations of GuHCl from 1 - 7 M was tested. The pH values are the average of two measurements, not including the initial pH values.

In Table 8.1, it is observed that the pH of the three buffer solutions after storage at 4 °C for two weeks were slightly decreased compared to the initial pH values. Furthermore, it is observed that the pH simultaneously decreases as a function of increasing GuHCl concentration in each of the three buffer solutions. The most significant change in pH is observed in the pH 10 buffer solution where the pH value decreases by approximately 2.3.

The changes observed in the pH 7 buffer and pH 4 buffer were approximately 1.6 and 0.5, respectively.

## 8.2 Thermal Denaturation

As described in Chapter 7, attempts were made to thermally denature HEWL in all three buffer solutions. The results were obtained from both steady-state fluorescence and CD spectroscopy, and the results for each buffer solution will be presented separately.

### 8.2.1 Sodium Acetate Buffer: pH 4

In order to thermally denature 0.1 g/L HEWL at pH 4, one temperature scan was executed using steady-state fluorescence spectroscopy, scanning from 25 to 88 °C, 3 °C per minute at 350 nm emission wavelength. In Figure 8.1 the average of three temperature scans is shown, plotting the emission intensity of Tryptophan in HEWL as a function of increasing temperature, along with the derivative of the emission intensity as a function of the increasing temperature.

Maximum temperatures of the HEWL solutions were 84.3 °C, 84.1 °C, and 84.5 °C, and bobbles were observed in all solutions after the temperature scans ended.

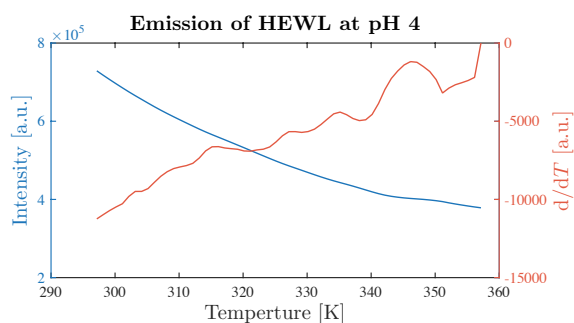


**Figure 8.1.** Average temperature scan of 0.1 g/L HEWL at pH 4 heated from 25 to 88 °C, 3 °C per minute at 350 nm emission wavelength by fluorescence spectroscopy. The emission intensity of Tryptophan in HEWL as a function of increasing temperature is displayed (blue), along with the derivative of the intensity as a function of increasing temperature (red). Maximum temperatures observed were 84.3 °C, 84.1 °C, and 84.5 °C. A peak in the derivative is observed at 346 K (73 °C) followed by a later peak.

In Figure 8.1, it is observed, that the emission intensity of Tryptophan in HEWL at 350 nm decreases as the temperature increases, and a small peak in the derivative of the intensity is observed at 346 K (73 °C) followed by a later peak.

Furthermore, by steady-state fluorescence spectroscopy, emission scans (300 - 455 nm) were executed, measuring the emission intensity of Tryptophan in HEWL as a function of wavelength at pH 4. Figure 8.2 displays the average of three emission scans carried out on 0.1 g/L native HEWL at room temperature, the average of three emission scans carried out on 0.1 g/L heated HEWL, which had been heated for 5 minutes at 80 °C, and the average of three emission scans carried out on 0.1 g/L refolded HEWL, which had been heated for 5 minutes at 80 °C and naturally cooled toward 20 - 25 °C for 30 minutes. The maximum temperatures of the heated HEWL solutions were 82 °C, 79 °C, and 82 °C. The maximum

temperatures observed for the refolded HEWL solutions for all were 26 °C. Every emission scan was carried out using 295 nm excitation of Tryptophan.

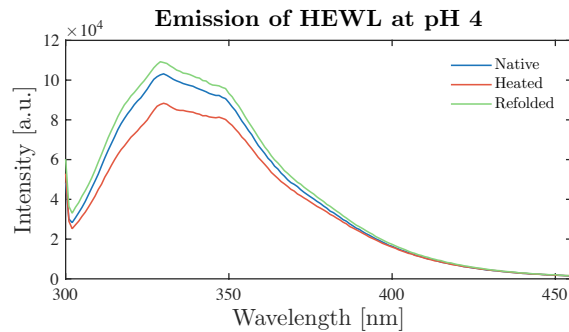


**Figure 8.2.** Average emission spectra (300 - 455 nm) by fluorescence spectroscopy at pH 4 and 295 nm excitation of Tryptophan in HEWL showing the emission intensity of the native HEWL solutions at room temperature (Native), the heated HEWL solutions, with maximum temperatures of 82 °C, 79 °C, and 82 °C (Heated), and the refolded HEWL solutions at 26 °C (Refolded), as a function of wavelength. It is observed that the emission intensity decreases as the protein has been heated and increases when refolded, compared to that of the native protein.

In Figure 8.2, no shift in maximum emission wavelength is observed as HEWL is heated, and when it has had a chance to refold. Furthermore, it is observed that the emission intensity of Tryptophan, compared to that of the native protein, decreases as the protein is heated, and the emission intensity increases when the protein has had a chance to refold. In Figure 8.3, a normalized version of the emission spectrum in Figure 8.2 is shown along with the ratio between the wavelengths 350 and 330 nm for the native, heated, and refolded HEWL.

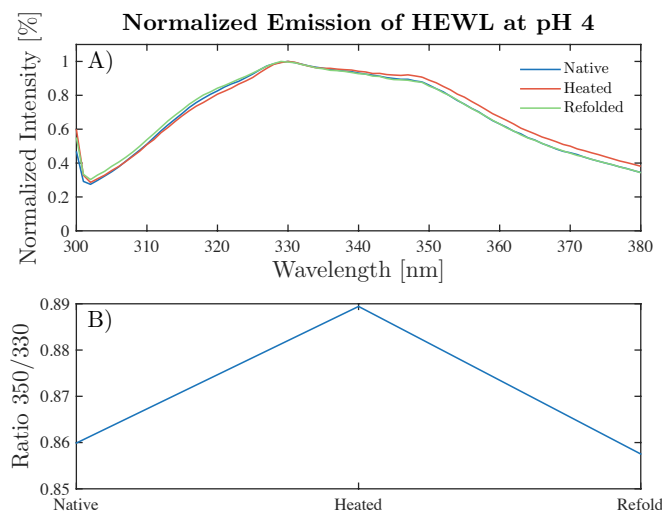


**Figure 8.3.** A) normalized emission spectra (300 - 380 nm) by fluorescence spectroscopy at pH 4 and 295 nm excitation of Tryptophan in HEWL showing the emission intensity of the native HEWL solutions at room temperature (Native), the heated HEWL solutions with maximum temperatures of 82 °C, 79 °C, and 82 °C (Heated), and the refolded HEWL solutions at 26 °C (Refolded) as a function of wavelength. B) the ratio between the wavelengths 350 and 330 nm derived from A) for the native, heated, and refolded HEWL. It is observed that the emission intensity shifts slightly towards 350 nm when the protein has been heated, and returns to the same ratio when the protein is refolded.

It is observed from Figure 8.3 that the emission intensity of Tryptophan in HEWL shifts slightly from 330 towards 350 nm when the protein has been heated, and returns to the same ratio when refolded, compared to the native protein.

As for the CD spectroscopy measurements at pH 4, Figure 8.4 displays the average of three CD spectra (190 - 250 nm) of the native, heated, and refolded HEWL solutions, respectively. The maximum temperatures observed of the native HEWL solutions were 20.86 °C, 20.87 °C, and 20.85 °C. The maximum temperatures observed of the heated HEWL solutions were 81 °C, 82 °C, and 79 °C. Lastly, the maximum temperatures observed for the refolded HEWL solutions were 22 °C, 26 °C, and 25 °C.

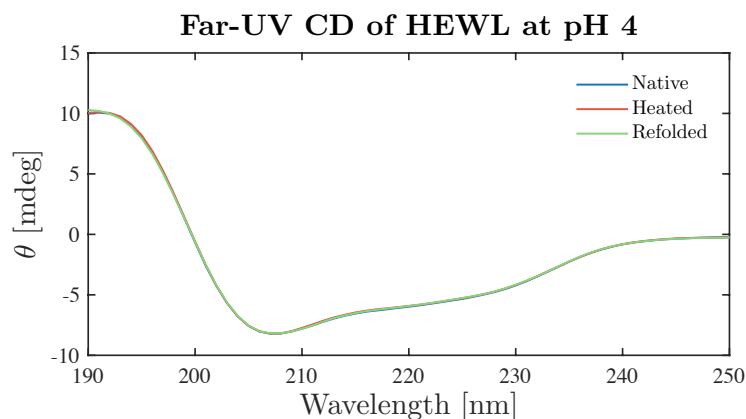


**Figure 8.4.** The average CD spectra (190 - 250 nm), showing average ellipticity as a function of wavelength at pH 4, measured on 0.1 g/L native, heated, and refolded HEWL solutions. The maximum temperatures observed of the native HEWL solutions were 20.86 °C, 20.87 °C, and 20.85 °C. The maximum temperatures observed of the heated HEWL solutions were 81 °C, 82 °C, and 79 °C. Lastly, the maximum temperatures observed for the refolded HEWL solutions were 22 °C, 26 °C, and 25 °C. No significant change in ellipticity is observed when the protein is heated and refolded compared to that of the native.

In Figure 8.4, no significant change in ellipticity as a function of wavelength is observed as the native protein is heated and refolded compared to the signal for the native HEWL.

## 8.2.2 Sodium Citrate Buffer: pH 7

In order to thermally denature 0.1 g/L HEWL at pH 7, one temperature scan was executed using steady-state fluorescence spectroscopy, scanning from 25 to 88 °C, 3 °C per minute at 350 nm emission wavelength. In Figure 8.5 the average of three temperature scans is shown, plotting the emission intensity of Tryptophan in HEWL as a function of increasing temperature, along with the derivative of the emission intensity as a function of the increasing temperature.

Maximum temperatures of the HEWL solutions were 84.5 °C, 84.4 °C, and 84.5 °C, and bobbles were observed in all solutions after the temperature scans ended.

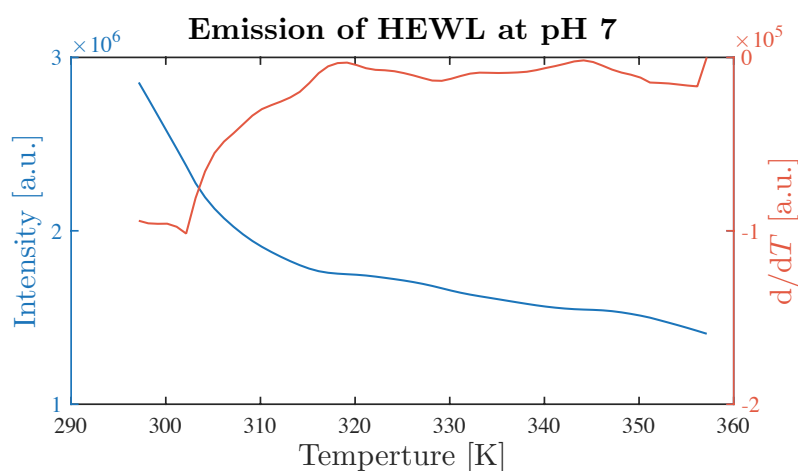
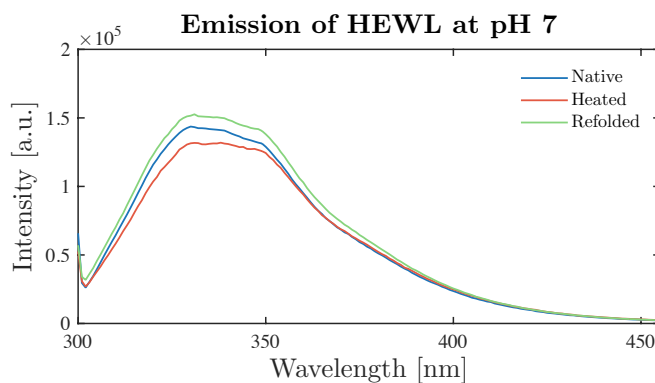


**Figure 8.5.** Average temperature scan of 0.1 g/L HEWL at pH 7 heated from 25 to 88 °C, 3 °C per minute at 350 nm emission wavelength by fluorescence spectroscopy. The emission intensity of Tryptophan in HEWL as a function of increasing temperature is displayed (blue), along with the derivative of the intensity as a function of increasing temperature (red). Maximum temperatures observed were 84.5 °C, 84.4 °C, and 84.5 °C. No significant peak in the derivative is observed, however, the emission intensity decreases significantly between 290 and 315 nm.

In Figure 8.5, it is observed, that the emission intensity of Tryptophan in HEWL at 350 nm decreases as the temperature increases, and no peaks in the derivative is observed. However, the emission intensity decreases significantly between 290 and 315 nm.

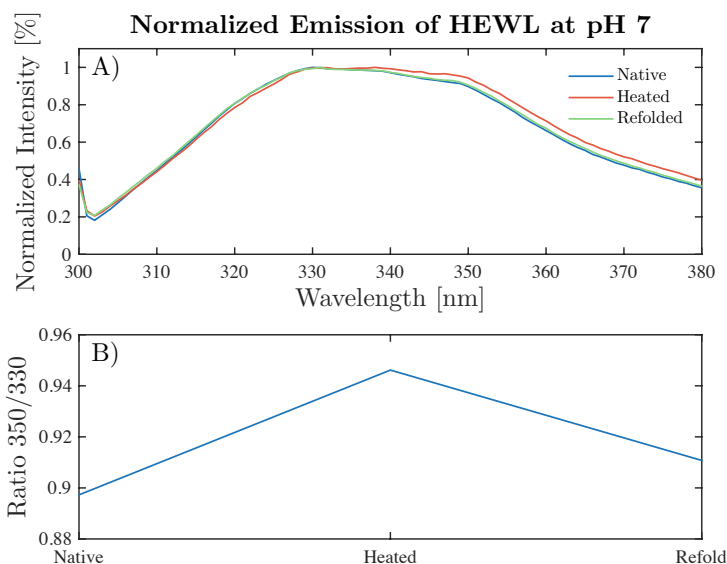
Furthermore, by steady-state fluorescence spectroscopy, emission scans (300 - 455 nm) were executed, measuring the emission intensity of Tryptophan in HEWL as a function of wavelength at pH 7.

Figure 8.6 displays the average of three emission scans carried out on 0.1 g/L native HEWL at room temperature, the average of three emission scans carried out on 0.1 g/L heated HEWL, which had been heated for 5 minutes at 80 °C, and the average of three emission scans carried out on 0.1 g/L refolded HEWL, which had been heated for 5 minutes at 80 °C and naturally cooled toward 20 - 25 °C for 30 minutes. The maximum temperatures of the heated HEWL solutions were 80 °C, 78 °C, and 81 °C. The maximum temperatures observed for the refolded HEWL solutions were 27 °C, 25 °C, and 27 °C. Every emission scan was carried out using 295 nm excitation of Tryptophan.



**Figure 8.6.** Average emission spectra (300 - 455 nm) by fluorescence spectroscopy at pH 7 and 295 nm excitation of Tryptophan in HEWL showing the emission intensity of the native HEWL solutions at room temperature (Native), the heated HEWL solutions, with maximum temperatures of 80 °C, 78 °C, and 81 °C (Heated), and the refolded HEWL solutions at 27 °C, 25 °C, and 27 °C (Refolded), as a function of wavelength. It is observed that the emission intensity decreases as the protein has been heated and increases when refolded, compared to that of the native protein.

In Figure 8.6, no shift in maximum emission wavelength is observed, as HEWL is heated, and when HEWL is heated and refolded. Furthermore, it is observed that the emission intensity of Tryptophan, compared to that of the native protein, decreases as the protein is heated, and the emission intensity increases when the protein has had a chance to refold. In Figure 8.7, a normalized version of the emission spectrum in Figure 8.6 is shown along with the ratio between the wavelengths 350 and 330 nm for the native, heated, and refolded HEWL.



**Figure 8.7.** A) normalized emission spectra (300 - 380 nm) by fluorescence spectroscopy at pH 7 and 295 nm excitation of Tryptophan in HEWL showing the emission intensity of the native HEWL solutions at room temperature (Native), the heated HEWL solutions with maximum temperatures of 80 °C, 78 °C, and 81 °C (Heated), and the refolded HEWL solutions at 27 °C, 25 °C and 27 °C (Refolded) as a function of wavelength. B) the ratio between the wavelengths 350 nm and 330 nm derived from A) for the native, heated, and refolded HEWL. It is observed that the maximum emission intensity shifts slightly toward 350 nm when the protein has been heated, and return to the same ratio when the protein is refolded.

It is observed from Figure 8.7 that the maximum emission intensity of Tryptophan in HEWL shifts slightly from 330 towards 350 nm when the protein has been heated, and returns to the same ratio when refolded when compared to the native protein.

As for the CD spectroscopy measurements at pH 7, Figure 8.8 displays the average of three CD spectra (190 - 250 nm) of the native, heated, and refolded HEWL solution, respectively. The maximum temperatures observed of the native HEWL solutions were 20.26 °C, 20.30 °C, and 20.88 °C. The maximum temperatures observed of the heated HEWL solutions were all 80 °C. Lastly, the maximum temperatures observed for the refolded HEWL solutions were 23 °C, 25 °C, and 26 °C.

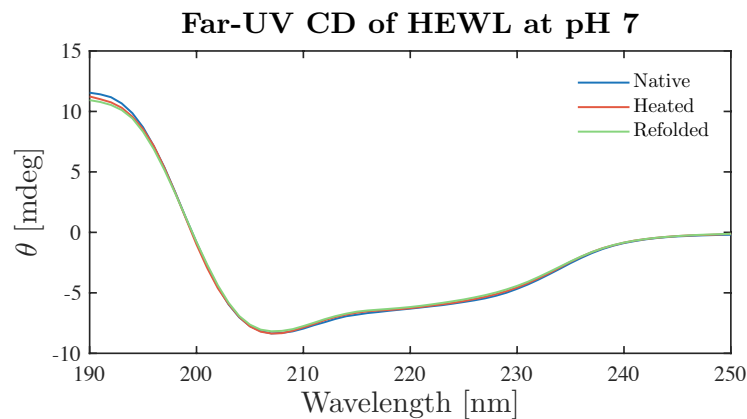


**Figure 8.8.** A) the average CD spectra (190 - 250 nm), showing average ellipticity as a function of wavelength at pH 7, measured on 0.1 g/L native, heated, and refolded HEWL solutions. The maximum temperatures observed of the native HEWL solutions were 20.26 °C, 20.30 °C, and 20.88 °C. The maximum temperatures observed of the heated HEWL solutions were all 80 °C. Lastly, the maximum temperatures observed for the refolded HEWL solutions were 23 °C, 25 °C, and 26 °C. No significant change in ellipticity is observed when the protein is heated and refolded compared to that of the native.

In Figure 8.8, no significant change in ellipticity as a function of wavelength is observed as the native protein is heated and refolded compared to the signal of the native HEWL.

### 8.2.3 Sodium Carbonate Buffer: pH 10

In order to thermally denature 0.1 g/L HEWL at pH 10, one temperature scan was executed using steady-state fluorescence spectroscopy, scanning from 25 to 88 °C, 3 °C per minute at 350 nm emission wavelength. In Figure 8.9 the average of three temperature scans is shown, plotting the emission intensity of Tryptophan in HEWL as a function of increasing temperature, along with the derivative of the emission intensity as a function of the increasing temperature.

Maximum temperatures of the HEWL solutions were 84.2 °C, 84.0 °C, and 84.5 °C, and bobbles and aggregates were observed in all solutions after the temperature scans ended. Furthermore, aggregates were observed in the solutions from the moment of dissolution of HEWL in the buffer solution.

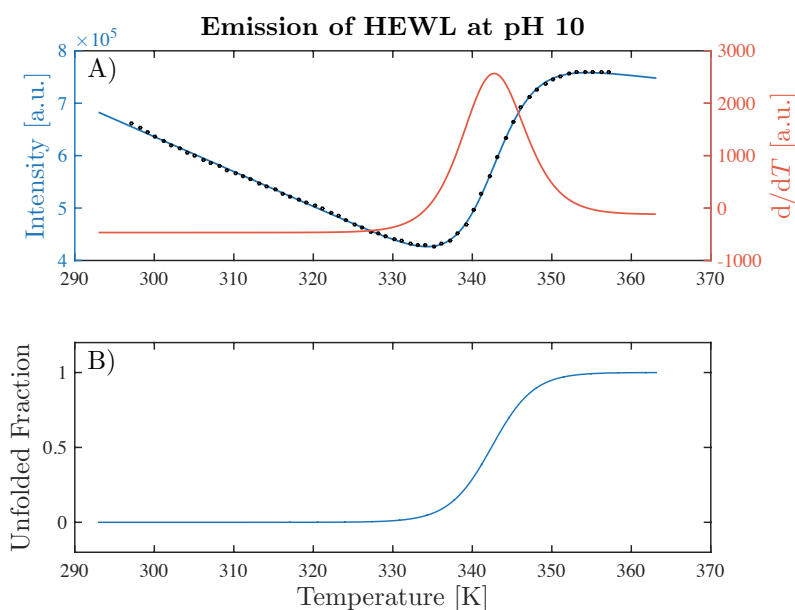


**Figure 8.9.** Average temperature scan of 0.1 g/L HEWL at pH 10 heated from 25 to 88 °C, 3 °C per minute at 350 nm emission wavelength by fluorescence spectroscopy. A) The emission intensity of Tryptophan in HEWL as a function of increasing temperature is displayed (blue), along with the derivative of the intensity as a function of increasing temperature (red). Maximum temperatures observed were 84.2 °C, 84.0 °C, and 84.5 °C. A significant peak in the derivative is observed at 342 K (69 °C). It is observed that the emission intensity decreases until 327 K followed by an increase toward 356 K. The data has been fitted using Equation (4.6). B) the fraction of unfolded HEWL as a function of temperature. It is observed that the unfolded fraction increases from 335 to 353 K. The fraction of unfolded HEWL was calculated using Equation (4.8).

In Figure 8.9, it is observed, that the emission intensity of Tryptophan in HEWL at 350 nm decreases until 335 K followed by an increase toward 353 K as the temperature is increased. A significant peak of the derivative is observed at 342 K (69 °C). The data have been fitted using Equation (4.6), and the fraction of unfolded HEWL was calculated using Equation (4.8). The best fit was obtained using Matlab, utilizing the seven parameters;  $A = 2.63 \cdot 10^6 \frac{1}{s}$ ,  $B = -6.65 \cdot 10^3 \frac{1}{s \cdot K}$ ,  $C = 1.37 \cdot 10^6 \frac{1}{s}$ ,  $D = -1.71 \cdot 10^3 \frac{1}{s \cdot K}$ ,  $\Delta H = 368 \frac{kJ}{mol}$ ,  $\Delta C_p = 3.75 \frac{kJ}{K \cdot mol}$ , and  $T_m = 342$  K.

The unfolded fraction was calculated using the parameters  $A$ ,  $B$ ,  $C$ , and  $D$  along with the intensity of the fluorescence  $y$ , calculated from Equation (4.6).

Furthermore, by steady-state fluorescence spectroscopy, emission scans (300 - 455 nm) were executed, measuring the emission intensity of Tryptophan in HEWL as a function of wavelength at pH 10.

Figure 8.10 displays the average of three emission scans carried out on 0.1 g/L native HEWL at room temperature, the average of three emission scans carried out on 0.1 g/L heated HEWL, which had been heated for 5 minutes at 80 °C, and the average of three emission scans carried out on 0.1 g/L refolded HEWL, which had been heated for 5 minutes at 80 °C and naturally cooled toward 20 - 25 °C for 30 minutes. The maximum temperatures of the heated HEWL solutions were 81 °C, 80 °C, and 79 °C. The maximum temperatures observed for the refolded HEWL solutions were all 25 °C. Every emission scan was carried out using 295 nm excitation of Tryptophan.

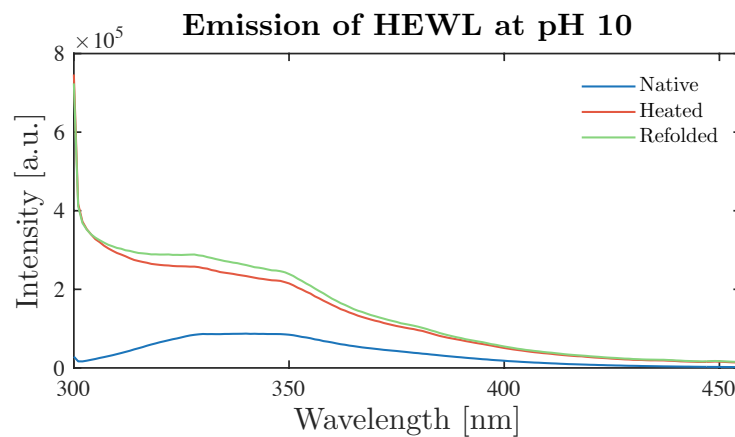


**Figure 8.10.** Average emission spectra (300 - 455 nm) by fluorescence spectroscopy at pH 10 and 295 nm excitation of Tryptophan in HEWL showing the emission intensity of the native HEWL solutions at room temperature (Native), the heated HEWL solutions, with maximum temperatures of 81 °C, 80 °C, and 79 °C (Heated), and the refolded HEWL solutions at 25 °C (Refolded), as a function of wavelength. It is observed that the emission intensity increases as the protein has been heated and refolded, compared to that of the native protein.

In Figure 8.10, it is observed that the emission intensity of Tryptophan, compared to that of the native protein, increases as the protein has been heated, and when the protein has had a chance to refold. It is observed that aggregates were formed, both before and after measurements.

As for the CD spectroscopy measurements at pH 10, Figure 8.11 displays the average of three CD spectra (190 - 250 nm) of the native, heated, and refolded HEWL solution, respectively. The maximum temperatures observed of the native HEWL solutions were 20.88 °C, 20.87 °C, and 20.88 °C. The maximum temperatures observed of the heated HEWL solutions were all 82 °C. Lastly, the maximum temperatures observed for the refolded HEWL solutions were 25 °C, 26 °C, and 25.5 °C. Furthermore, Figure 8.11 displays the average change in ellipticity at 222 nm for the native, heated, and refolded protein.

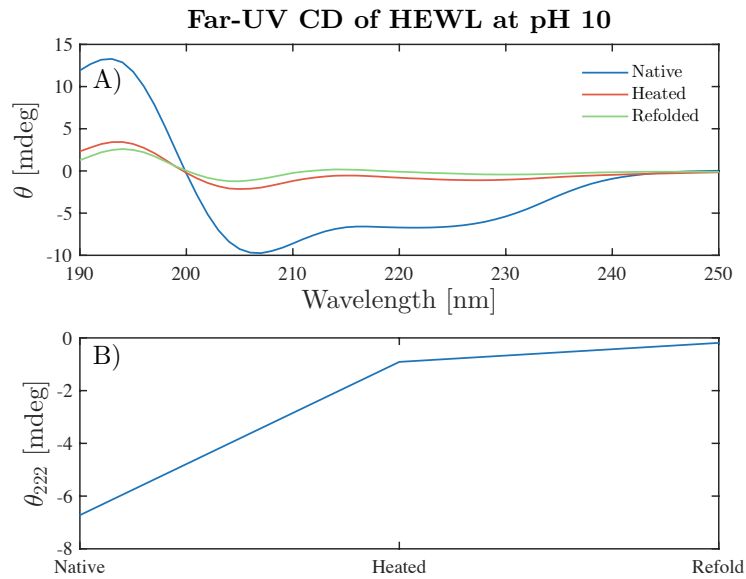


**Figure 8.11.** A) the average CD spectra (190 - 250 nm), showing average ellipticity as a function of wavelength at pH 10, measured on 0.1 g/L native, heated, and refolded HEWL solutions. The maximum temperatures observed of the native HEWL solutions were 20.88 °C, 20.87 °C, and 20.88 °C. The maximum temperatures observed of the heated HEWL solutions were all 82 °C. Lastly, the maximum temperatures observed for the refolded HEWL solutions were 25 °C, 26 °C, and 25.5 °C. B) the average change in ellipticity at 222 nm for the native, heated, and refolded protein. It is observed that the ellipticity is approaching zero when the protein is heated and refolded compared to that of the native protein.

In Figure 8.11, a significant change in ellipticity as a function of wavelength is observed as the native protein is heated and refolded compared to the signal for the native HEWL. However, the ellipticity of the heated and refolded protein is approximately equal but with a slight displacement.

## 8.3 Chemical Denaturation

As described in Chapter 7, HEWL was chemically denatured by GuHCl in all three buffer solutions. The results were obtained from both steady-state fluorescence and CD spectroscopy, and the results for each buffer solution will be presented separately. 8 concentrations of GuHCl were tested; 0 M, 1 M, 2 M, 3 M, 4 M, 5 M, 6 M, and 7 M.

### 8.3.1 Sodium Acetate Buffer: pH 4

In order to chemically denature HEWL at pH 4 by GuHCl, one emission scan (300 - 455 nm) was executed using steady-state fluorescence spectroscopy, measuring the emission intensity of Tryptophan as a function of wavelength for each concentration of GuHCl.

Figure 8.12 displays the average of three emissions scans carried out on 0.1 g/L HEWL at room temperature for each GuHCl concentration. Every emission scan was carried out at 295 nm excitation of Tryptophan.

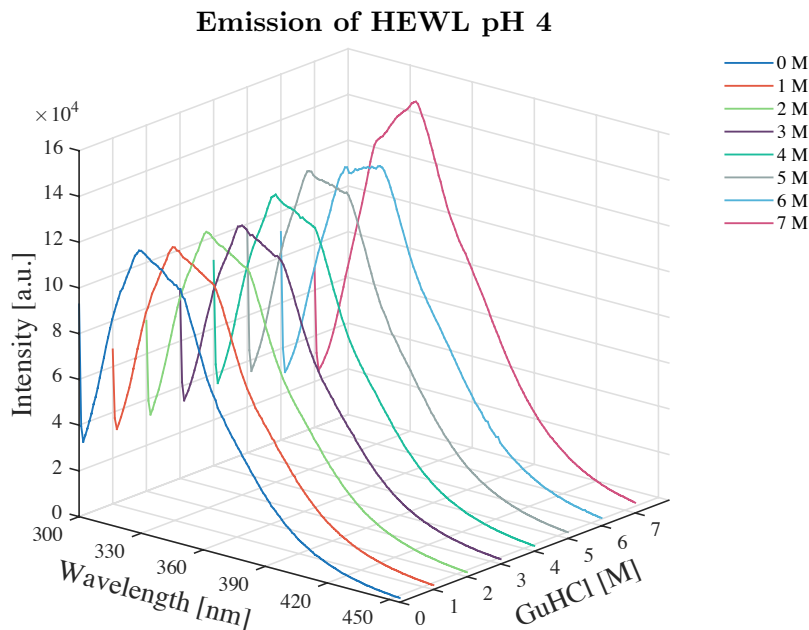


**Figure 8.12.** The average emission spectra (300 - 455 nm) by fluorescence spectroscopy at pH 4 and 295 nm excitation of Tryptophan in HEWL showing the emission intensity of 0.1 g/L HEWL solutions containing 0 - 7 M GuHCl. It is observed that the emission intensity increases as a function of increasing GuHCl concentration.

In Figure 8.12, it is observed that when the concentration of GuHCl increases, the emission intensity increases as well. Furthermore, a significant shift in maximum emission wavelength occurs as the concentration of GuHCl increases.

In Figure 8.13, a normalized version of the emission spectra in Figure 8.12 is shown along with the ratio between the wavelengths 350 and 330 nm and the normalized intensity at 330 nm as a function of GuHCl concentration.

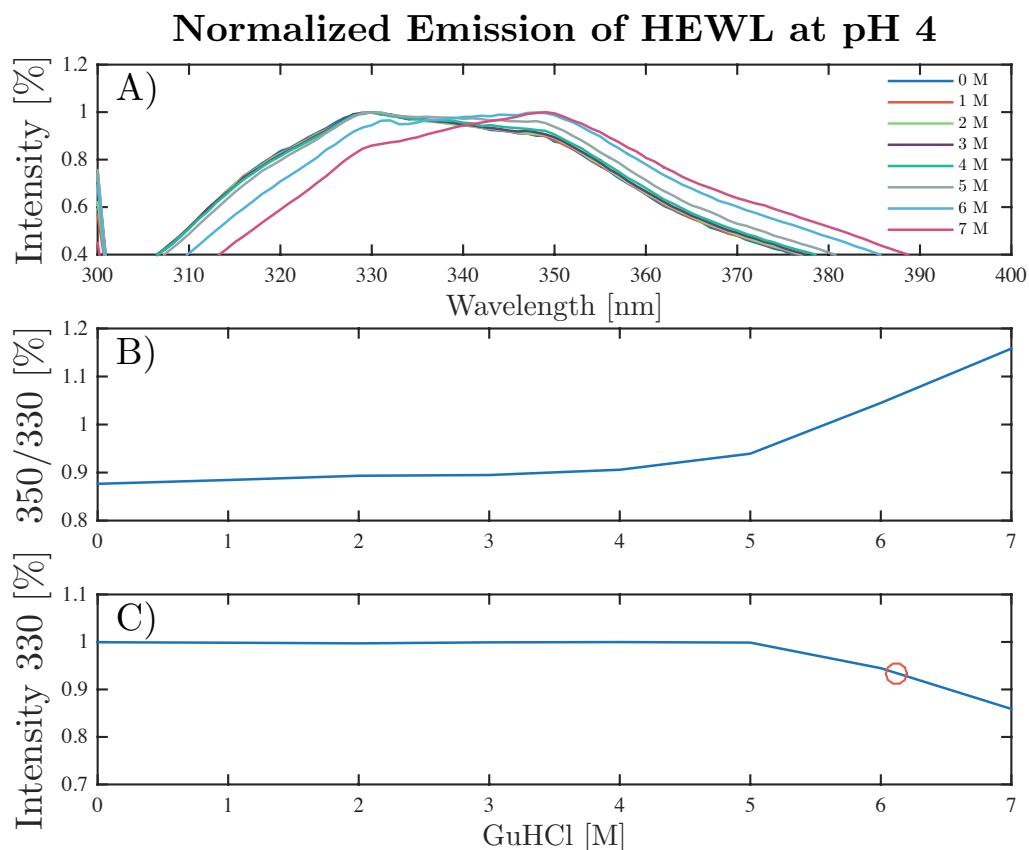


**Figure 8.13.** A) normalized emission spectra (300 - 400 nm) by fluorescence spectroscopy at pH 4 and 295 nm excitation of Tryptophan in HEWL showing the emission intensity at GuHCl concentrations from 0 - 7 M. B) the ratio between the wavelengths 350 and 330 nm derived from A) for each concentration of GuHCl. C) the normalized emission intensity at 330 nm as a function of increasing GuHCl concentration. The red circle indicates the transition point, which is  $[D_{50\%}] = 6.1238$  M GuHCl. It is observed that the maximum emission wavelength increases from 5 to 7 M GuHCl toward 350 nm, thus the emission intensity at 330 nm decreases at those concentrations.

In Figure 8.13, a significant change in maximum emission wavelength is observed, as it shifts from 330 toward 350 nm as the concentration of GuHCl increases. The change is observed from 5 to 7 M GuHCl in A) and 4 to 7 M in B). The red circle in C) is the determined transition point. The transition point was determined by the average concentration between 5 to 7 M GuHCl in the normalized emission intensity at 330 nm. The transition point is  $[D_{50\%}] = 6.1238$  M GuHCl, which, using Equation (4.10), means that  $\Delta G_{\text{solvent}} = 14.27$  kcal mol<sup>-1</sup>. It should be noted, that in order to determine the transition point, it is assumed, the the protein begins to denature at 5 M and is fully denatured at 7 M.

As for the CD spectroscopy measurements, Figure 8.14 shows the average of three CD spectra (190 - 250 nm) of 1.0 g/L HEWL solutions containing concentrations of GuHCl from 0 to 7 M at pH 4 and room temperature. Furthermore, Figure 8.14 shows the ellipticity at 222 nm as a function of increasing GuHCl concentration.

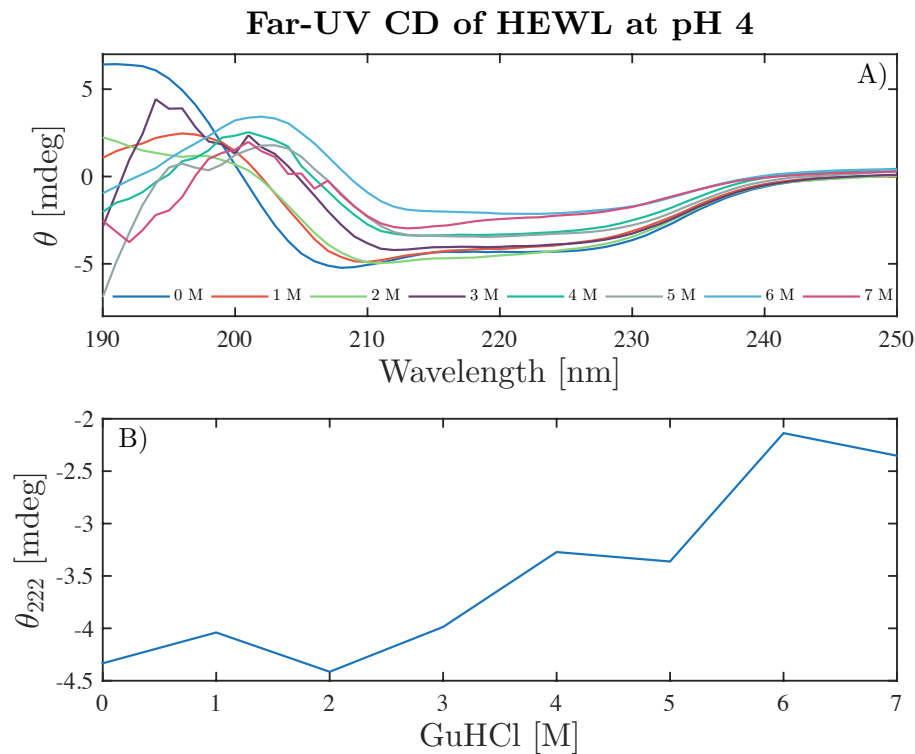


**Figure 8.14.** A) the average CD spectra (190 - 250 nm) of 1.0 g/L HEWL in solutions with GuHCl concentrations from 0 - 7 M at pH 4 and room temperature, showing ellipticity as a function of wavelength, and B) the average change in ellipticity at 222 nm as a function of increasing GuHCl concentration. It is observed that 2, 5, and 7 M GuHCl CD signals are slightly displaced, and that salt effects occur at wavelengths of approximately 205 nm and below. The observed tendency is that the ellipticity approaches zero as the GuHCl concentration increases.

In Figure 8.14, it is observed that the average 2, 5, and 7 M GuHCl CD spectra are slightly displaced in ellipticity as a function of wavelength since a chronological tendency should occur. It is also observed that some salt effects are occurring at wavelengths of approximately 205 nm and below. Furthermore, it is observed that the ellipticity by tendency approaches zero as a function of increasing GuHCl concentration. Since the ellipticity approaches zero gradually, it is difficult to determine any transition point.

### 8.3.2 Sodium Citrate Buffer: pH 7

In order to chemically denature HEWL at pH 7 by GuHCl, one emission scan (300 - 455 nm) was executed using steady-state fluorescence spectroscopy, measuring the emission intensity of Tryptophan as a function of wavelength for each concentration of GuHCl.

Figure 8.15 displays the average of three emissions scans carried out on 0.1 g/L HEWL at room temperature for each GuHCl concentration. Every emission scan was carried out at 295 nm excitation of Tryptophan.

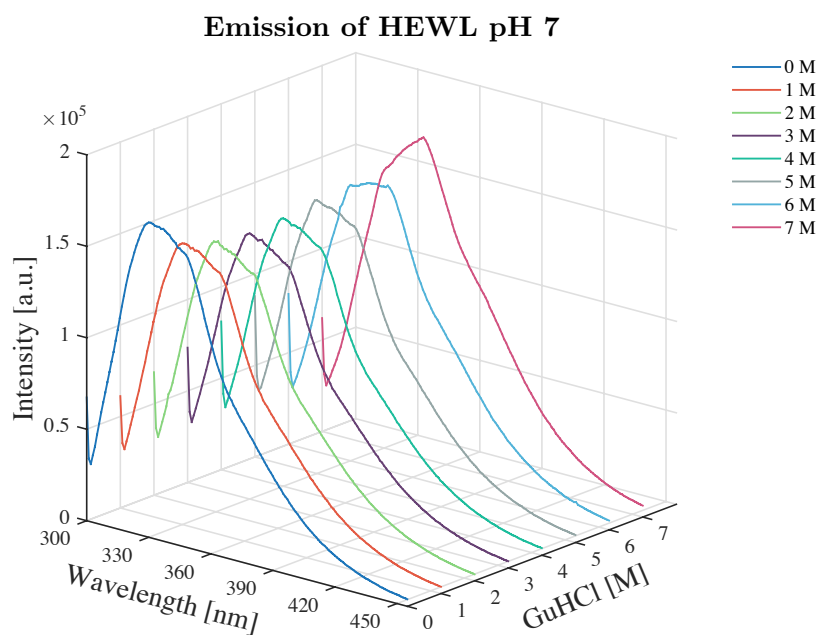


**Figure 8.15.** The average emission spectra (300 - 455 nm) by fluorescence spectroscopy at pH 7 and 295 nm excitation of Tryptophan in HEWL showing the emission intensity of 0.1 g/L HEWL solutions containing 0 - 7 M GuHCl. It is observed that the emission intensity decreases at 0 to 2 M followed by an increase at 3 to 7 M GuHCl.

In Figure 8.15, a decrease in intensity is observed from 0 to 3 M GuHCl, followed by an increase from 3 to 7 M GuHCl.

Furthermore, a significant shift in maximum emission wavelength occurs as the concentration of GuHCl increases.

In Figure 8.16, a normalized version of the emission spectra in Figure 8.15 is shown along with the ratio between the wavelengths 350 and 330 nm and the normalized intensity at 330 nm as a function of GuHCl concentration.

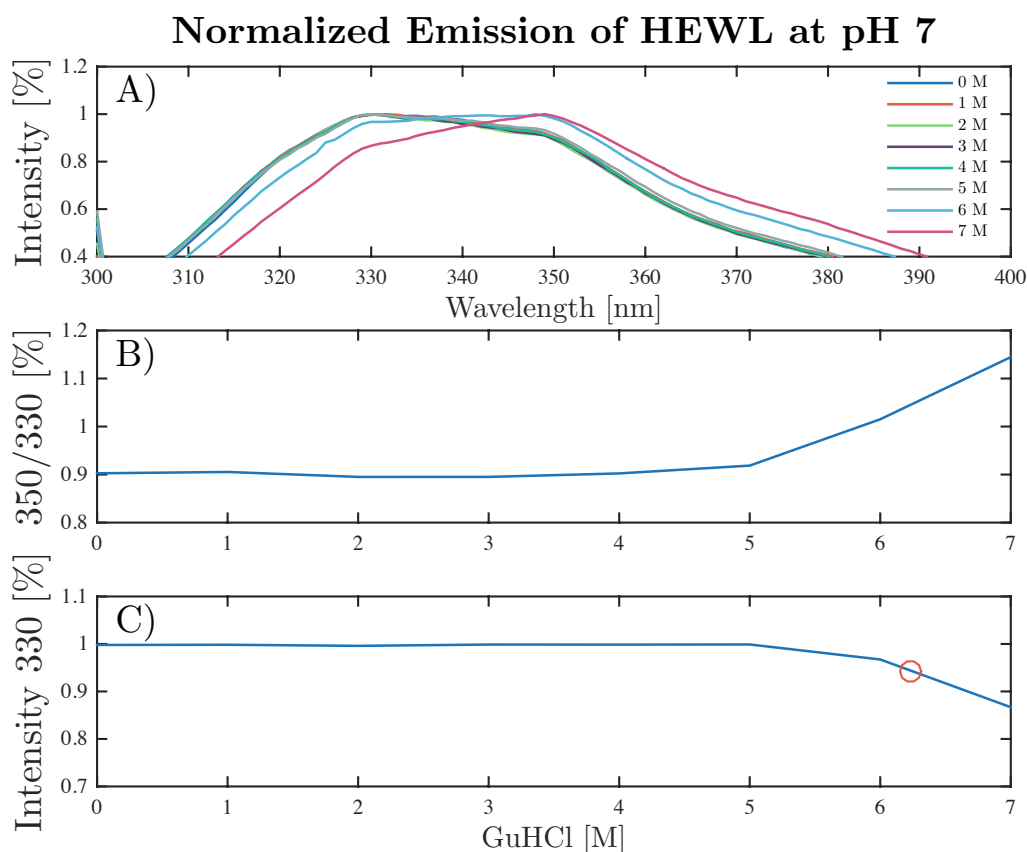


**Figure 8.16.** A) normalized emission spectra (300 - 400 nm) by fluorescence spectroscopy at pH 7 and 295 nm excitation of Tryptophan in HEWL showing the emission intensity at GuHCl concentrations from 0 - 7 M. B) the ratio between the wavelengths 350 and 330 nm derived from A) for each concentration of GuHCl. C) the normalized emission intensity at 330 nm as a function of increasing GuHCl concentration. The red circle indicates the transition point, which is  $[D_{50\%}] = 6.2286$  M GuHCl. It is observed that the maximum emission wavelength increases from 5 to 7 M GuHCl toward 350 nm, thus the emission intensity at 330 nm decreases at those concentrations.

In Figure 8.16, a significant change in maximum emission wavelength is observed, as it shifts from 330 toward 350 nm as the concentration of GuHCl increases. The change is observed from 6 to 7 M GuHCl in A) and 5 to 7 in B).

The red circle in C) is the determined transition point. The transition point was determined by the average concentration between 5 to 7 M GuHCl in the normalized emission intensity at 330 nm. The transition point is  $[D_{50\%}] = 6.2286$  M GuHCl, which, using Equation (4.10), means that  $\Delta G_{\text{solvent}} = 14.51$  kcal mol<sup>-1</sup>. It should be noted, that in order to determine the transition point, it is assumed, the the protein begins to denature at 5 M and is fully denatured at 7 M.

As for the CD spectroscopy measurements, Figure 8.17 shows the average of three CD spectra (190 - 250 nm) of 1.0 g/L HEWL solutions containing concentrations of GuHCl from 0 - 7 M at pH 7 and room temperature. Furthermore, Figure 8.17 shows the ellipticity at 222 nm as a function of increasing GuHCl concentration.

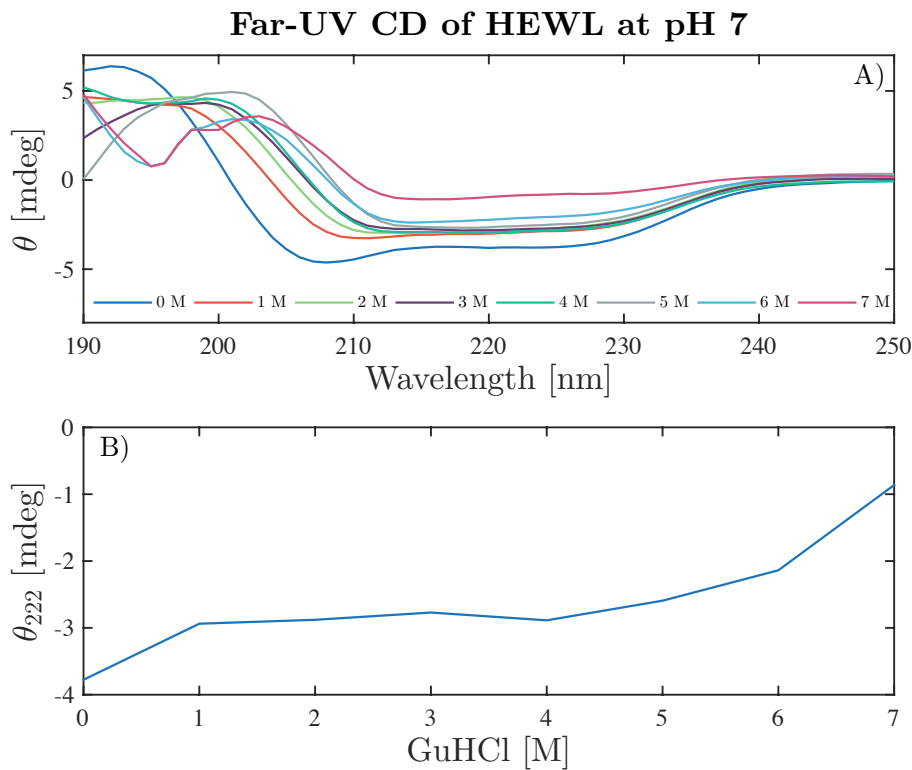


**Figure 8.17.** A) the average CD spectra (190 - 250 nm) of 1.0 g/L HEWL in solutions with GuHCl concentrations 0 - 7 M at pH 7 and room temperature showing ellipticity as a function of wavelength, and B) the average change in ellipticity at 222 nm as a function of increasing GuHCl concentration. It is observed that the 4 M GuHCl CD signal is slightly displaced, and that salt effects occur at wavelengths approximately of 205 nm and below. The observed tendency is that the ellipticity approaches zero as the GuHCl concentration increases.

In Figure 8.17, it is observed that the average 4 M GuHCl CD spectrum is slightly displaced in ellipticity as a function of wavelength since a chronological tendency should occur. It is also observed that some salt effects are occurring at wavelengths approximately 205 nm and below. Furthermore, it is observed that the ellipticity approaches zero as a function of increasing GuHCl concentration. Since the ellipticity approaches zero gradually, it is difficult to determine any transition point.

### 8.3.3 Sodium Carbonate Buffer: pH 10

In order to chemically denature HEWL at pH 10 by GuHCl, one emission scan (300 - 455 nm) was executed using steady-state fluorescence spectroscopy, measuring the emission intensity of Tryptophan as a function of wavelength for each concentration of GuHCl.

Figure 8.18 displays the average of three emissions scans carried out on 0.1 g/L HEWL at room temperature for each GuHCl concentration. Every emission scan was carried out at 295 nm excitation of Tryptophan.

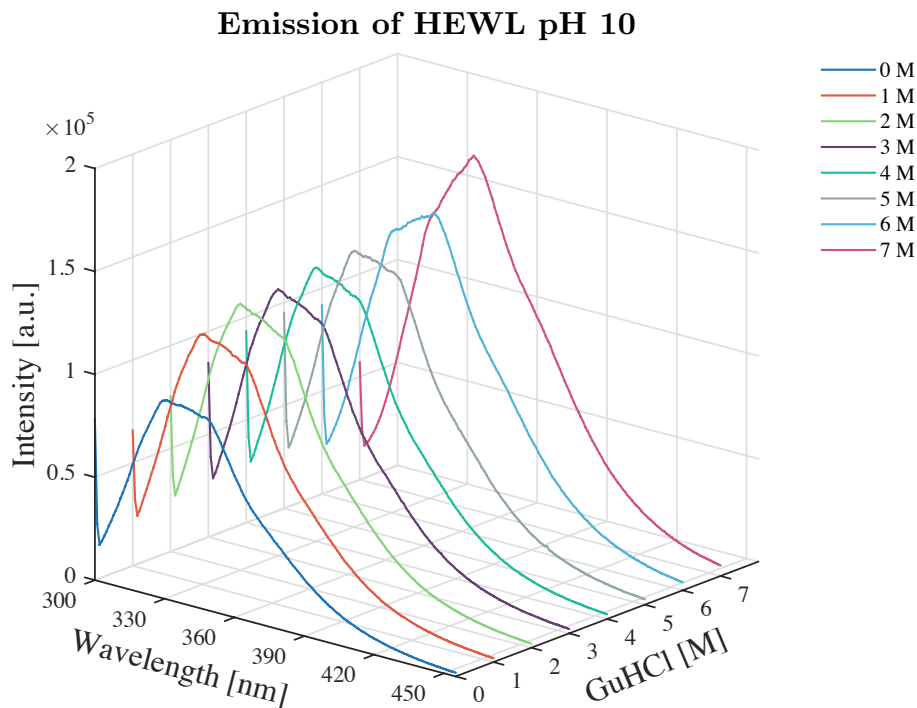


**Figure 8.18.** The average emission spectra (300 - 455 nm) by fluorescence spectroscopy at pH 10 and 295 nm excitation of Tryptophan in HEWL showing the emission intensity of 0.1 g/L HEWL solutions containing 0 - 7 M GuHCl. It is observed that the emission intensity increases as a function of increasing GuHCl concentration.

In Figure 8.18, it is observed that when the concentration of GuHCl increases, the emission intensity increases as well. Furthermore, a significant shift in maximum intensity wavelength occurs as the concentration of GuHCl increases.

In Figure 8.19, a normalized version of the emission spectra in Figure 8.18 is shown along with the ratio between the wavelengths 350 and 330 nm and the normalized intensity at 330 nm as a function of GuHCl concentration.

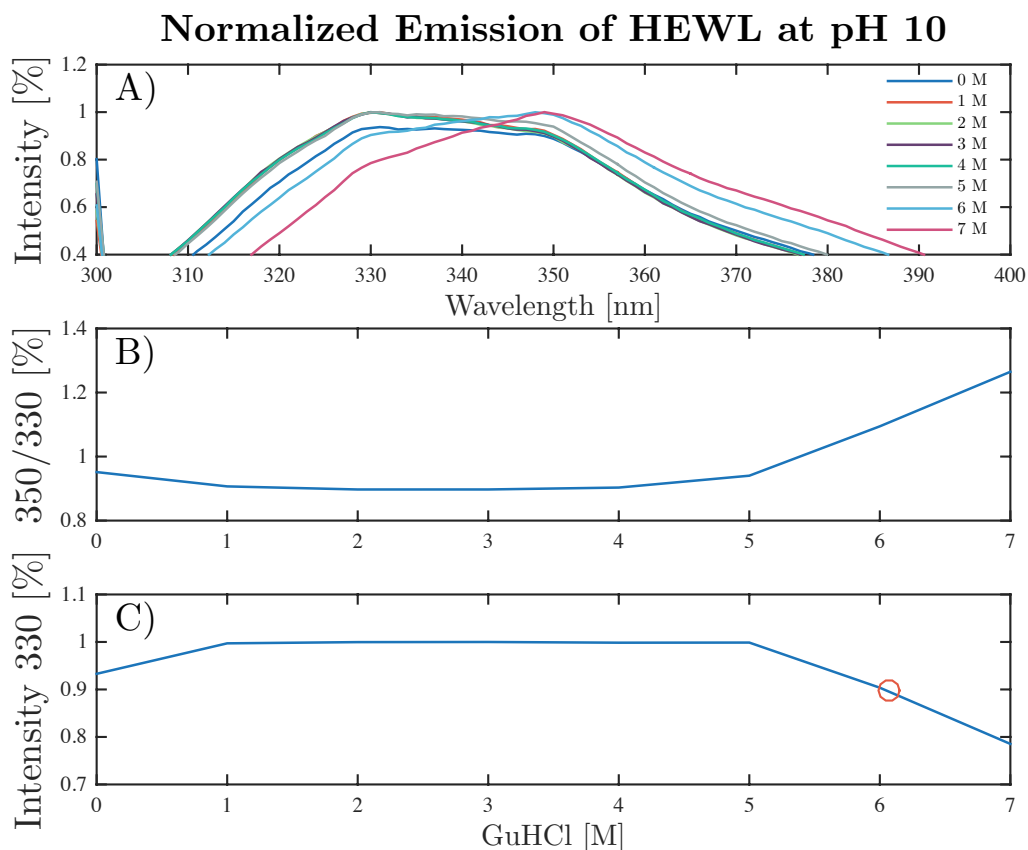


**Figure 8.19.** A) normalized emission spectra (300 - 400 nm) by fluorescence spectroscopy at pH 10 and 295 nm excitation of Tryptophan in HEWL showing the emission intensity at GuHCl concentrations from 0 - 7 M. B) the ratio between the wavelengths 350 and 330 nm derived from A) for each concentration of GuHCl. C) The normalized emission intensity at 330 nm as a function of increasing GuHCl concentration. The red circle indicates the transition point, which is  $[D_{50\%}] = 6.0656$  M GuHCl. It is observed that the maximum emission wavelength shifts from 330 nm toward 350 nm at concentrations above 5 M GuHCl, and that the emission intensity and ratio of the 0 M GuHCl solution is low compared to that of 1 to 4 M GuHCl.

In Figure 8.19, a significant change in maximum emission wavelength is observed, as it shifts from 330 toward 350 nm as the concentration of GuHCl increases. The change is observed from 6 to 7 M GuHCl in A) and 5 to 7 M in B). Furthermore, it is observed that the emission intensity of 0 M GuHCl is displaced in comparison to concentrations 1 to 4 M. The red circle in C) is the determined transition point. The transition point was determined by the average concentration between 5 to 7 M GuHCl in the normalized emission intensity at 330 nm. The transition point is  $[D_{50\%}] = 6.0656$  M GuHCl, which, using Equation (4.10), means that  $\Delta G_{\text{solvent}} = 14.13$  kcal mol<sup>-1</sup>. It should be noted, that in order to determine the transition point, it is assumed, the protein begins to denature at 5 M and is fully denatured at 7 M.

As for the CD spectroscopy measurements, Figure 8.20 shows the average of three CD spectra (190 - 250 nm) of 1.0 g/L HEWL solutions containing concentrations of GuHCl from 0 - 7 M at pH 10 and room temperature. Furthermore, Figure 8.20 shows the ellipticity at 222 nm as a function of increasing GuHCl concentration.

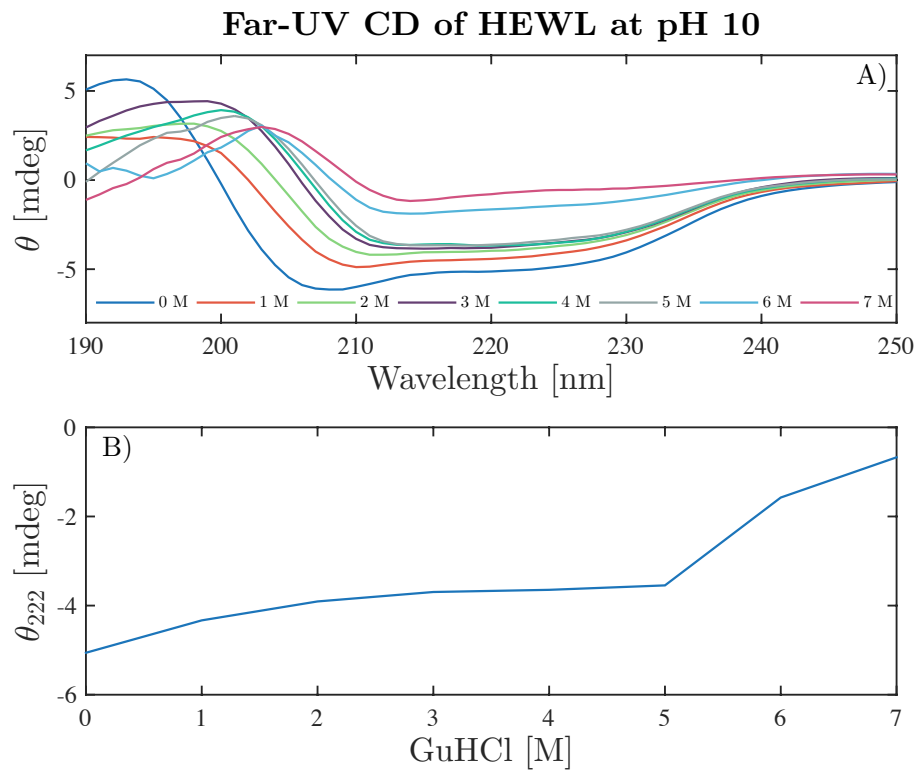


**Figure 8.20.** A) the average CD spectra (190 - 250 nm) of 1.0 g/L HEWL in solutions with GuHCl concentrations from 0 to 7 M at pH 10 and room temperature showing ellipticity as a function of wavelength, and B) the average change in ellipticity at 222 nm as a function of increasing GuHCl concentration. Salt effects are observed to occur at wavelengths of approximately 205 nm and below. The observed tendency is that the ellipticity approaches zero as the GuHCl concentration increases.

In Figure 8.20, it is observed that the ellipticity as a function of wavelength occurs as a chronological tendency. It is also observed that some salt effects occurs at wavelengths of approximately 205 nm and below. Furthermore, it is observed that the ellipticity approaches zero as a function of increasing GuHCl concentration. Since the ellipticity approaches zero gradually, it is difficult to determine any transition point.

## 8.4 Helical Content

In all experiments using CD spectroscopy, it is possible to calculate the helical content of HEWL during thermal and chemical denaturation using Equation (5.3). In Figure 8.21 the  $\alpha$ -helix content in HEWL during thermal and chemical denaturation is plotted for the native, heated, and refolded protein, and as a function of increasing GuHCl concentration, respectively.

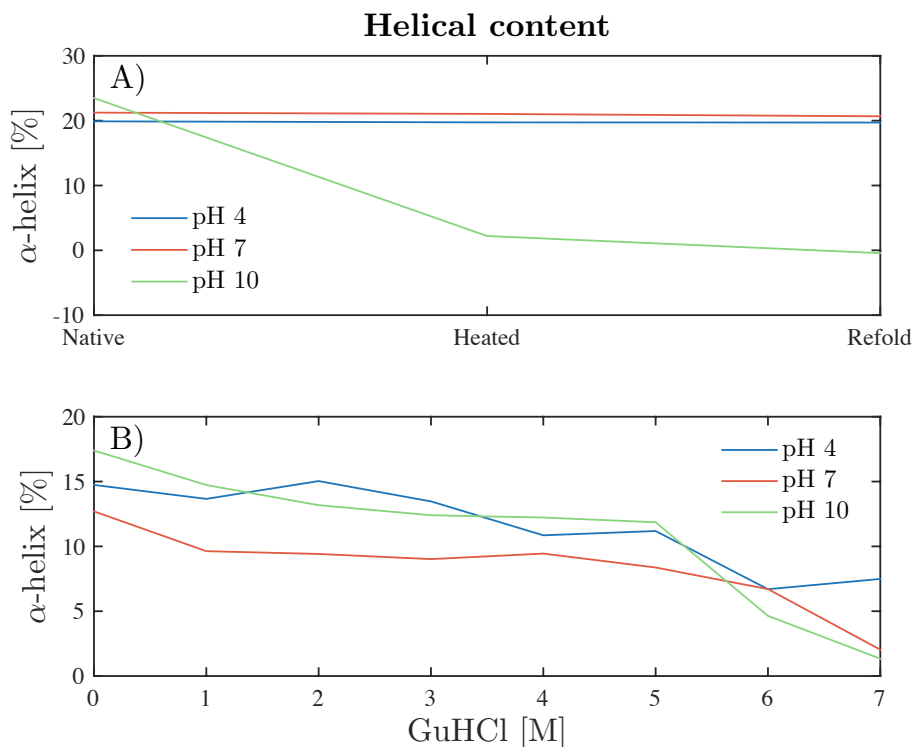


**Figure 8.21.** A) the  $\alpha$ -helix content in percent for the 0.1 g/L native HEWL solutions at room temperature, 0.1 g/L heated HEWL solutions heated at 80 °C for 5 minutes, and 0.1 g/L refolded HEWL solutions at 20 - 25 °C, which was heated at 80 °C for 5 minutes and naturally cooled for 30 minutes. It is observed that the helical content is unchanged at pH 4 and 7 during unfolding and refolding, where the content decreases at pH 10 when the protein is heated and refolded. B) the  $\alpha$ -helix content in percent for the 1.0 g/L HEWL solution as a function of increasing GuHCl concentration. It is observed that the helical content gradually decreases in each of the buffer solutions as the GuHCl concentration increases.

In Figure 8.21, it is observed that the  $\alpha$ -helix content is unchanged at pH 4 and 7 while heating and refolding, where the content decreases at pH 10 when the protein is heated and refolded during thermal denaturation. Furthermore, the  $\alpha$ -helix content in percent gradually decreases in each of the buffer solutions as the GuHCl concentration increases during chemical denaturation.

---

## 9. Discussion

---

### 9.1 Considerations in Relation to Buffer Solutions

As mentioned in Section 7.1, the buffer solutions were selected due to their pH range, water solubility, and pH stability during temperature changes. Thus they follow the criteria for buffers used in biochemistry set forth by Good *et al.* [71].

In order to minimize salt effects during CD spectroscopy measurements, the concentration of the buffer solutions were 1.0 mM. This proved effective in each of the three buffer solutions during thermal and chemical denaturation.

However, as seen in Table 8.1, the pH of the buffer solutions decreased significantly as the concentration of GuHCl was increased. Thus the low concentration of the buffer solution resulted in a buffer system not able to withstand the high concentrations of GuHCl, which is suspected to produce hydrogen chloride when dissolved, since the pH decreased drastically, especially at pH 10. Furthermore, the low concentration of buffer solutions resulted in that the ratio between denaturant and buffer solution was 7000 at the highest concentration of GuHCl.

Experiments involving protein stability normally utilizes concentrations of buffer solutions resulting in a ratio of 100. Dunbar *et al.*, Laurents *et al.*, and Makhatadze *et al.* applied buffer solutions with concentrations between 0.03 - 0.1 M, hence their ratios were between 70 and 700 [59, 72, 73].

The pH of the sodium carbonate buffer decreased by a maximum of 2.3, when GuHCl was added, which is a dramatic decrease, and the trend is persistent in the two other buffers as well, although not as dramatic. Lapanje *et al.* report similar results, as their pH values decrease with increasing concentration of GuHCl [74].

Chirgwin *et al.* have argued that the decrease in pH could have been minimized if the pH of the GuHCl stock solutions were adjusted toward a desired pH. They prepared GuHCl solutions with pH 7.5, which they adjusted with sodium citrate towards pH 7. After the adjustment, the solutions were stable for 1 month at room temperature without showing any change in pH [75]. Liu *et al.* adjusted their GuHCl solutions toward pH 4.5 by adding aqueous hydrogen chloride and sodium hydroxide [76]. This approach, by adjusting with sodium hydroxide, would account for the decrease in pH in the solutions containing GuHCl without increasing the buffer concentration, which could result in further salt effects. Another approach is to adjust the pH of the HEWL solutions tested by fluorescence and CD spectroscopy, however, the ratio between HEWL, buffer, and GuHCl would be inexact, and measurements would not be comparable.

Furthermore, in the case of sodium citrate and sodium carbonate, their optimal pH range is 3.0 - 6.2 and 9.2 - 10.8, respectively. Those ranges correspond to the pKa values of the acid in the buffers. However, a buffer is most stable and persistent in its optimal pH range, and since the sodium citrate and sodium carbonate buffer solutions were adjusted to pH 7.18 and 10.81, respectively, one could argue that those pH values are on the border of the optimal pH ranges of the buffers, thus resulting in less stability of the buffers.

Other buffers may have been better suited for the experiments performed in this project.

Instead of sodium citrate, Rashid *et al.* have applied sodium phosphate, which have a pH range between 5.8 and 8 [43]. Sodium phosphate is an excellent buffer, which works very well with CD spectroscopy measurements. Correa *et al.* reports that sodium phosphate can be used in CD spectroscopy measurements down to 190 nm in concentrations of 20 mM, and in measurements down to 200 nm in 100 mM concentrations [53]. Kelly *et al.* and Greenfield *et al.* agree, and recommend using sodium phosphate for CD spectroscopy measurements [10, 77]. Kelly *et al.* also recommend a borate buffer, which can be applied at pH 9.5, and will not display salt effects during the CD spectroscopy measurements [10]. Makki has applied a citric acid - sodium phosphate buffer in order to obtain pH 4 conditions [32].

## 9.2 Thermal Denaturation

Stock HEWL solutions were prepared as described in Chapter 7, and during the experiment period, HEWL dissolved in the sodium acetate buffer solution (pH 4) and the sodium citrate buffer solution (pH 7) revealed no aggregation, precipitation etc. after hours of storage and application. However, HEWL dissolved in the sodium carbonate buffer solution (pH 10) resulted from the moment of dissolution in a cloudy solution, suggested to originate from aggregates. This corresponds well with the fact that HEWL is stable in most acidic environments, but has limited stability in alkaline solutions, due to the reduction of at least one disulphide bond [12]. Although HEWL solutions were stored at 4 °C in order to slow denaturation caused by the pH conditions of the solutions, this was not a success considering the pH 10 buffer. However, the aggregation of HEWL at pH 10 occurred before storage, thus making storage conditions ineffective and irrelevant. On the other hand, storage conditions may have proved effective when considering HEWL at pH 4 and 7, since there were no aggregates, precipitates etc. observed in those solutions. However, this could be a result of HEWL's fine stability in acidic and neutral environments.

Each quartz cuvette applied during experiments were cleansed in 2 % Hellmanex, 70 % ethanol, and fresh Milli-Q water, in that order. This was done to minimize emission effects from other organic molecules, proteins, microorganisms, and HEWL from earlier measurements. However, it was observed in the 10.0 mm quartz cuvette, which was applied during fluorescence spectroscopy measurements (both thermal and chemical denaturation), that insoluble aggregates impossible to remove chemically and mechanically accumulated early onto the inner surface of the cuvette. This effect could interfere with emission measurements from Tryptophan. Furthermore, as to further minimize effects from other proteins, molecules, or microorganisms, pipette tips and buffer and GuHCl solutions were autoclaved at 121 °C, one bar above atmospheric pressure for 30 minutes. Some buffer solutions cannot be autoclaved, since they degrade upon heating. However, this should not be the case of sodium acetate, sodium citrate, or sodium carbonate buffer solutions, as no precipitation, discolouring etc. were observed after autoclaving. Autoclaving the GuHCl solutions should neither result in precipitation, discolouring etc., and no precipitation due to GuHCl should occur, since it is a salt. No precipitation, discolouring etc. were observed in the GuHCl solutions after autoclaving and storage at 4 °C. Furthermore, since no precipitation was observed in the GuHCl solutions, it is suggested that the buffers do not react with GuHCl, at least when considering precipitation. Every autoclaved solution was cooled down before application as to minimize thermal effects.

Plastic containers were used in all experiments, as proteins tend to adsorb in a lesser degree onto plastic than onto glass [78]. There is, however, still adsorption occurring, and this could have had a decreasing effect on the concentration of protein in the solutions throughout all experiments.

In order to thermally denature HEWL, the protein was presented with temperatures between 25 and 88 °C. This method resulted in denaturation being supposedly successful at pH 4 and pH 10. As is visible in Figure 8.9, the emission intensity of Tryptophan is decreasing as the temperature increases at pH 10, but at 69 °C a significant increase in the intensity is observed. This is likely the transition point. The decrease in emission intensity as a function of increasing temperature is most likely due to thermal quenching, as described in Section 6, where the water becomes a better quencher as the temperature increases, decreasing the emission intensity of Tryptophan. Another explanation is photobleaching. However, one can argue that any photobleaching effect is strongly minimized, since the sample was being stirred when measured upon, and a slit width of 3 nm was applied, meaning the intensity of light hitting the sample was not significantly great, thus photobleaching effects would be small or insignificant. The increase in intensity can be explained by protein denaturation. As the protein unfolds, Tryptophan is exposed to water, and although water is a quencher, it is less effective than the other residues and protein bonds in which Tryptophan has been in close relation to while folded. Hence the intensity of Tryptophan increases as the solvent becomes the primary quencher. As is visible in Figures 8.1 and 8.5, the emission intensity at pH 4 and 7 also decreases, however, this time throughout the entire experiment. The decrease is again explained by thermal quenching, although the emission intensity decreases significantly between 290 and 315 nm, and since there is no increase in emission intensity, HEWL is supposedly not successfully thermally denatured. However, in Figure 8.1 a small peak in the derivative of the emission is observed at 73 °C at pH 4. It is suggested that, at the center of the peak half of the proteins are denatured and the other half remain native (transition point). According to the literature, HEWL should denature at temperatures from 70 to 77 °C at pH values around 4 [28, 34, 79, 80]. The argument could therefore be made, that the protein is denatured at 73 °C, but it can also be seen, that the derivative begins to increase again as the temperature reaches 84 °C. This could mean that the protein begins to denature at 84 °C, but this is not possible to conclude based on the temperature ranges used in these experiments. Furthermore, HEWL is found to be most thermally stable at pH 5, according to the literature, but even at this pH value, Venkataramani *et al.* manages to denature the protein with temperatures of 71.9 °C [34].

The CD spectroscopy measurements yielded no evidence of any conformational changes in HEWL at pH 4 when heated toward 85 °C, as is evident from Figure 8.4, and from the non-existent change in  $\alpha$ -helix content, see Figure 8.21. Emission scans, visible in Figures 8.2 and 8.3, however, shows an expected change in emission intensity, and a small change in the ratio between the wavelengths 350 and 330 nm. Though small, the ratio indicates some change in the tertiary structure of the protein at pH 4. If the protein indeed begins to denature at 73 °C, as Figure 8.1 might suggest, it is interesting that it is only conformational changes to the tertiary structure of the protein which is observable. This could indicate some form of an intermediate structure resembling the MG, where the tertiary structure is disrupted, but the secondary structure resembles the native form.

According to theory, small proteins tend to form intermediates like the MG when thermally denatured [6]. There is still, however, a debate going as to whether this actually occurs in HEWL, see Chapter 4.

At pH 7, there are no significant peaks in the derivative of the emission intensity as a function of temperature, see Figure 8.5. According to several studies, HEWL should denature at a temperature ranging from 70 - 73 °C at pH 7. [28, 34, 70, 81], but this is not the case in these experiments. CD spectroscopy measurements yielded no indication of any changes in the secondary structure or the helical content of the protein, and the emission spectra at different temperatures revealed the same results as in pH 4. Again, a small change in the maximum emission wavelengths was observed, and so were corresponding changes in the emission intensity.

In contrast to the experiments at pH 7, the protein clearly did denature at pH 10. Although no studies denaturing HEWL at pH 10 could be found in order to obtain comparison, Makki mentions, that HEWL is dramatically less stable at higher pH values compared to the lower ones [32]. This conforms with this project, since HEWL is denatured at lower temperatures at pH 10 compared to pH 4. This, coupled with the fact that the pI for HEWL is at 11 [17], strengthens the argument that a protein is not necessarily most stable at its pI value. Furthermore, the fact that no studies using pH 10 could be found, stems from the fact that HEWL aggregates very easily at such high pH values [30].

CD spectroscopy measurements at pH 10 show a significant change in the secondary structure of the protein, and a dramatical loss in helical structure, going from around 20 % to almost no  $\alpha$ -helices at all. It should be noted, that when native, the helical content in all buffers were around 20 %, which partly conforms with the study by Chen *et al.*, who calculates it to be 24 % [56]. Moreover, there was not much refolding, and this could possibly be because of severe aggregation in the samples after measurements. This is supported by the emission spectra, visible in Figure 8.10, where the emission intensity of the spectrum is significantly altered after the protein is heated, and after refolding. As well as aggregation, many bubbles were observed in each of the three buffers after heating, which could contribute to the high intensity of the emission scan in the form of scattering. Aggregation of HEWL in the pH 10 solution conforms with the fact that HEWL is very unstable at such high pH values, and once aggregation has been onset, Buswell *et al.* argues that native proteins can be incorporated into aggregates during refolding [82].

The changes in heat capacity and enthalpy are two important factors in the denaturation of proteins. According to Gomez *et al.*, the heat capacity of a native and a denatured protein at the same temperature varies significantly, as the heat capacity of the denatured protein is higher than that of the native [83]. This is in agreement with the results presented in this project, as the heat capacity of HEWL was observed to increase by  $\Delta C_p = 3.75 \frac{\text{kJ}}{\text{K mol}}$ . The heat capacity of the denatured protein is higher than that of the native, due to the surface area between the hydrophobic residues and water increases, as the protein denatures. The enthalpy also increases, because of the energy transferred to the protein during heating of the solvent.

In relation to the experimental method used to thermally denature HEWL, it should be noted, that when the samples were heated toward 80 °C in order to measure the emission spectra of Tryptophan and CD spectra of the secondary structure, two different volumes were heated. For CD spectroscopy measurements, 0.9 mL was heated, and for emission scans, 1.5 mL was heated. This is suggested to result in, that the samples applied

during CD spectroscopy measurements had been heated more effectively, thus making denaturation more likely. The fact that no change was observed in the CD spectrum only contributes to the thermal stability of the secondary structure at pH 4 and 7.

### 9.3 Chemical Denaturation

In order to chemically denature HEWL, the protein was presented with denaturing conditions relying on concentrations of GuHCl in the range of 0 - 7 M. This range was selected on the basis of other studies which have chemically denatured HEWL in between these concentrations at different pH values [40, 41, 74, 84]. Furthermore, GuHCl is a well-known protein denaturant [44, 72, 76, 84], and during experiments, GuHCl had proven to be an excellent denaturant of HEWL in each of the three buffers in concentrations over 5 M.

In the case of chemical denaturation of HEWL at pH 4 and 10, it is observed that, as the concentration of GuHCl is increased, the emission intensity of Tryptophan increases as well, see Figures 8.12 and 8.18. An increase in intensity as a function of increased denaturant concentration, can be explained by quenching where unfolding and exposure of Tryptophan residues to water will induce an increase in emission intensity according to Khalifeh *et al.* [68]

As for HEWL at pH 7, a decrease in emission intensity is observed at 0 to 3 M GuHCl continued by an increase from 3 to 7 M GuHCl. Again, the increase from 3 M GuHCl is explained by the exposure of Tryptophan residues to water. However, the decrease in emission intensity from 0 to 3 M GuHCl is suspected to originate from the decrease in the pH of the solution. The pH of the solution decreased from 7.18 to 5.745 in 0 to 3 M GuHCl. Combining that HEWL is well known to be very stable in acidic conditions (pH 5), and that concentrations of 4 and 5 M GuHCl is a requirement for chemical denaturation [57], it is proposed that the acidity of GuHCl solutions contribute to a higher level of stability, which will decrease emission intensity as quenching of protein residues and bonds is increased. This effect, however, is neutralized and vanquished as the concentration of GuHCl approaches and exceeds the value of which it denatures HEWL.

At pH 10, the emission intensity is very low at 0 M GuHCl and the ratio between the wavelengths 350 and 330 nm is somewhat close to 1. At pH 10, the pH of the buffer decreased from 10.63 to 8.355 in 0 - 7 M GuHCl. Again one can argue, that transferring GuHCl to the HEWL solution decreases the pH, thereby increasing the stability of HEWL. This effect is, however, again neutralized and vanquished as the concentration of GuHCl approaches and exceeds the value of which it denatures HEWL. As for the radical increase in intensity from 0 to 1 M, it is suspected that the spectrum originates from an aggregated HEWL when comparing the intensity to that of Figure 8.18, which was also aggregated. Furthermore, according to Aune and Tandford the resultant volume of denatured HEWL is relatively small compared to that of other proteins [85]. This means that the residues are closer to each other than in most random coiled proteins, and that contact interactions between side chains are relatively frequent. This effect will, on the contrary to Khalifeh *et al.*, reduce the emission intensity of Tryptophan during denaturing, as residues are better quenchers. However, this effect must be relatively small since the emission intensity still increases as a function of increasing concentration of GuHCl at pH 4 and 10, and from 3 to 7 M GuHCl in pH 7. On the other hand, this increase may have been larger if the quenching effect of residues had been smaller.

One could argue that high concentrations of GuHCl may also exhibit some quenching effects in the solution. However, according to Pajot, choosing proper excitation wavelengths excludes effects of other fluorescing and absorbing groups or species. Thus choosing excitation of 295 nm, which is the excitation wavelength of Tryptophan, excludes effects from GuHCl. The emission of Tryptophan in solutions containing 6 M GuHCl did not show any change in fluorescence compared to solutions not containing GuHCl. [86]

It is observed in each of the three buffers that the maximum emission wavelength shifts from 330 toward 350 nm as the protein is chemically denatured by GuHCl. The shift occurs in all three buffers from 5 to 7 M GuHCl. This effect is the aforementioned red shift, which occurs as the exposed imide groups of Tryptophan form hydrogen bonds with surrounding water, changing the electron structure of the imide. Furthermore, the red shift effect is suggested to be an effect of solvent relaxation.

The transition points in the three buffers were 6.1238, 6.2286, and 6.0656 M, respectively. At this point, there exist equilibrium between the denatured and native HEWL. The values for the Gibbs Free Energy follows the tendency of the transition points.

According to Aune and Tandford, the concentration of GuHCl needed to denature HEWL decreases as the pH is reduced in a pH range of 1 - 8 [85]. This effect is observed in HEWL at pH 4 and 7. However, the changes are small and much smaller than the ones obtained by Aune and Tandford. In the case of HEWL at pH 10, the transition point is at its lowest concentration of GuHCl. This can be explained by the reduced stability of HEWL in alkaline environments. The effect may have been more profound if GuHCl did not decrease the pH of the protein solutions, thus enhancing protein stability. Furthermore, according to Pajot, HEWL requires a rather long period of time for denaturation by GuHCl. He suggests that an incubation time of 30 minutes at pH 8 is usually sufficient for most soluble proteins [86]. An incubation time of 30 minutes, instead of the applied 15 during experiments, may have elucidated the tendency in transitions points, and thus the Gibbs Free Energy of the protein in the three buffers would have been more segregated, and it would be easier to conclude on the stability of HEWL at different pH values.

In relation to the calculated Gibbs Free Energies, it should be noted that the  $m$  value used was the same for all three pH values, but, as stated in Section 4.2, the  $m$  value has been shown to depend heavily on pH values, and the one applied in this project were determined at pH 7 by Ahmad *et al.* [40]. Thus, these calculations can give rise to false interpretation of the stability at different pH values. It is well proven that HEWL is very stable at acidic conditions, but have a very limited stability in alkaline conditions, and the results obtained from experiments in this project show only a slight increase and decrease in stability at those conditions.

It is evident that the tertiary structure of HEWL indeed is affected by GuHCl in concentrations over 5 M from the emission spectrums of HEWL in each of the three buffers. As for the secondary structure of the HEWL, it is evident in the overall tendency from the CD spectroscopy measurements and determined  $\alpha$ -helix contents that GuHCl continuously influences the secondary structure of HEWL as well. In each of the three buffers, the ellipticity at 222 nm approached 0 due to the decreased difference in absorption of  $\mathcal{R}$ - and  $\mathcal{L}$ -CPL, which indicates that the proteins loose structure and chirality.

The tendency of the CD spectra to approach 0 in ellipticity, as the concentration of GuHCl increases, ought to be a chronological tendency since least ellipticity is expected in the so-

lution with highest concentration of GuHCl. However, at pH 4 and 7, containing 2, 5, and 7 M, and 4 M GuHCl, respectively, the ellipticity were slightly displaced. It was noted during experiments, as each measurement were repeated three times, that the observed tendency in each solution occurred somewhat random. Even though pipette tips and buffer and GuHCl solutions were autoclaved before application, and pipette tips were stored at 60 °C in order to keep them dry and free of growth of microorganisms, the tendency still occurred at random. The ellipticity is concentration dependent, thus only differences in concentrations of chiral molecules may displace a CD spectrum. However, if pipette tips and solutions were autoclaved and the risk of microorganisms and other proteins minimized, then the aberration must be found in preparation of the solutions themselves. Buffer, GuHCl, and HEWL were diluted in order to obtain 1.0 g/L HEWL, 1.0 mM buffer, and 0 - 7 M GuHCl in each tested solution. However, some problems occurred in the accuracy of one of the Eppendorf pipettes during the experiment period, and it is unknown if these problems have resulted in random concentrations of protein in the solutions. In order to deal with the problem at the time, some of the Eppendorf pipettes were tested by weighting volumes of water, and only small aberrations were observed. Other possible explanations could include wrong concentrations of HEWL due to wrongly calculated volumes, or simply the uncertainty of man work. However, calculated values were confirmed more than twice, and the dilution of solutions into right concentrations was carefully double checked throughout the experiments. The randomness of the displacement of CD spectra can therefore only be explained by two things. The inaccuracy of Eppendorf pipettes and the pipetting by hand, or that some solutions may have become contaminated by microorganisms or other proteins. One last approach to the randomness of the CD spectra is the applied 0.10 mm quartz cuvette. The cuvette was applied in order to minimize salt effects of GuHCl. However, when the optical path length is very small, the measurements are very sensitive to concentration variations of HEWL, both local, or due to aforementioned inaccurate metering. Local concentration aberrations may have been excluded if more accumulations were applied along with more repetitions of the experiment. Furthermore, it was difficult to exclude bubbles from the sample, but it was established, that no large visible bubbles were at the center of the cuvette. As two optical quartz plates comprise the cuvette, which then is compressed by hand before measurement, it was uncertain if any fingerprints, or other contamination occurred on the outer site of the cuvette. However, gloves were worn throughout the experiments, but this does not exclude this uncertainty entirely.

One could argue that when measuring with UV light, the protein may become denatured by the light rather than denaturants. However, in fluorescence spectroscopy the samples were only measured for about 3 minutes and approximately 13 minutes at CD spectroscopy. The intensity of the incident light was only 150 W where a slit width of 3 nm was applied. Thus UV denaturation is insignificant and ignored. However, the intensity of the incident light was not determined during the experiment period.

GuHCl affects both the tertiary and the secondary structure of HEWL. The effect is attributed to several denaturing factors. Firstly, GuHCl is suggested to participate in hydrogen bonds with water and self-associate in a stacking fashion, which ultimately disrupts the hydrophobic interactions of the protein, thus destabilizing it. Furthermore, in

high concentrations of GuHCl, the solvent is supplied with a high ionic strength, which may increase electrostatic interactions between the pH induced charged amino acids of the protein and GuHCl. Lastly, as GuHCl is introduced into the system, the dielectric constant of the solution will increase as the polarity of the solvent increases, and it will minimize ionic interactions between the proteins. According to Harrison *et al.*, the increase in dielectric constant will favour salting out effects, leading to aggregation and precipitation of the protein [46]. However, according to the Hofmeister series, the guanidium ion is a strong salting in ion that denatures proteins, which also is the obtained tendency by the experiments. One can then argue, that since each guanidium ion participates in 4.5 hydrogen bonds, on average, with water, the polarization effect of GuHCl is decreased and the hydrogen layer surrounding the protein is relaxed. Moreover, according to Chaplin, the dielectric constant of water will decrease if the hydrogen bonding network is weakened, and one could argue that this is the method of attack of the guanidium ion [87]. This conforms with the fact that the surface tension of water also decreases as the hydrogen bonding network is weakened, and this is suggested by the Hofmeister series to be one of the denaturation effects by salting in ions. Although one could argue, that the dielectric constant of water, after all, is unaffected or decreased by GuHCl even though it is a salt, thus favouring denaturation over aggregation and precipitation. No studies have been found in order to confirm this argument.

One could argue that, as the tertiary and secondary structure is disrupted in each of the three buffer solutions, the protein, in at least 7 M, is completely unfolded, thus a random coil. This corresponds to the theory that small proteins often are converted into a random coil in high concentrations of denaturant. On the other hand, at the high concentrations, 6 to 7 M GuHCl in each of the buffer solutions, the protein maintain some structure and chirality. This effect is clear at pH 4 where 6 to 7 M, although 7 M is slightly displaced, contain some sort of chirality, see Figure 8.14. At pH 7, the effect is only observed for 7 M GuHCl, see Figure 8.17, and at pH 10 the effect is less obvious, see Figure 8.20.

In a CD spectra of random coils, see Figure 5.3, it is observed that random coils have some chiral quality. This observation can explain why HEWL at high concentrations of GuHCl maintain some structure while being a random coil. Furthermore, a CD spectrum is a linear combination of CD signals from random coils,  $\alpha$ -helices, and  $\beta$ -structures. Thus one could argue that, as the concentration of denatured proteins, which are supposed random coils, is increased during denaturation, the CD spectra of HEWL will approach zero since the ellipticity, when measuring random coils, are close to and exceeds zero at wavelengths where the ellipticity is highest for  $\alpha$ -helices and  $\beta$ -structures.

However, according to Vernaglia *et al.*, which have obtained similar results to this project, when HEWL is fully denatured, at 4 and 5 M GuHCl at pH 6 to 7, the protein still contains some residual structure due to the presence of the four disulphide bonds, and thus full denaturation of HEWL results in a partially unfolded protein [57]. Furthermore, Imoto *et al.* have reported that HEWL is not completely unfolded in 5 M GuHCl at pH 5 [62]. If this is true, then HEWL, when presented with high concentrations of GuHCl, may form some intermediate structure rather than the random coil. Both Vernaglia *et al.* and Aune and Tanford reports that the denatured structure of HEWL is a random coiled polypeptide chain cross-linked by disulphide bonds, but maintains no fixed non-covalent interactions [57, 85]. Thus proteins containing disulphide bonds are never true

random coils when denatured by GuHCl, as GuHCl does not affect those bonds. This could explain why, in each of the three buffers, even at high concentrations of GuHCl, the proteins maintain some structural ordering and chirality. They are simply not fully denatured into a true random coil, but rather a partially unfolded structure. This is an important notion if one will want to induce fibrillar-HEWL.

There is a divide, where some, argue that HEWL can form a MG like structure at mild denaturation conditions [5, 15, 16, 88], other argue that it does not form any intermediate [19, 20, 21, 85]. However, Hameed *et al.* reports that MG structures of HEWL do not occur in solutions with pH 1 - 11, but is obtained at pH 11.75, and a fully denatured random coil is obtained at pH 13.2 due to loss of disulphide bonds. Furthermore, they report that a decrease in ellipticity is observed when measuring the MG structure by CD spectroscopy, suggesting loss of secondary structure without affecting the basic format compared to the native protein. They also report that 6 M GuHCl at pH 11.75 completely unfolds the HEWL protein like pH 13.2. Thus one could argue that at pH 10 in high concentrations of GuHCl, HEWL might be fully denatured into a random coil without disulphide bonds. In each of the three buffers, the ellipticity approaches zero as the GuHCl concentration is increased, however, 1 to 3 M at pH 4, 1 to 6 M at pH 7, and 1 to 5 M at pH 10 shows only a slight increase and the curves maintain most of their basic format. Initially, this made it difficult to determine transition points from the CD spectra, and secondly it could represent an MG-like structure since there exists mild denaturing conditions in most cases, and since most of the secondary structure is maintained. However the maximum emission wavelength in these concentrations suggest that the tertiary structure seems somewhat unaffected, at least when including the normalized emission spectra. Lastly, Bhattacharjya *et al.* suggest that the MG structure presents Tryptophan with an environment not very different from that of the native, and this effect was especially significant at low pH values. However, the emission intensity of Tryptophan was observed to gradually increase in these concentrations, with exception of 0 to 3 M GuHCl at pH 7, which could indicate a change in the tertiary structure due to change in main quenchers.

Whether a MG-like structure is obtained or the results indicate a partially denatured HEWL maintaining only disulphide bonds in some solutions, is unclear. Some supporters of the MG theory will conclude, that the results indicate MG-like structures due to the maintained basic format of ellipticity and GuHCl concentrations. Others will argue that the pH and the intensity, along with the CD spectroscopy measurements and change in maximum emission wavelength, only results in a denatured HEWL in the form of a random coil, which have retained its four disulphide bonds. However, it is clear that some interruption of both the secondary and the tertiary structure occurred while chemically denaturing HEWL by GuHCl.

## 9.4 Further Studies

Other methods often used for studying proteins are able to give important information about the stability and kinetics of the protein.

In this project, CD spectroscopy was used to study the secondary structure of HEWL. However, fourier transform infrared spectroscopy (FTIR) could also be used for the same goal. FTIR uses infrared light (IR) instead of UV light, which would eliminate any interference by UV light. In relation to the concentrations of proteins, FTIR can measure

samples with concentrations of 200 g/L, which is significantly higher than anything possible to measure upon using CD spectroscopy. For this particular reason, FTIR is a useful tool when investigating aggregates of proteins, which often occur at high concentrations. Although the problems with UV are minimized, and higher concentrations of protein are possible to measure, it is important to have in mind, that IR light causes energy to build up in the sample leading to evaporation. This can cause the hydration level in the sample to decrease, which means the concentration of the protein would increase. To eliminate the interference from both UV and IR light, both methods could be utilized and compared. [89]

If FTIR was applied in this project, it would have been possible to observe additional characteristics of the aggregates which was observed, when HEWL was heated at pH 10. To investigate the kinetics of the interactions between the protein and GuHCl, a technique termed Stopped-Flow can be utilized. This technique is used in many different spectroscopy methods such as FTIR, CD, and fluorescence and is popular for studying proteins. One would start a flow of two solutions and mix them inside the spectrophotometer. The flow then stops, allowing the solutions to react in a specific amount of time. After the reaction, a new solution is introduced in order to stop the reaction, or the measurement is simply stopped. With this technique it is possible to study the events which occur when the two solutions react. This technique has many applications such as to study refolding of a protein, the interactions with a denaturant, or the effects of a certain pH value. In this project, only the effects of the reaction between GuHCl and HEWL were observed after 15 minutes, whereas, using Stopped-Flow, it would be possible to uncover details about how they interact, during the reaction, continuously. [90]

The thermodynamics of proteins are of particular interest, and many forms of calorimetry can provide vital insight, not otherwise obtainable. Using calorimetry, it is possible to directly observe the specific heat capacity of a protein during specific reactions. The heat capacity, and how it changes during a reaction, can provide much information about the thermodynamics of a protein, and thus the stability of it. Two methods of calorimetry are; differential scanning calorimetry (DSC), which measures the heat capacity in relation to a reference as a function of temperature, and isothermal titration calorimetry (ITC), which measures the heat evolution during titration. The DSC could be used as temperature experiments to observe how the heat capacity changes throughout thermal denaturation of HEWL. In this project, DSC would give additional, more precise information about the heat capacity. ITC could be used to observe the heat capacity, when titrating HEWL with GuHCl. [91]

As stated in Chapter 2, a medically very interesting field in the study of protein stability and folding is amyloid fibrillation. It is evident from several studies, that an easy way to create, and thereby study amyloid fibrils, is by having proteins, in a partially folded state, aggregate in this particular manner. According to the results presented in this project, it would seem, that it would be necessary to employ either a specific temperature corresponding to a partially unfolded state in the sample, a concentration of GuHCl, also corresponding to this state of stability, or a combination of the two. According to the results in this project, HEWL would be too unstable at pH 10, and too stable at pH 7. At pH 4, the protein seemed to be denatured at high temperatures in some experiments, but still maintaining a stable secondary structure in other experiments. It would seem,

based on these results, that heating HEWL at a pH around 4 perhaps, combined with some concentration of GuHCl, would be ideal for fibrillation. According to the literature, various pH values have been tested, and a study done by Arnaudov *et al.* suggests that the optimal pH range for creating fibrils is between pH 2 - 4 [58]. This conforms with the fact, that at pH 4, HEWL should be very thermally stable. Vernaglia *et al.* however, used pH 6.5, and they could induce fibril formation in HEWL in under 2 hours using 3 M GuHCl at 50 °C. They confirmed the formation of fibrils using transmission electron microscopy, atomic force microscopy, and fluorescence spectroscopy utilizing the fluorescence of Thioflavin T. [57]

As far as the temperature goes, this project is not able to predict what temperature is optimal, if a pH value around 7 was used for fibrillation, as in the study by Vernaglia *et al.*. It could be wise to rely on their method, which did produce amyloid fibrils in a short time, using 50 °C. [57]

In relation to the concentration of denaturant, however, this project can provide some insight, as it was possible to denature HEWL at pH 7 using concentrations up to 7 M GuHCl. It was, however, around a concentration of 5 M, that the protein began to denature, and when the denaturant is used in combination with temperature, it might be best not to use excessive concentrations. Too high concentrations of denaturants can, as studied before, break down the fibrils. This partly conforms with the study by Vernaglia *et al.*, who uses a concentration of 3 M, which they show to be optimal for fibrillation of HEWL. [57]

Another interesting method for producing fibrils is suggested by Krebs *et al.*, who study the effects of seeds, parts of fibrils added to the proteins, on the time scale of fibrillation. They found, that using seeds could significantly speed up the fibrillation process [92]. Arnaudov *et al.* were able to create fibrils using incubation at 57 °C for 13 days at pH 2. They confirmed their results using atomic force microscopy and transmission electron microscopy. [58]

In summation, it is clearly possible to produce amyloid fibrils using a combination of the different denaturing environments introduced in this project.



---

## 10. Conclusion

---

In this project, the aim was to determine the stability of HEWL, using thermal and chemical denaturation. After being evaluated, the stability should be able to yield information concerning the creation of amyloid fibrils, which is an important field of medical research.

HEWL was arguably found to denature at 73 °C at pH 4, and it clearly denatured at 69 °C at pH 10. At pH 7 however, thermal denaturation was unsuccessful. This is in conformation with the current literature, apart from the fact that HEWL did not denature at pH 7. According to various studies, the most stable pH value of HEWL is pH 5, thus HEWL should denature more easily at pH 7 than at pH 4.

The chemical denaturation was carried out using GuHCl as a denaturant at all three pH values. At pH 4, the transition point was calculated to be at 6.1238 M GuHCl. The experiments yielded similar results in the other pH values, with the transition point being at 6.2286 M GuHCl at pH 7 and 6.0656 M at pH 10. This points to HEWL being most unstable in pH 10 and most stable between pH 4 and 7, although the differences are very small, which conforms with the literature.

The results yield information about the stability of HEWL, which can be utilized when producing amyloid fibrils. Amyloid fibrils are produced in mildly denaturing environments, which favour a partially unfolded state of HEWL. According to the experiments done in this project, these conditions should be present at pH 4, 5 M GuHCl, and a temperature a little under 69 °C. This partly conforms with the literature, that suggests using pH 6.5 or 7, since HEWL is too stable at pH 4.



---

# Bibliography

---

- [1] Christopher M Dobson. Principles of protein folding, misfolding and aggregation. In *Seminars in cell & developmental biology*, volume 15, pages 3–16. Elsevier, 2004.
- [2] Thomas R Jahn and Sheena E Radford. The yin and yang of protein folding. *Febs Journal*, 272(23):5962–5970, 2005.
- [3] Leila M Luheshi and Christopher M Dobson. Bridging the gap: from protein misfolding to protein misfolding diseases. *FEBS letters*, 583(16):2581–2586, 2009.
- [4] Biao Cheng, Hao Gong, Hongwen Xiao, Robert B Petersen, Ling Zheng, and Kun Huang. Inhibiting toxic aggregation of amyloidogenic proteins: a therapeutic strategy for protein misfolding diseases. *Biochimica et Biophysica Acta (BBA)-General Subjects*, 1830(10):4860–4871, 2013.
- [5] Dennis J Selkoe. Folding proteins in fatal ways. *Nature*, 426(6968):900–904, 2003.
- [6] Alexei V Finkelstein and Oleg Ptitsyn. *Protein physics: a course of lectures*. Academic Press, 2002.
- [7] L Stryer. *Biochemistry, 7th edition*. WH Freeman and Co., New York, NY, 2012.
- [8] Paul M Dewick. *Essentials of organic chemistry: for students of pharmacy, medicinal chemistry and biological chemistry*. John Wiley & Sons, 2006.
- [9] Frank Albert Cotton, Geoffrey Wilkinson, Paul L Gaus, and Rosa Bryant. *Basic inorganic chemistry*, volume 1. Wiley New York, 1995.
- [10] Sharon M Kelly and Nicholas C Price. The use of circular dichroism in the investigation of protein structure and function. *Current protein and peptide science*, 1(4):349–384, 2000.
- [11] Claude Sauter, Fermin Otalora, Jose Antonio Gavira, Olga Vidal, Richard Giege, and Juan Ma Garcia-Ruiz. Structure of tetragonal hen egg-white lysozyme at 0.94 Å from crystals grown by the counter-diffusion method. *Acta Crystallographica Section D: Biological Crystallography*, 57(8):1119–1126, 2001.
- [12] P Michael Davidson, John N Sofos, and A Larry Branen. *Antimicrobials in food*. CRC press, 2005.
- [13] James D Gunton, Andrey Shirayayev, and Daniel L Pagan. *Protein condensation: kinetic pathways to crystallization and disease*. Cambridge university press, 2007.
- [14] The Scop authors. Protein: Lysozyme from chicken (callus gallus). Scop database, 06 2009.
- [15] OB Ptitsyn and VN Uversky. The molten globule is a third thermodynamical state of protein molecules. *FEBS letters*, 341(1):15–18, 1994.

- 
- [16] OB Ptitsyn, Roger H Pain, GV Semisotnov, E Zerovnik, and OI Razgulyaev. Evidence for a molten globule state as a general intermediate in protein folding. *FEBS letters*, 262(1):20–24, 1990.
- [17] Mahrukh Hameed, Basir Ahmad, Khalid Majid Fazili, Khurshid Andrabi, and Rizwan Hasan Khan. Different molten globule-like folding intermediates of hen egg white lysozyme induced by high pH and tertiary butanol. *Journal of biochemistry*, 141(4):573–583, 2007.
- [18] Takatoshi Ohkuri and T Tadashi Imoto, Taiji Imoto. Characterization of refolded hen egg lysozyme variant lacking two outside disulfide bonds. *Bioisci. Biotechnol. Biochem.*, 2005.
- [19] Jui-Yoa Chang and Li Li. The unfolding mechanism and the disulfide structures of denatured lysozyme. *FEBS letters*, 511(1):73–78, 2002.
- [20] Els Pardon, Petra Haezebrouck, Annie De Baetselier, Shaun D Hooke, Katherine T Fancourt, Johan Desmet, Christopher M Dobson, Herman Van Dael, and Marcel Joniau. A  $Ca^{2+}$ -binding chimera of human lysozyme and bovine  $\alpha$ -lactalbumin that can form a molten globule. *Journal of Biological Chemistry*, 270(18):10514–10524, 1995.
- [21] Shintaro Sugai and Masamichi Ikeguchi. Conformational comparison between  $\alpha$ -lactalbumin and lysozyme. *Advances in biophysics*, 30:37–84, 1994.
- [22] Donald Templeton Haynie. *Biological thermodynamics*. Cambridge University Press, 2001.
- [23] Rodney Cotterill. *Biophysics: an introduction*. John Wiley & Sons, 2003.
- [24] Charlotte W Pratt and Kathleen Cornely. *Essential biochemistry*. Wiley Global Education, 2012.
- [25] Bengt Noeltig. *Protein folding kinetics: biophysical methods*. Springer Science & Business Media, 2005.
- [26] Mikael Oliveberg, Stephane Vuilleumier, and Alan R Fersht. Thermodynamic study of the acid denaturation of barnase and its dependence on ionic strength: evidence for residual electrostatic interactions in the acid/thermally denatured state. *Biochemistry*, 33(29):8826–8832, 1994.
- [27] C Nick Pace and J Martin Scholtz. Measuring the conformational stability of a protein. *Protein structure: A practical approach*, 2:299–321, 1997.
- [28] Shigeki Arai and Mitsuhiro Hirai. Reversibility and hierarchy of thermal transition of hen egg-white lysozyme studied by small-angle x-ray scattering. *Biophysical journal*, 76(4):2192–2197, 1999.
- [29] Alice Blumlein and Jennifer J McManus. Reversible and non-reversible thermal denaturation of lysozyme with varying pH at low ionic strength. *Biochimica et Biophysica Acta (BBA)-Proteins and Proteomics*, 1834(10):2064–2070, 2013.

- [30] Michael Schaefer, Michael Sommer, and Martin Karplus. pH-dependence of protein stability: Absolute electrostatic free energy differences between conformations. *The Journal of Physical Chemistry B*, 101(9):1663–1683, Feb 1997.
- [31] K Linderström-Lang. On the ionization of proteins. *CR Trav Lab Carlsberg*, 15(7):1–29, 1924.
- [32] Farid Makki. *Thermal Inactivation Kinetics of Lysozyme and Preservative Effect in Beer*. PhD thesis, University of British Columbia, 1996.
- [33] Madaisy Cueto, M Jesús Dorta, Obdulia Mungu, et al. New approach to stability assessment of protein solution formulations by differential scanning calorimetry. *International journal of pharmaceuticals*, 252(1):159–166, 2003.
- [34] Sathyadevi Venkataramani, Jeremy Truntzer, and Denis R Coleman. Thermal stability of high concentration lysozyme across varying pH: A fourier transform infrared study. *Journal of pharmacy & bioallied sciences*, 5(2):148, 2013.
- [35] C Pace, Roy W Alston, and Kevin L Shaw. Charge–charge interactions influence the denatured state ensemble and contribute to protein stability. *Protein science*, 9(07):1395–1398, 2000.
- [36] Giovanni Salvi, Paolo De Los Rios, and Michele Vendruscolo. Effective interactions between chaotropic agents and proteins. *Proteins: Structure, Function, and Bioinformatics*, 61(3):492–499, 2005.
- [37] Donald B. Watlafer, Sunit K. Malik, Leon. Stoller, and Ronald L. Coffin. Nonpolar group participation in the denaturation of proteins by urea and guanidinium salts. model compound studies. *Journal of the American Chemical Society*, 86(3):508–514, Feb 1964.
- [38] Ronald Breslow and Tao Guo. Surface tension measurements show that chaotropic salting-in denaturants are not just water-structure breakers. *Proceedings of the National Academy of Sciences*, 87(1):167–169, 1990.
- [39] Gavin R. Hedwig, Terence H. Lilley, and Helen Linsdell. Calorimetric and volumetric studies of the interactions of some amides in water and in 6 mol dm<sup>-3</sup> aqueous guanidinium chloride. *Faraday Trans.*, 87(18):2975, 1991.
- [40] Faizan Ahmad and Charles C Bigelow. Estimation of the free energy of stabilization of ribonuclease a, lysozyme, alpha-lactalbumin, and myoglobin. *Journal of Biological Chemistry*, 257(21):12935–12938, 1982.
- [41] Saeed Emadi and Maliheh Behzadi. A comparative study on the aggregating effects of guanidine thiocyanate, guanidine hydrochloride and urea on lysozyme aggregation. *Biochemical and biophysical research communications*, 450(4):1339–1344, 2014.
- [42] DJ Haas, DR Harris, and HH Mills. The crystal structure of guanidinium chloride. *Acta crystallographica*, 19(4):676–679, 1965.

- 
- [43] Fouzia Rashid, Sandeep Sharma, and Bilqees Bano. Comparison of guanidine hydrochloride (gdnhcl) and urea denaturation on inactivation and unfolding of human placental cystatin (hpc). *The protein journal*, 24(5):283–292, 2005.
- [44] Farshad Rahimpour and Mohsen Pirdashti. The effect of guanidine hydrochloride on phase diagram of peg-phosphate aqueous two-phase system. *International Journal of Chemical & Biomolecular Engineering*, 1(1), 2008.
- [45] Robert L Baldwin. How hofmeister ion interactions affect protein stability. *Biophysical journal*, 71(4):2056, 1996.
- [46] Roger Harrison. *Protein purification process engineering*, volume 18. CRC Press, 1993.
- [47] Lorenz M Mayr and Franz X Schmid. Stabilization of a protein by guanidinium chloride. *Biochemistry*, 32(31):7994–7998, 1993.
- [48] Philip E Mason, George W Neilson, John E Enderby, Marie-Louise Saboungi, Christopher E Dempsey, Alexander D MacKerell, and John W Brady. The structure of aqueous guanidinium chloride solutions. *Journal of the American Chemical Society*, 126(37):11462–11470, 2004.
- [49] Jinbing Xie, Meng Qin, Yi Cao, and Wei Wang. Mechanistic insight of photo-induced aggregation of chicken egg white lysozyme: The interplay between hydrophobic interactions and formation of intermolecular disulfide bonds. *Proteins: Structure, Function, and Bioinformatics*, 79(8):2505–2516, 2011.
- [50] Ling-Zhi Wu, Yue-Biao Sheng, Jin-Bin Xie, and Wei Wang. Photoexcitation of tryptophan groups induced reduction of disulfide bonds in hen egg white lysozyme. *Journal of Molecular Structure*, 882(1):101–106, 2008.
- [51] Bernard Valeur and Mário Nuno Berberan-Santos. *Molecular fluorescence: principles and applications*. John Wiley & Sons, 2012.
- [52] Eugene Hecht and A Zajac. *Optics 4th (International) Edition*. 2002.
- [53] Daniel HA Correa and Carlos HI Ramos. The use of circular dichroism spectroscopy to study protein folding, form and function. *African J Biochem Res*, 3(5):164–173, 2009.
- [54] Jonathan D Hirst and Charles L Brooks. Helicity, circular dichroism and molecular dynamics of proteins. *Journal of molecular biology*, 243(2):173–178, 1994.
- [55] EA Roman, J Santos, and FL Gonzalez-Flecha. The use of circular dichroism methods to monitor unfolding transitions in peptides, globular and membrane proteins. *Circular Dichroism, Theory and Spectroscopy*, pages 217–254, 2011.
- [56] Yee-Hsiung Chen, Jen Tsi Yang, and Hugo M Martinez. Determination of the secondary structures of proteins by circular dichroism and optical rotatory dispersion. *Biochemistry*, 11(22):4120–4131, 1972.

- [57] Brian A Vernaglia, Jia Huang, and Eliana D Clark. Guanidine hydrochloride can induce amyloid fibril formation from hen egg-white lysozyme. *Biomacromolecules*, 5(4):1362–1370, 2004.
- [58] Luben N Arnaudov and Renko de Vries. Thermally induced fibrillar aggregation of hen egg white lysozyme. *Biophysical journal*, 88(1):515–526, 2005.
- [59] DV Laurents and RL Baldwin. Characterization of the unfolding pathway of hen egg white lysozyme. *Biochemistry*, 36(6):1496–1504, 1997.
- [60] Yu Chen and Mary D Barkley. Toward understanding tryptophan fluorescence in proteins. *Biochemistry*, 37(28):9976–9982, 1998.
- [61] Joseph R Lakowicz. *Principles of fluorescence spectroscopy*. Springer Science & Business Media, 2007.
- [62] T Imoto, Leslie S Forster, JA Rupley, and Fumio Tanaka. Fluorescence of lysozyme: emissions from tryptophan residues 62 and 108 and energy migration. *Proceedings of the National Academy of Sciences*, 69(5):1151–1155, 1972.
- [63] Mary E Denton, David M Rothwarf, and Harold A Scheraga. Kinetics of folding of guanidine-denatured hen egg white lysozyme and carboxymethyl (cys6, cys127)-lysozyme: a stopped-flow absorbance and fluorescence study. *Biochemistry*, 33(37):11225–11236, 1994.
- [64] Matias Moller and Ana Denicola. Protein tryptophan accessibility studied by fluorescence quenching. *Biochemistry and Molecular Biology Education*, 30(3):175–178, 2002.
- [65] Eugene A Permyakov. *Luminescent spectroscopy of proteins*. CRC press, 1992.
- [66] Alexey S. Ladokhin. *Fluorescence Spectroscopy in Peptide and Protein Analysis*. John Wiley & Sons, Ltd, 2006.
- [67] Yu Chen, Bo Liu, Hong-Tao Yu, and Mary D Barkley. The peptide bond quenches indole fluorescence. *Journal of the American Chemical Society*, 118(39):9271–9278, 1996.
- [68] Khosrow Khalifeh, Bijan Ranjbar, Khosro Khajeh, Hossein Naderi-Manesh, Mehdi Sadeghi, and Sara Gharavi. A stopped-flow fluorescence study of the native and modified lysozyme. *Biologia*, 62(3):258–264, 2007.
- [69] MA Ansari, S Zubair, SM Atif, M Kashif, N Khan, M Rehan, T Anwar, A Iqbal, and M Owais. Identification and characterization of molten globule-like state of hen egg-white lysozyme in presence of salts under alkaline conditions. *Protein and peptide letters*, 17(1):11–17, 2010.
- [70] Tatsuyuki Yamamoto, Noriko Fukui, Akihiro Hori, and Yoshihisa Matsui. Circular dichroism and fluorescence spectroscopy studies of the effect of cyclodextrins on the thermal stability of chicken egg white lysozyme in aqueous solution. *Journal of molecular structure*, 782(1):60–66, 2006.

- 
- [71] Norman E Good, G Douglas Winget, Wilhelmina Winter, Thomas N Connolly, Seikichi Izawa, and Raizada MM Singh. Hydrogen ion buffers for biological research\*. *Biochemistry*, 5(2):467–477, 1966.
- [72] Jennifer Dunbar, Hemant P Yennawar, Soojay Banerjee, Jiabin Luo, and Gregory K Farber. The effect of denaturants on protein structure. *Protein science*, 6(8):1727–1733, 1997.
- [73] George I Makhatadze and Peter L Privalov. Protein interactions with urea and guanidinium chloride: a calorimetric study. *Journal of molecular biology*, 226(2):491–505, 1992.
- [74] Savo Lapanje and Ingemar Wadso. A calorimetric study of the denaturation of lysozyme by guanidine hydrochloride and hydrochloric acid. *European Journal of Biochemistry*, 22(3):345–349, 1971.
- [75] John M Chirgwin, Alan E Przybyla, Raymond J MacDonald, and William J Rutter. Isolation of biologically active ribonucleic acid from sources enriched in ribonuclease. *Biochemistry*, 18(24):5294–5299, 1979.
- [76] Wei Liu, Troy Cellmer, David Keerl, John M Prausnitz, and Harvey W Blanch. Interactions of lysozyme in guanidinium chloride solutions from static and dynamic light-scattering measurements. *Biotechnology and bioengineering*, 90(4):482–490, 2005.
- [77] Norma J Greenfield. Using circular dichroism spectra to estimate protein secondary structure. *Nature protocols*, 1(6):2876–2890, 2006.
- [78] CH Suelter and Marlene DeLuca. How to prevent losses of protein by adsorption to glass and plastic. *Analytical biochemistry*, 135(1):112–119, 1983.
- [79] NN Khechinashvili, PL Privalov, and EI Tiktopulo. Calorimetric investigation of lysozyme thermal denaturation. *FEBS letters*, 30(1):57–60, 1973.
- [80] Alan Cooper, Stephen J Eyles, Sheena E Radford, and Christopher M Dobson. Thermodynamic consequences of the removal of a disulphide bridge from hen lysozyme. *Journal of molecular biology*, 225(4):939–943, 1992.
- [81] Phoebe Shih, Jack F Kirsch, and Debra R Holland. Thermal stability determinants of chicken egg-white lysozyme core mutants: Hydrophobicity, packing volume, and conserved buried water molecules. *Protein Science*, 4(10):2050–2062, 1995.
- [82] A Mark Buswell and Anton PJ Middelberg. Critical analysis of lysozyme refolding kinetics. *Biotechnology progress*, 18(3):470–475, 2002.
- [83] Javier Gomez, Vincent J Hilser, Dong Xie, and Ernesto Freire. The heat capacity of proteins. *Proteins: Structure, Function, and Bioinformatics*, 22(4):404–412, 1995.
- [84] Edward P O’Brien, Ruxandra I Dima, Bernard Brooks, and D Thirumalai. Interactions between hydrophobic and ionic solutes in aqueous guanidinium chloride and urea solutions: lessons for protein denaturation mechanism. *Journal of the American Chemical Society*, 129(23):7346–7353, 2007.

- [85] Kirk C Aune and Charles Tanford. Thermodynamics of the denaturation of lysozyme by guanidine hydrochloride. i. dependence on ph at 25. *Biochemistry*, 8(11):4579–4585, 1969.
- [86] Patrick PAJOT. Fluorescence of proteins in 6-m guanidine hydrochloride. *European Journal of Biochemistry*, 63(1):263–269, 1976.
- [87] Martin F Chaplin. Water’s hydrogen bond strength. *Water and Life: The unique properties of H2O*, 20:69, 2010.
- [88] Surajit Bhattacharjya and Padmanabhan Balaram. Hexafluoroacetone hydrate as a structure modifier in proteins: Characterization of a molten globule state of hen egg-white lysozyme. *Protein science*, 6(5):1065–1073, 1997.
- [89] Ye Zou and Gang Ma. A new criterion to evaluate water vapor interference in protein secondary structural analysis by ftir spectroscopy. *International journal of molecular sciences*, 15(6):10018–10033, 2014.
- [90] A Gomez-Hens and D Perez-Bendito. The stopped-flow technique in analytical chemistry. *Analytica chimica acta*, 242:147–177, 1991.
- [91] Ninad V Prabhu and Kim A Sharp. Heat capacity in proteins. *Annu. Rev. Phys. Chem.*, 56:521–548, 2005.
- [92] Mark RH Krebs, Deborah K Wilkins, Evonne W Chung, Maureen C Pitkeathly, Aaron K Chamberlain, Jesus Zurdo, Carol V Robinson, and Christopher M Dobson. Formation and seeding of amyloid fibrils from wild-type hen lysozyme and a peptide fragment from the  $\beta$ -domain. *Journal of molecular biology*, 300(3):541–549, 2000.



---

# A.

---

## APOLAR BASIC POLAR ACIDIC

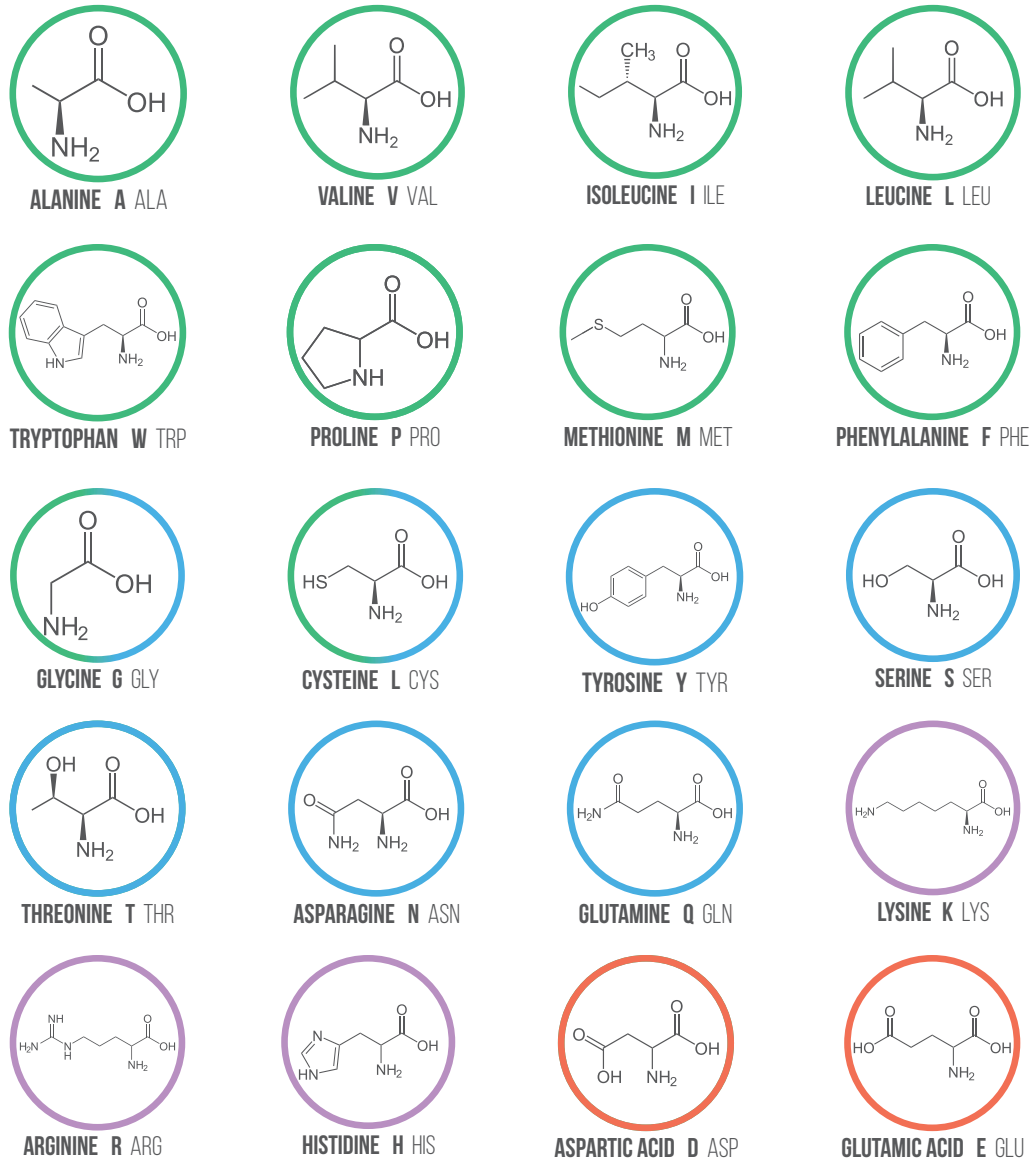


**Figure A.1.** Chemical representation of the 20 natural amino acids comprising proteins.